Sudden Stratospheric Warmings

Mark P. Baldwin[1], Blanca Ayarzagüena[2], Thomas Birner[3], Neal Butchart[4], Amy H. Butler[5], Andrew J. Charlton-Perez[6], Daniela I. V. Domeisen[7], Chaim I. Garfinkel[8], Hella Garny[9], Edwin P. Gerber,[10], Michaela I. Hegglin[6], Ulrike Langematz[11], Nicholas M. Pedatella[12,13]

[1]Global Systems Institute and Department of Mathematics, University of Exeter, United Kingdom
[2]Dpto. de Fsica de la Tierra y Astrofsica, Facultad de CC. Fsicas, Universidad Complutense de Madrid, Madrid, Spain
[3]Meteorological Institute, Ludwig-Maximilians-University Munich, Munich, Germany
[4]Met Office Hadley Centre, Exeter, United Kingdom
[5]NOAA Chemical Sciences Laboratory, Boulder, CO, USA
[6]Department of Meteorology, University of Reading, Reading, United Kingdom
[7]Institute for Atmospheric and Climate Science, ETH Zurich, Zurich, Switzerland
[8]The Fredy & Nadine Herrmann Institute of Earth Sciences, The Hebrew University, Jerusalem, Israel
[9]Deutsches Zentrum fr Luft- und Raumfahrt (DLR), Institut fr Physik der Atmosphre, Oberpfaffenhofen, Germany
[10]Courant Institute of Mathematical Sciences, New York University, New York, NY, USA
[11]Institut fr Meteorologie, Freie Universität Berlin, Berlin, Germany
[12]High Altitude Observatory, National Center for Atmospheric Research, Boulder, CO, USA
[13]COSMIC Program Office, University Center for Atmospheric Research, Boulder, CO, USA

Key Points:

- Sudden stratospheric warmings are dramatic events of the polar stratosphere that affect the atmosphere from the surface to the thermosphere.
- Our understanding of sudden stratospheric warmings has accelerated recently, particularly the predictability of surface weather effects.
- More observations, improved climate models, and big data methods will address uncertainties in key aspects of sudden stratospheric warmings.

This is the author manuscript accepted for publication and has undergone full peer review but has not been through the copyediting, typesetting, pagination and proofreading process, which may lead to differences between this version and the Version of Record. Please cite this article as doi: 10.1029/2020RG000708

Corresponding author: Mark P. Baldwin, m.baldwin@exeter.ac.uk

Abstract

Sudden stratospheric warmings (SSWs) are impressive fluid dynamical events in which large and rapid temperature increases in the winter polar stratosphere (∼10–50km) are associated with a complete reversal of the climatological wintertime westerly winds. SSWs are caused by the breaking of planetary-scale waves that propagate upwards from the troposphere. During an SSW, the polar vortex breaks down, accompanied by rapid descent and warming of air in polar latitudes, mirrored by ascent and cooling above the warming. The rapid warming and descent of the polar air column affects tropospheric weather, shifting jet streams, storm tracks, and the Northern Annular Mode, making cold air outbreaks over North America and Eurasia more likely. SSWs affect the atmosphere above the stratosphere, producing widespread effects on atmospheric chemistry, temperatures, winds, neutral (non-ionized) particles and electron densities, and electric fields. These effects span both hemispheres. Given their crucial role in the whole atmosphere, SSWs are also seen as a key process to analyze in climate change studies and subseasonal to seasonal prediction. This work reviews the current knowledge on the most important aspects of SSWs, from the historical background to dynamical processes, modelling, chemistry, and impact on other atmospheric layers.

Plain Language Summary

The stratosphere is the layer of the atmosphere from ∼10 to 50km, with pressures decreasing to ∼1 hPa (0.1% of surface pressure) at the top. The polar stratosphere during winter is normally very cold, with strong westerly winds. Roughly every two years in the Northern Hemisphere, the quiescent vortex suddenly warms over a week or two, and the winds slow dramatically, resulting in easterly winds that are more similar to the summer. These events, known as sudden stratospheric warmings (SSWs) were discovered in the early 1950s, and today they are observed in detail by satellites. After several decades researching SSWs, considerable progress has been made in dynamical aspects of SSWs, but our understanding of how they affect both surface weather and the upper atmosphere is incomplete. We observe that variability of the stratospheric circulation (SSWs being an extreme event) is associated with shifts in the jet stream and the paths of storms, with associated effects on rainfall and temperatures. The likelihood of cold weather spells and damaging wind storms is also affected. Almost all SSWs have occurred in the Northern Hemisphere, but there was one spectacular major SSW in 2002 in the Southern Hemisphere.

1 Introduction

Sudden stratospheric warmings (SSWs) are the most dramatic stratospheric phenomenon. During SSWs, the normally strong wintertime westerly stratospheric circulation breaks down in a few days, and is replaced by weak easterly winds. This is accompanied by polar warming by up to 50°C; the effects extend to Earth's surface as well as through the mesosphere and beyond. The climatology of both the mean flow and planetary-scale wave amplitudes determines the overall likelihood of SSWs, which occur only during extended winter and almost exclusively in the Northern Hemisphere.

The variation of insolation with latitude and season drives a strong annual cycle in the stratosphere. During winter the polar stratosphere is characterized by a strong, westerly, cold polar vortex. The polar vortex is formed primarily through radiative cooling and is characterized by a band of strong westerly winds at mid- to high latitudes. Typical temperatures are ∼-65° to -55°C (∼208 to 218 K) in the polar Northern Hemisphere at 10 hPa. Roughly every two years, the wintertime vortex is disrupted by planetary-scale waves to such an extent that this circulation breaks down, with westerly winds becoming weak easterly, and temperatures climbing several tens of °C—essentially summertime conditions—and occasionally (e.g., January 2009) climbing above 0°C at some local points. SSWs happen very rapidly, i.e., in a few days, resulting in one of the most dramatic atmospheric events. Figure 1 illustrates a sudden warming event in 2018–2019, together with the background climatology and variability of zonal wind, and the average temperature from 65°–90°N at 10 hPa. It is important to highlight that both the lowest and highest recorded temperatures occurred in mid-winter. Outside of winter, the stratosphere is quiescent. The warming event (red curve) was followed, after more than a month, by anomalously low temperatures and strong winds in the middle stratosphere. Figure 2 illustrates zonal mean temperature anomalies averaged over days 0–30 following SSW events. The upper stratosphere cools, and that there is slight cooling in the mid-latitudes and tropics in compensation for the downward adiabatic warming over the polar cap. Vectors illustrate the approximate motion consistent with the temperature anomalies (and pressure anomalies, not shown). See Baldwin, Birner, and Ayarzagüena (2019) for details of the calculation. In particular, note the poleward movement of mass near the surface at high latitudes. This leads to higher Arctic surface pressure following SSWs.

The effects of SSWs are not only identified in the middle stratosphere. SSWs last much longer in the lower stratosphere and troposphere than they do in the upper stratosphere. Figure 3a illustrates a lag composite of temperature anomalies for SSW events in JRA-55 reanalyses (1958–2015). Above 30 km, the SSW events end within two to three weeks, while in the lowermost stratosphere SSWs last more than two months, on average. This is largely due to the faster radiative time scale in the upper stratosphere. Pressure anomaly composites (Figure 3b) are similar to temperature, except that surface effects are clearly visible. The "lumpiness" of the surface signal is due to averaging of a relatively small number of SSWs. Averaged over days 0–60 the surface pressure anomaly is 2.1 hPa, but is only 0.74 hPa near the tropopause. This is called "surface amplification" of the stratospheric signal (Baldwin, Birner, & Ayarzagüena, 2019). The fact that the pressure anomaly from SSWs is largest at the surface is important. It means that tropospheric near-surface processes must be reinforcing the stratospheric signal, raising surface pressure over the polar cap (See Section 7).

SSWs are fascinating from a fluid dynamical perspective, and perhaps the simplest and most insightful way of viewing the dynamics is maps of potential vorticity (PV; see Section 4) (McIntyre & Palmer, 1983, 1984). Maps of PV in the middle stratosphere show that planetary-scale wave breaking erodes the polar vortex, sharpening its edge. All SSWs are preceeded by erosion of the vortex, which forms a "surf zone" surrounding the vortex. With fine enough resolution, one can see filamentation—thin streamers—of PV being stripped away from the vortex and mixed into the surf zone. This horizontal view complements the zonal mean, which shows mainly rapid temperature rises as air descends over the polar cap, accompanied by slowing of the zonal winds. Over time, differing mechanisms have been suggested to explain the occurrence of SSWs. Some of the mechanisms are complementary descriptions from different perspectives, e.g., the zonal-mean perspective of wave, mean-flow interaction, vs. the horizontal perspective of wave breaking and potential vorticity. These issues are discussed in Section 4.

An underlying question is whether or not SSWs are dynamically unique extreme events. Given the observed distributions of temperatures, winds, PV, etc., do SSWs stand out as outliers from the distribution? Or is it that SSWs simply occupy one tail of the distribution? In the Northern Hemisphere (NH), it appears that SSWs occupy one tail of the distribution (e.g., of wintertime of zonal mean wind at 60°N, 10 hPa). There is a broad continuum of warmings, from very minor to major deviations from climatology (Coughlin & Gray, 2009). Thus, defining an SSW as having occurred or not comes down to defining a fixed threshold (e.g., of absolute stratospheric fields such as polar wind and/or temperature at some level) or a relative field (e.g., based on the variability of the polar stratosphere such as the Northern Annular Mode or just the variability of the polar temperature (Butler et al., 2015)). As summarized in Section 3, many different criteria have been proposed for detecting major SSW events. They often identify the most disruptive events but differ in the quantitative size and timing of the events. However, the use of different algorithms in studies can lead to inconsistent conclusions among studies, particularly when using different models or under different climate states (McLandress & Shepherd, 2009a).

So far we have mainly focused on the NH, since all major SSWs occurred in the NH prior to 2002. In fact, in the Southern Hemisphere (SH) there has been only one major SSW (in 2002), and it was indeed spectacular (Kruger et al., 2005). In terms of daily zonal wind anomalies, the event was approximately eight standard deviations from the mean—far outside the distribution up to that time. As rare as this event was, in early September 2019 a similarly anomalous event occurred, though it did not technically qualify as a major SSW by established criteria (Hendon et al., 2019; Rao, Garfinkel, White, & Schwartz, 2020). Southern Hemisphere warming events are important because they inhibit strong heterogeneous ozone depletion—essentially preventing the formation of the ozone hole—and because these events affect jet streams, precipitation (and droughts) especially across Australia (e.g Thompson et al., 2005; Lim et al., 2019).

The effects of SSWs are not confined to the polar stratosphere. SSWs affect the circulation in the tropical stratosphere (e.g. Kodera et al., 2011) and beyond, mixing chemical constituents such as ozone, as indicated in Section 9. The large descent over the polar cap associated with the SSW is balanced by upwelling south of $\sim$50°N that extends into the Southern Hemisphere (Figure 2). Also visible is ascent (cooling) in the polar upper stratosphere, that extends into the mesosphere (Krnich & Becker, 2010). SSWs can affect thermospheric chemistry, temperatures, winds, electron densities, and electric fields, across both hemispheres (Chau et al., 2012). These effects are discussed in Section 8.

Some of the most important impacts of SSWs occur in the troposphere, and this is actually one of the SSW features that has received most of the attention in literature in the last decade—as summarized in Section 7. On average, SSWs are observed to have substantial, long-lasting effects on surface weather and climate, especially on sea-level pressure (SLP) and the Northern Annular Mode (NAM), with associated shifts in the jet streams, storm tracks, and precipitation (e.g Baldwin & Dunkerton, 2001). These effects are much larger than can be explained by dynamical theories such as PV inversion (e.g. Charlton et al., 2005) or the tropospheric response to stratospheric wave forcing. Tropospheric processes, possibly involving low-level Arctic temperature anomalies, act to amplify the stratospheric signal (Baldwin, Birner, & Ayarzagüena, 2019). This picture of SSW impacts on surface weather becomes clear when analysis over many SSWs is averaged together. Despite the extensive efforts of the scientific community, it is still impossible to predict which individual SSW will have a visible downward impact—meaning that the tropospheric anomalies (e.g., NAM index or pressure) are of the same sign as as those in the stratosphere. Some SSWs may have a tropospheric impact, but not enough to be obvious.

Given the relevance of SSW events on the whole atmosphere, several efforts have been made in investigating their predictability. SSWs can be predicted relatively well 10-15 days in advance (Tripathi et al., 2015; Karpechko, 2018; Domeisen, Butler, et al., 2020a). Several phenomena outside the polar stratosphere have been identified, in the observations, as possible modulators of the likelihood of SSWs. Some of them are related to the tropical stratosphere such as the Quasi-Biennial Oscillation (QBO) and Semi-Annual Oscillation (SAO) of the equatorial stratosphere. Others are related to ocean-atmosphere system such as the El Niño-Southern Oscillation (ENSO) and Madden Julian Oscillation (MJO), and some others even refer to external phenomena such as the 11-yr solar cycle. With multiple possible influences, and only around 40 SSWs since 1958, quantifying these relationships is challenging.

In this study, we offer a review of our current understanding of most aspects of SSWs. Most of the previous reviews of SSWs were published several decades ago and only or mostly focused on the explanation of the dynamics involved in the occurrence of these events (e.g. Schoeberl, 1978; Holton, 1980; McIntyre, 1982). Around 1980 the availability of observations in the stratosphere was very limited, mainly because meteorological satellites were just starting to operate. This hindered the investigation of SSW aspects such as the effects on the upper atmosphere. Surface weather effects were not widely recognised until 1999 (e.g. Baldwin & Dunkerton, 1999). Another limitation was that general circulation models (GCMs) in the 1970s and 1980s had low vertical resolution of the stratosphere. The biggest increase in the number models with well-resolved stratospheres was relatively recent, during the Coupled Model Intercomparison Project Phase 5 (CMIP5) (Charlton-Perez et al., 2013). Model development has not only allowed the advance in knowledge on known dynamical and chemistry aspects, but also the exploration of new SSW perspectives such as the benefits of including stratospheric information to improve medium-range to subseasonal predictions of surface weather. Research on SSWs has accelerated in very recent decades with a large increase in the number of publications on this topic. Summaries have been written by O'Neill et al. (2015) and Padatella et al. (2018), but not in detail, or just covering the most common aspects such as dynamics, types of events, history or tropospheric fingerprint. For instance, O'Neill et al. (2015) do not address the effects of SSWs on the atmosphere above the stratopause, whereas Padatella et al. (2018) provide just an overview of SSWs influence on the whole atmosphere without going much in detail. Still, as anticipated previously, many questions remain open. The present review aims to provide a general overview of SSWs by covering the major aspects of SSWs, their impacts, and the outstanding research challenges. In Section 2 a brief historical background is provided and Section 3 describes the classification of these events. Dynamical theories for the occurrence of SSWs are included in Section 4, and possible external factors driving SSWs are discussed in Section 5. The predictability of SSWs is discussed in Section 6, and their effects on climate and weather are presented in Section 7. Effects above the stratosphere are described in Section 8, and chemical/tracer aspects are shown in Section 9. Finally, the outlook/conclusion is provided in Section 10.

2 Historical background

SSWs were discovered by Richard Scherhag in radiosonde temperature measurements above Berlin, Germany. Scherhag started regular radiosonde measurements from the area of the former Tempelhof airport in Berlin in January 1951. As professor and head of the recently founded Institute of Meteorology at Freie Universität Berlin he was interested in exploring the stratosphere. With the help of the U.S. allies in post-war Berlin he was able to employ a new type of American radiosonde using neoprene balloons which provided regular measurements of the stratosphere up to ∼30 km altitude (∼10 hPa). In a first publication in spring 1952, Scherhag reported an explosive-type warming of the high stratosphere in January 1952 and concluded that the observed warming was too strong to be explained by advection (Scherhag, 1952a). This "Berlin Phenomenon", as Scherhag called the warming, developed as follows: "While all measured stratospheric temperatures ranged between –56° and –69°C on January 26, only two days later –37°C were measured at 13 hPa. This means a sudden warming of 30 degrees had started on January 27. On January 30, the temperature reached –23°C in 10 hPa, followed by a rapid cooling." Scherhag also found that the warming slowly propagated downward to the 200 hPa pressure level within one week. This first warming pulse was followed by a second, even stronger warming about one month later, with a temperature maximum of –12.4°C (a warming of ∼ 37°C within 2 days) at 10 hPa on February 23 and a change in circulation to south-easterly winds in the middle stratosphere. Figure 4 shows the Tempelhof radiosonde temperature measurements of February 21 (before the warming), February 23 (at the peak of the SSW), and on February 28 (after the peak) (Wiehler, 1955). Also in February 1952, upper-level wind data from radiosondes over the northern U.S. indicated an increase of the frequency of easterly winds at 50 hPa associated with a closed

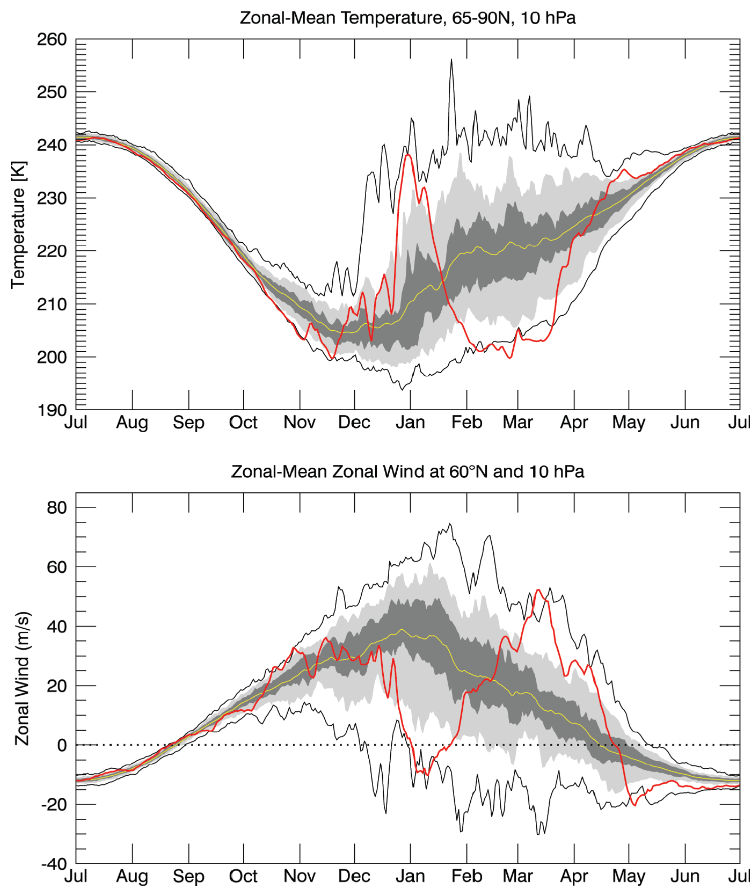

Figure 1. 10-hPa 65°–90°N ERA-Interim reanalysis (Dee et al., 2011) zonal-mean temperatures (top) and zonal-mean wind at 60°N (bottom) for July 2018–June 2019 (red lines). An SSW event is seen as the upward spike in temperature and the reduction to less than 0 m/s in zonal wind (easterlies). The yellow lines signifies the average conditions in the stratosphere for that time of year, while the gray shading show 70th (dark) and 90th (light) percentiles. Solid black lines show the max/min for prior winters 1979–2018. The month ticks indicate the first day of the month.

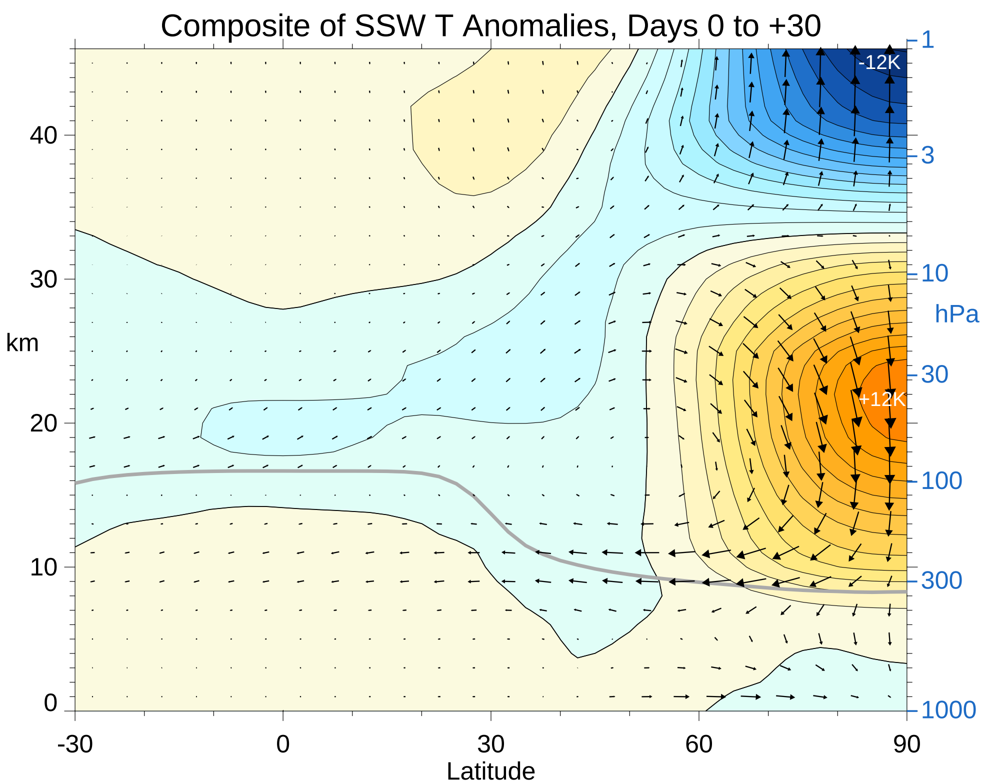

Figure 2. Composite temperature anomalies averaged during days 0–30 following 36 SSW events during 1958–2015 in JRA-55 data (1116 day mean) (Kobayashi et al., 2015). The SSWs dates are defined based on the reversal of the zonal mean zonal wind at 60°N and 10 hPa, applying the criterion of Charlton and Polvani (2007). The contour interval is 1K. The vertical component of the vectors represent the approximate displacement (from the climatological basic state) to form the temperature anomalies shown. Similarly, the horizontal components represent the north-south movement consistent with pressure regressions (not shown). The vectors are derived statistically from regressions, and are not a dynamical circulation. Beginning with the basic state, atmospheric movement defined by the vectors would create temperature and pressure anomalies approximately equal to the regression values. The calculation was performed in height coordinates. The pressure labels are approximate. The lapse-rate tropopause (gray line) is shown for the days in the composite.

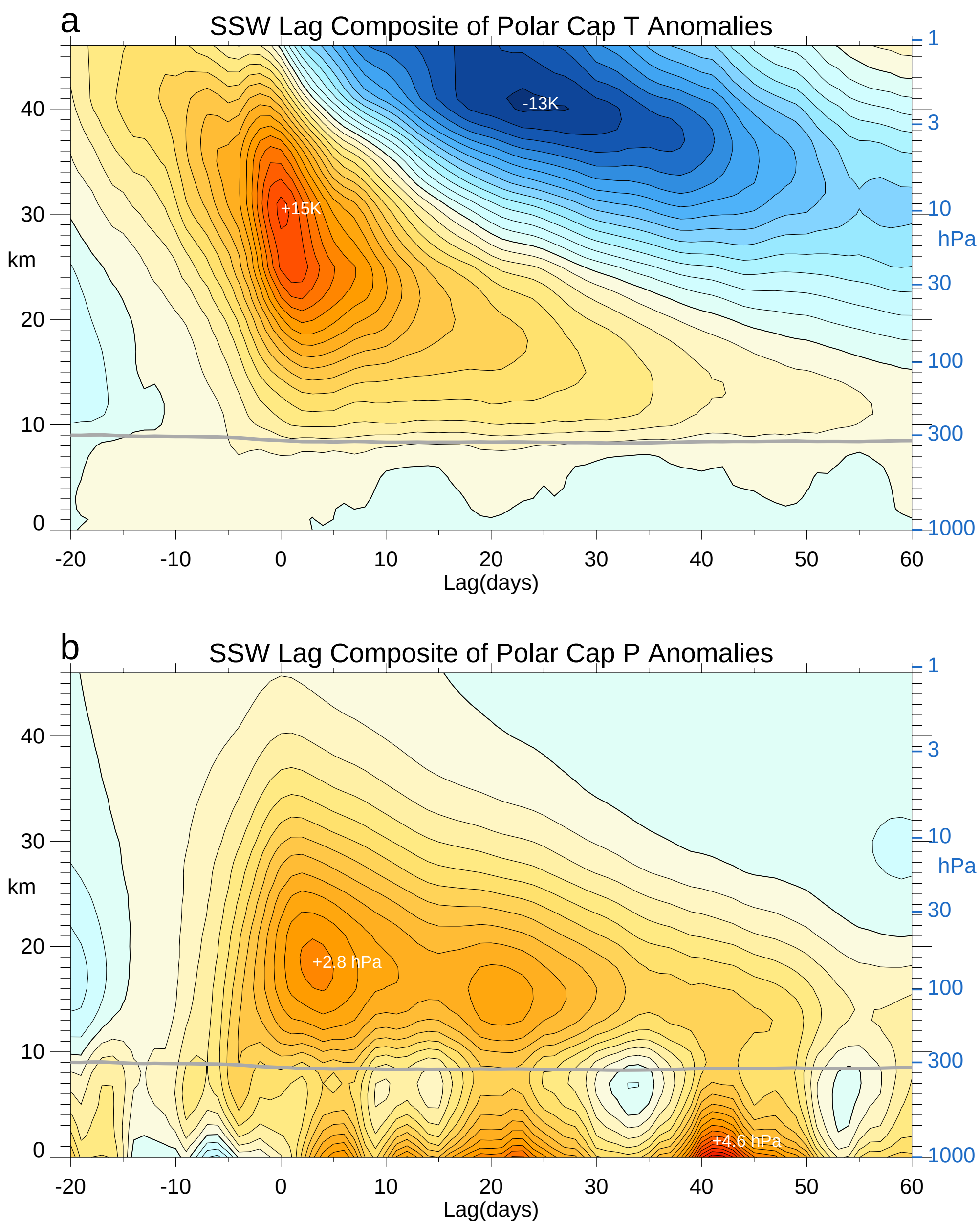

Figure 3. (a) Lag-composite of polar cap (65°–90°N) mean temperature anomalies from 36 SSW events during 1958–2015 in JRA-55 data. The SSWs dates are defined based on the reversal of the zonal mean zonal wind at 60°N and 10 hPa, applying the criterion of Charlton and Polvani (2007). The contour interval is 1K. The tropopause (gray line) is depressed by ~750m following the warmings. (b) as in (a) except for polar cap pressure anomalies. Contour interval 0.25 hPa

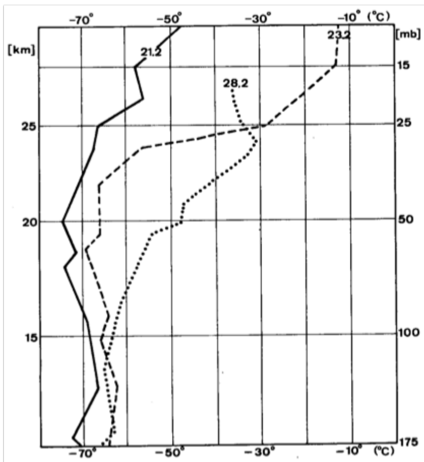

Figure 4. Radiosonde temperature measurements in Berlin-Tempelhof during the first recorded Sudden Stratospheric Warming in February 21-28, 1952. Figure from Wiehler (1955).

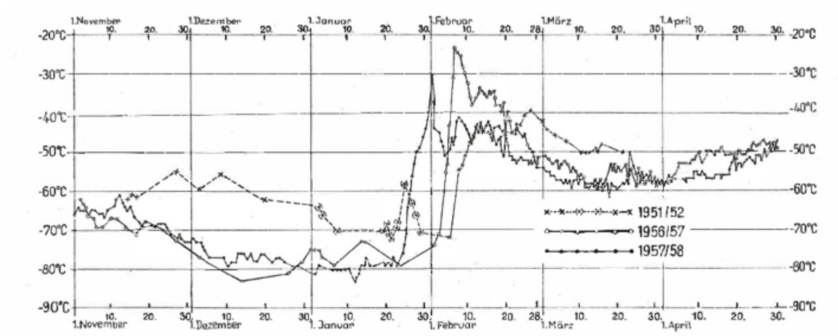

Figure 5. 50 hPa temperature time series over Alert, Ellesmere Land, during the 3 winters with stratospheric warmings in the 1950s. Figure from Warnecke (1962).

persistent anticyclonic circulation northwest of Hudson Bay and a warming over Canada and Greenland (Darling, 1953).

In a first attempt to explain the unexpected warming of the winter stratosphere, Scherhag (1952b) and Willett (1952) suspected a severe solar eruption on February 24 to be the source. While we now know that solar effects are not strong enough to force individual SSWs, a statistical relation between the occurrence of SSWs and solar activity is actively discussed until the present day. A similar stratospheric warming had also been noted the year before, in February 1951, from British Meteorological Office radiosonde and radar measurements over England and Scotland. It was accompanied by a reversal of the lower stratospheric winds to easterlies which were followed again by westerlies before the transition to summertime easterlies (Scrase, 1953). It then took until the winters 1956/57 and 1957/58 that similarly strong SSWs were analysed in maps which had been specifically produced on stratospheric pressure levels (Teweles, 1958; Teweles & Finger, 1958). Figure 5 shows the evolution of 50 hPa temperature over Alert, Ellesmere Land, during 3 winters with stratospheric warmings in the 1950s.

With the start of the International Geophysical Year (IGY) in July 1957, the number of radiosonde balloons reaching altitudes above 30 km increased. Stratospheric maps (daily or every five days, at 100, 50, 30 and 10 hPa) for the Northern Hemisphere were published by several centers, e.g., the US Weather Bureau, the Arctic Meteorology Research Group of McGill University Montreal and the Stratospheric Research Group of Freie Universität Berlin. Meteorological rocketsondes provided new insights: It was found, for example, that the strong stratospheric warming over Fort Churchill in January 1958 occurred a couple of days earlier in the altitude region above 40 km than in the layers below (Stroud et al., 1960). Moreover, intense warmings were detected in the upper stratosphere which were never detected below 10 hPa. In order to obtain an increased number of high-altitude soundings during stratospheric warmings, the STRATWARM warning system was established by the WMO in 1964. These alerts included information on the intensity and movement of the warmings and were distributed internationally from the meteorological centers at Melbourne, Tokyo, Berlin and Washington D.C. As suggested in the WMO/IQSY (1964) report, SSWs were classified according to their time of occurrence ("mid-winter warmings" versus "final warmings" in late winter) and their intensity. While "minor mid-winter warmings" were characterized by a strong warming of the Arctic stratosphere at 10 hPa and higher levels, "major mid-winter warmings" had to be additionally accompanied by a complete circulation reversal from westerlies to easterlies polewards of 60°N at the same levels. Alternative SSW definitions that were developed later are discussed in Section 3.

In a plea for additional upper air data, Scherhag et al. (1970) raised the question of "whether an intimate knowledge of the stratospheric circulation would prove valuable in, for example, forecasting." They stated that phase relationships between events in the stratosphere and troposphere must be known for a full exploration of forecast probabilities. In fact, Scherhag had speculated about the impact of SSWs on surface weather as early as in his initial 1952 report, in which he pointed out a drop in forecast skill score following the February 1952 SSW (perhaps related to the fact that stratospheric information was not included in the forecasts). Indeed, some early studies had pointed at a potential interaction of tropospheric and stratospheric zonal wavenumber 2 during the 1967/68 warming (Johnson, 1969) and the role of tropospheric blockings for the onset of stratospheric warmings (Julian & Labitzke, 1965). An early example of stratosphere-troposphere coupling is illustrated in Figure 6 which shows 10 hPa height maps at the beginning (January 18, left panel) and peak (January 27, middle panel) of the 1963 stratospheric warming, and the surface pressure map of January 31 (Fig 6, right panel) (Scherhag, 1965). A few days after the stratospheric warming, a surface anticyclone developed over Greenland which extended through the troposphere up to the middle stratosphere. This was consistent with Labitzke (1965) who described the occurrence of a tropospheric blocking about ten days after a stratospheric warming and Quiroz (1977) who found tropospheric temperature changes after a stratospheric warming.

With the beginning of the satellite era in 1979 much improved data coverage allowed new breakthroughs in our understanding of stratospheric dynamics and SSWs. McIntyre and Palmer (1983) showed the first observationally derived hemispheric scale maps of PV on a mid-stratospheric potential temperature surface (850 K) based on the then newly available radiance data from the Stratospheric Sounding Unit (SSU). These maps clearly demonstrate the existence of large amplitude planetary wavenumber 1 preceding the 1979 SSW event with subsequent evolution showing wave breaking. The maps furthermore illustrate the split of the vortex during the 1979 major SSW as seen in PV at 850 K. Satellite data have continued to provide valuable observational constraints on the dynamics and transport characteristics surrounding SSW events [e.g., Manney, Harwood, et al. (2009); see also Section 9].

3 Types and classification of SSWs

In the early decades after the discovery of SSWs, the WMO developed an international monitoring program called STRATALERT, led by Karin Labitzke of Freie Universität Berlin, to detect SSWs. Early metrics to measure these events were based on

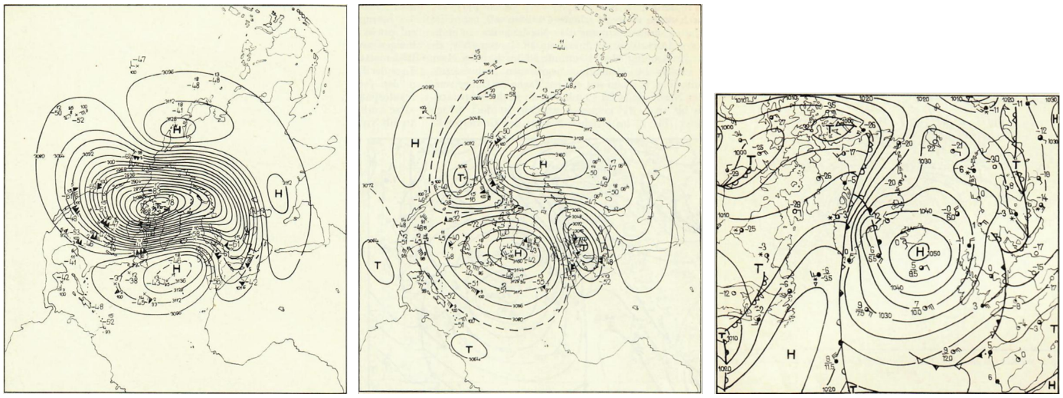

Figure 6. 10 hPa height map on January 18, 1963 (left) and January 27, 1963 (middle) and sea level pressure on January 31, 1963 (right) (From Scherhag (1965). ©Springer. Used with permission.)

temperature changes, as the sudden and rapid warming of the stratosphere were key features measurable by radiosondes and rocketsondes. WMO/IQSY (1964) established that "major" SSWs were separated from more minor events by requiring a reversal (from westerly to easterly) of the zonal winds poleward of 60° latitude and an increase in the zonal-mean temperature polewards of 60° at 10 hPa (WMO/IQSY, 1964; McInturff, 1978; Labitzke, 1981). The inclusion of a zonal circulation reversal criteria stems from wave-mean flow theory which stipulates that quasi-stationary planetary-scale waves cannot propagate into easterly flow (Charney & Drazin, 1961; Matsuno, 1971; Palmer, 1981). Thus, an obvious dynamical distinction between a major and minor SSW is that vertical wave propagation from the troposphere is prohibited beyond the middle stratosphere following a major event. A remarkable aspect of these early metrics is the extent to which they still form the basis of SSW detection, despite being based on a very small number of observations.

The most commonly used metric to detect major SSWs was proposed by Charlton and Polvani (2007) (hereafter CP07) and adapted from earlier definitions: the reversal of the daily-mean zonal-mean zonal winds from westerly to easterly at 60°N latitude and 10 hPa from November to April[1]. The earlier criteria for a temperature gradient increase was found to be largely redundant since, by thermal wind balance, this occurs in almost all cases of a zonal wind reversal. While the detection of major SSWs using the CP07 definition is sensitive to the particular latitude, altitude, and threshold of the zonal wind weakening (Butler et al., 2015), the choice of a reversal at 10 hPa and 60°N optimizes key features and impacts of major SSWs (Butler & Gerber, 2018). Having a common metric for major SSWs allows for consistent intercomparison of models (Charlton-Perez et al., 2013; Kim et al., 2017; Ayarzagüena et al., 2018) and reanalyses (Palmeiro et al., 2015; Butler et al., 2017; Martineau et al., 2018; Ayarzagüena et al., 2019).

It should be noted that the CP07 metric was developed during a time when the increased availability of global climate model simulations necessitated the evaluation of the model stratosphere in large gridded datasets (Charlton-Perez et al., 2013). Thus, a major criterion for the CP07 metric was that the data request needed for the calculation should be as small as possible. In the current era, with greater availability of dy-

[1] By CP07, wind reversals must be separated by 20 consecutive days of westerly winds, and must return to westerly for at least 10 consecutive days prior to 30 April, to be classified as a mid-winter SSW.

namical metrics output from model simulations (Gerber & Manzini, 2016), this requirement is not as stringent. Thus, it is worth emphasizing the intended use of the CP07 definition as a simple metric for polar vortex weak extremes, rather than as an infallible selection of events that should be deemed "important". This metric yields on average 6 major SSWs per decade in the NH. There is however significant decadal variability in the frequency of SSW events (Reichler et al., 2012), with the 1990s exhibiting only two SSWs (in 1998 and 1999) and the 2000s exhibiting 9 events according to the CP07 metric. According to a reconstruction of SSW frequency based on the surface NAO, recent decades since 1970 show stronger decadal variability in SSW frequency than the period in the middle of the 20th century, with the 1990s likely representing the longest absence of SSW events since 1850 (Domeisen, 2019).

The application of the CP07 metric to the SH polar vortex (where zonal-mean zonal wind reversals at 60°S and 10 hPa between May-October are considered) reveals only one major SH SSW in the reanalysis back to 1958, which occurred on 26 September 2002 (Shepherd et al., 2005). This highlights important differences in dynamics and climatology between the NH and SH. However, in mid-September of 2019 an extremely anomalous weakening of the SH vortex occurred (Hendon et al., 2019; Rao, Garfinkel, White, & Schwartz, 2020) that did not meet the CP07 criterion for a major SSW. Nonetheless, this event should not be disregarded simply because the circulation failed to meet one metric; the event set new records for mid-stratospheric temperatures in September, and the downward influence from this SSW was associated with an extremely persistent equatorward shift of the SH jet stream that led to significant impacts on surface climate, such as extensive Australian bushfires (Lim et al., 2019). Further diagnostics should thus be considered for evaluating the relevance of extreme vortex events in both hemispheres for surface weather effects; a so-called minor SSW can have major societal impacts.

In addition to major versus minor SSWs, there is also classification of the morphology of the event. During a SSW, the polar vortex can either be displaced off the pole or split into two pieces. Several different methods have been developed to classify split versus displacements (CP07; Mitchell et al., 2011; Seviour et al., 2013; Lehtonen & Karpechko, 2016). About a third of the observed 36 major SSWs in the 1958-2012 period can be unambiguously classified across all methods as splits and another third as displacements (Gerber et al., 2020). The rest of the events are more ambiguous across methods, perhaps because in some cases the polar vortex both displaces and splits within a period of several days (Rao, Garfinkel, et al., 2019).

Furthermore, SSWs have been classified by the zonal wavenumber of the tropospheric precursor patterns leading up to the SSW. These predominantly wave-1 and wave-2 patterns tend to precede SSWs (Tung & Lindzen, 1979a; Woollings et al., 2010; Garfinkel et al., 2010; Cohen & Jones, 2011). In particular, blocking (a persistent anomalous high pressure) over the Pacific region and North Atlantic/Scandinavian region has been tied to wave-2 driving of split vortex events (Martius et al., 2009). Anomalous low pressure over the North Pacific/Aleutians with Euro-Atlantic blocking has been tied to wave-1 driving of primarily displacement vortex events (Castanheira & Barriopedro, 2010). While displacements of the vortex are nearly always preceded by wave-1 forcing, splits of the vortex can be preceded by either wave-1 or wave-2 forcing (Bancalá et al., 2012; Barriopedro & Calvo, 2014) and often proceed with an increase in wave-1 followed by a subsequent increase in wave-2.

While the focus of this review is on SSWs, which represent the weakest polar vortex extremes, SSWs are just one extreme within a broad spectrum of polar stratospheric dynamic variability. A wide range of variations (see Figure 1, daily maximum and minimum values in black lines)—from more minor deviations from climatology, to the strongest polar vortex extremes—can influence stratosphere-troposphere coupling, transport, and chemical processes. Polar stratospheric variability peaks from January–March in the Northern Hemisphere, and from September–November in the Southern Hemisphere (though variability is less). Early winter extremes may evolve differently than late winter extremes; for example, *Canadian Warmings* are amplifications of the Aleutian High in the lower and middle NH stratosphere, and are the dominant type of stratospheric warming in early boreal winter (Labitzke, 1977). *Final warmings* refer to the seasonal transition of the polar vortex from its westerly to easterly state. In the NH the timing and other characteristics of this transition present a large interannual variability that in turn may have surface impacts, often distinct from those associated with mid-winter SSW (Ayarzagüena & Serrano, 2009; Hardiman et al., 2011; Butler et al., 2019; Thiblemont et al., 2019). In the SH, the timing of the final warming drives a substantial fraction of surface climate variability in austral late spring and summer (Byrne & Shepherd, 2018; Lim et al., 2018).

Additional metrics have been proposed to better capture the full spectrum of polar stratospheric variability. A number of studies consider metrics based on empirical orthogonal functions (EOFs). For example, the first EOF of geopotential height anomalies, also known as the "annular mode", (Baldwin & Dunkerton, 1999, 2001; Baldwin & Thompson, 2009; Gerber et al., 2010) captures mass fluctuations between the polar cap and extratropics. EOFs of vertical polar-cap temperature profiles have been used to identify weak vortex extremes (SSWs) that have the most extended recovery periods, called "Polar-night Jet Oscillations" (PJO) (Kuroda & Kodera, 2004; Hitchcock & Shepherd, 2012; Hitchcock et al., 2013). An advantage to EOF-based techniques is that thresholds for extremes are based on anomalies (deviations from the climatology) rather than absolute values, as in the CP07 zonal wind metric. Thus, EOF metrics can capture anomalous events relative to any changes in the climatology (McLandress & Shepherd, 2009b; Kim et al., 2017).

4 Development of dynamical theories

SSWs have been interpreted as a manifestation of strong two-way interactions between upward propagating planetary waves and the stratospheric mean flowalthough the extreme flow disruptions stretch the concept of waves on a mean flow. The polar vortex can be disrupted by large wave perturbations, primarily planetary-scale zonal wavenumber 1–2 quasi-stationary waves. Sufficient wave forcing of the mean flow by these waves can result in an SSW, with the breakdown of the westerly polar vortex, and easterly winds replacing westerlies near 10 hPa, 60°N. When the winds in the polar vortex slow, air is forced to move poleward to conserve angular momentum, with descent over the polar cap (arrows in Figure 2). The adiabatic heating associated with this descent results in the observed rapid increases in polar cap temperatures on time scales of just a few days.

Strong westerly winds in the polar night jet inhibit all but the largest, planetary scale waves from propagating into the stratosphere (Charney & Drazin, 1961). While planetary scale waves can spontaneously be generated by baroclinic instability (Hartmann, 1979; Domeisen & Plumb, 2012) or via upscale cascade from synoptic scale waves (Scinocca & Haynes, 1998), they are chiefly forced by planetary scale features at the surface: topography and land-sea contrast (Garfinkel, White, et al., 2020). The relative zonal symmetry of the austral hemisphere explains why SSWs are almost exclusively a boreal hemispheric phenomena, but this does not imply that the stratosphere just passively responds to wave driving from the troposphere.

The diversity of observed SSWs demonstrates that some SSWs appear to be forced by anomalous bursts of planetary wave activity from the troposphere, while in other SSWs the stratosphere itself acts to regulate upward wave propagation. All theories agree, however, that it is the sustained dissipation of wave activity in the stratosphere, chiefly through nonlinear wave breaking and irreversible mixing (Eliassen-Palm flux convergence), that generates a deep, sustained warming of the polar vortex. Once the vortex is destroyed, strong radiative cooling helps to rebuild the vortex provided there is time before the end of winter, but this radiatively controlled process can take several weeks (see Figure 3). Rotation and stratification couple the poleward transport of heat by waves to a downward transport of westerly momentum. Thus, the warming of the polar stratosphere occurs in concert with an eradication of the climatological vortex in a major warming event.

4.1 Wave-mean flow interactions, dissipation, and SSWs

The wintertime stratospheric polar vortex is formed primarily through radiative cooling, as the variation of insolation with latitude and season decreases the absorption of UV radiation by ozone at higher latitudes. Much of the theory of how SSWs occur relies on the basic assumption of waves propagating on a zonal mean flow. Although this assumption is violated during the extreme flow disruptions of SSWs (particularly at high latitudes), wave mean-flow interaction theory has been remarkably successful in explaining (at least qualitatively) the dynamics of how SSWs occur.

Upward propagation of a Rossby wave on a zonal-mean flow is associated with a poleward heat flux, $\overline{v'\theta'}$ (e.g., Eliassen & Palm, 1961; Charney & Drazin, 1961) (see also Vallis (2017), Chapt. 10). Warming of the vortex could then, in principle, be provided by convergence of the heat flux on the poleward flank of an upward propagating planetary wave. However, an opposing tendency arises due to the fact that the wave also induces vertical advection, producing adiabatic cooling where the heat flux would otherwise warm the air. (Likewise, the air on the equatorward side, which would be cooled by the poleward heat flux, sinks and adiabatically warms.) For conservatively propagating waves, i.e., a case with no dissipation, the two tendencies exactly cancel when integrated over the wave and no net warming or cooling occurs:

$$\overline{\omega}_r \frac{\partial \overline{\theta}}{\partial p} = -\frac{\frac{\partial}{\partial \varphi}(\cos\varphi \overline{v'\theta'})}{a\cos\varphi}\,. \tag{1}$$

Wave transience, say due to a wave propagating into the region of interest, gives rise to temporary polar cap warming and slowing down of the vortex with reversed tendencies as the wave leaves the region. In eq. 1, ω corresponds to vertical velocity in pressure coordinates, θ is the potential temperature, v refers to the meridional wind, a is the Earth's radius and φ refers to latitude. Overbar and primes denote zonal mean and deviation from it, respectively. Here, we have adopted the notation $\overline{\omega}_r$ to refer to the reversible component of zonal mean vertical motion that arises due to conservatively propagating waves. The nonacceleration theorem states that for steady waves with no dissipation and no critical levels, waves propagate through the mean flow without leading to accelerations or decelerations. In the presence of dissipation or diabatic processes, the full vertical velocity $\omega \neq \omega_r$, but the reversible component ω_r can still be identified from (1).

The calculus changes when the waves are allowed to dissipate, either damped by radiation and/or friction, or more cataclysmically, through non-linear breaking (though dissipation still plays a role, as breaking simply moves energy to smaller scales). Rossby waves carry easterly momentum owing to their intrinsic easterly phase speed; this easterly momentum is transferred to the mean flow during dissipation. The resulting easterly body force not only decelerates the vortex but also causes poleward flow, due to the Coriolis torque, and downwelling over the polar cap. This downwelling opposes the wave-induced upward motion described above. With extreme wave dissipation, it completely overwhelms the upwelling tendency and drives the spectacular warming of the polar stratosphere characterized by an SSW.

From this perspective, formalized in the "Transformed Eulerian Mean" representation of atmospheric dynamics (Andrews & McIntyre, 1976; Edmon et al., 1980), it is the residual (∼Lagrangian) downwelling that gives rise to warming of the polar cap when planetary waves dissipate. Neglecting diabatic heating during the onset of the warming, this can be written as in equation 2:

$$\frac{\partial\overline{\theta}}{\partial t} \approx -\overline{\omega}\frac{\partial\overline{\theta}}{\partial p} - \frac{\frac{\partial}{\partial\varphi}(\cos\varphi\overline{v'\theta'})}{a\cos\varphi} = -\overline{\omega}\frac{\partial\overline{\theta}}{\partial p} + \overline{\omega}_r\frac{\partial\overline{\theta}}{\partial p} = -\overline{\omega}^*\frac{\partial\overline{\theta}}{\partial p}, \tag{2}$$

where $\overline{\omega}^* \equiv \overline{\omega} + \frac{\frac{\partial}{\partial\varphi}(\cos\varphi\overline{v'\theta'})}{(a\cos\varphi)\frac{\partial\overline{\theta}}{\partial p}}$ is a modified vertical velocity that incorporates the effect of reversible wave-induced vertical motion and therefore corresponds to the net, residual vertical motion that gives rise to adiabatic warming (residual downwelling) or cooling (residual upwelling). Full temperature tendency needs to also take into account diabatic (radiative) heating.

Planetary wave dissipation gives rise to polar cap warming. This warming can at times be explosive, resulting in SSWs even if the waves themselves remain linear, due to the nonlinear nature of the wave-mean flow coupling (e.g., Geisler, 1974; Holton & Mass, 1976; Plumb, 1981). However, the vortex may be displaced from the pole or split in two, clearly violating the assumption of waves propagating on a zonal mean flow. The wave-induced deceleration of the vortex and the associated polar cap warming are at extreme levels; exactly how such extreme interactions between the waves and mean flow get triggered and unfold to the point of complete breakdown of the vortex is still not fully understood.

The wave breaking associated with a specific SSW is shown in Figure 7, illustrated with maps of potential vorticity (PV) on isentropic surfaces. Potential vorticity is defined by

$$PV = -g\frac{\partial\theta}{\partial p}(\zeta_\theta + f), \tag{3}$$

where g is gravity, θ is potential temperature, p is pressure, ζ_θ is relative vorticity perpendicular to an isentropic surface, and f is the Coriolis parameter. PV combines the conservation of mass and angular momentum. It is thus materially conserved in the absence of diabatic processes, and hence provides an effective diagnostic tool on the time scales associated with SSWs. Maps of PV on isentropic surfaces, as in Figure 7, show the breaking of planetary-scale Rossby waves in the "surf zone" (McIntyre & Palmer, 1983, 1984). As winter progresses, wave breaking in the surf zone sharpens the edge of the vortex, and if the wave breaking persists, the vortex can be displaced from the pole or even split in two. This can be viewed on horizontal maps of PV, or simply by measuring the size of the polar vortex in terms of PV (e.g. Butchart & Remsberg, 1986; Baldwin & Holton, 1988).

Two different perspectives exist in the literature regarding the role of the troposphere in initiating wave breaking events in the stratosphere (see section 4.2 below). Early work focused on the role of anomalous wave fluxes from the troposphere that drive the SSW, i.e., provide sufficient additional wave drag in the stratosphere to destroy the vortex, especially if it accumulates over a sufficiently long period of time. A second view holds that, given a wave field provided by the troposphere—which does not need to be anomalously strong—the stratospheric polar vortex may spontaneously feed back onto the wave field such that both get mutually amplified, reminiscent of resonance phenomena (e.g., Plumb, 1981).

Regardless of the perspective on the triggering mechanisms of SSWs, once the primary circulation breaks down and easterlies ensue, vertical propagation of stationary Rossby waves is inhibited. (Stationary wave can only exist if there are mean westerlies to offset their intrinsic easterly propagation.) The resulting "critical line" drives an accumulation of wave dissipation just below it, associated with more easterly acceleration and rapid lowering of the critical line (Matsuno, 1971). The corresponding downward progression of easterly zonal wind anomalies is mechanistically similar to the QBO (Plumb & Semeniuk, 2003), but acts on a much faster timescale, on the order of days, not years.

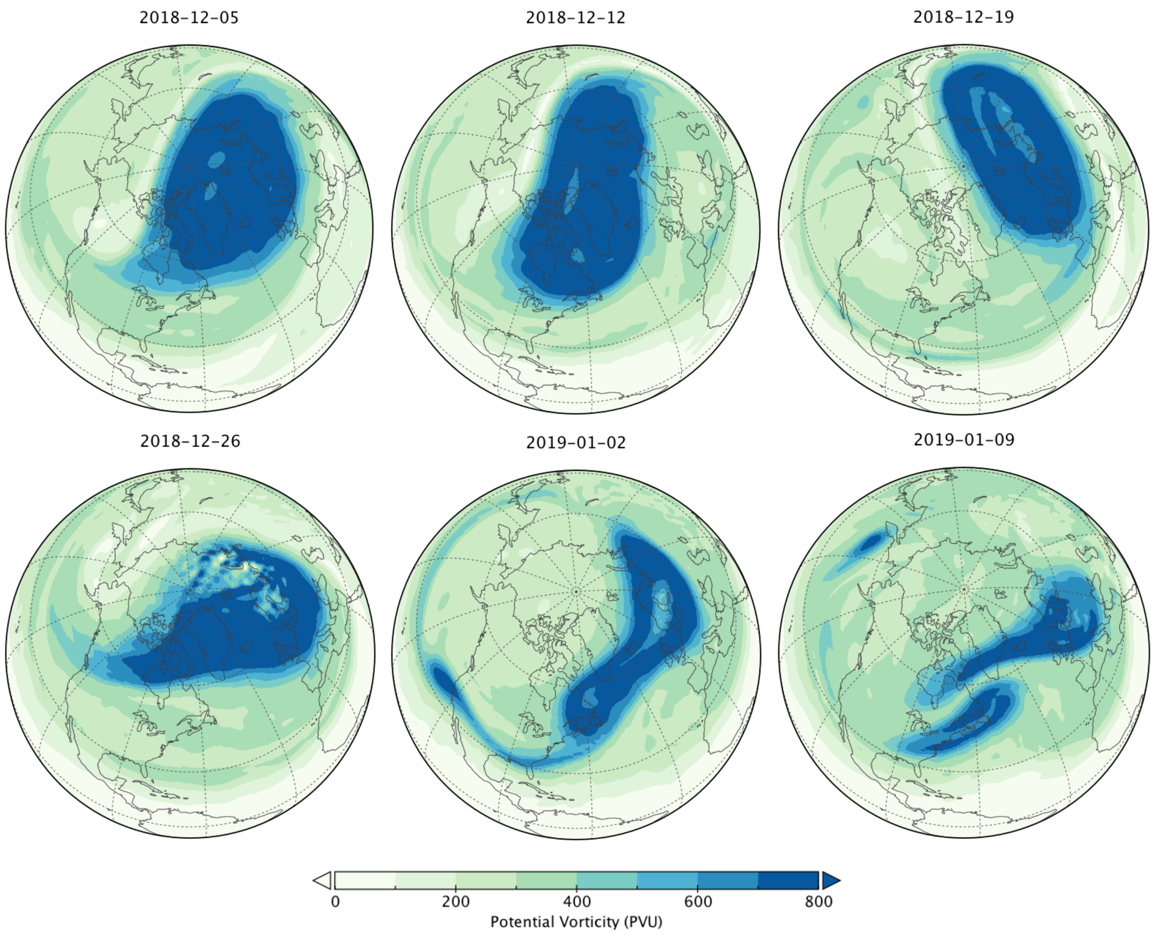

Figure 7. Illustration of the evolution of the polar vortex during an SSW in the winter 2018/19. Panels show PV on the 850K isentropic surface on six dates, showing a sequence illustrating a displacement of the vortex off the pole with concomitant stripping away of vortex filaments into the surf zone. Once the vortex is fully displaced off the pole (bottom middle) it then further splits into two smaller vortices (bottom right). From Baldwin, Birner, Brasseur, et al. (2019) ©American Meteorological Society. Used with permission.

4.2 Bottom up or top down: An evolving understanding on the mechanism(s) driving SSWs

A "bottom up" perspective, focused on the role of enhanced tropospheric wave forcing, is inherent in Matsuno's seminal work on showing that SSWs are dynamically forced. Matsuno (1971) prescribed a switch-on planetary wave 2 forcing at the lower boundary (approximately the tropopause) of a general circulation model. The model produced a strong split SSW in response to this pulse from below.

Matsuno's work suggests two key criteria for forcing an SSW. (1) SSWs only happen with sufficiently strong planetary wave forcing from the troposphere, and (2) SSWs require a pulse of anomalously strong wave forcing from the troposphere to initiate. Support for the first criterion includes the simple observation that warming events are much more prevalent in the Northern versus Southern Hemisphere. Additional support for a necessary minimum amount of wave forcing from the troposphere was established in a conceptual model developed by Holton and Mass (1976), who sought to distill an SSW down to its most basic elements.

The Holton and Mass model consists of a single planetary wave of constant amplitude, prescribed as input forcing to the stratosphere at its lower boundary. The mean flow (i.e, the vortex) exists either in a strong state with weak wave amplitudes (corresponding to weak wave-mean flow interaction), or a weak state with strong wave amplitudes (corresponding to strong wave-mean flow interaction similar to the dynamics involved in SSWs). More recently, idealized GCM studies have found a sharp increase in SSW frequency as planetary scale zonal asymmetries in the underlying flow are increased, either by topography (e.g., Taguchi and Yoden (2002); Gerber and Polvani (2009)) or thermal perturbations (Lindgren et al., 2018), though both topography and land-sea contrast may need to be present if represented in a realistic manner (Garfinkel, White, et al., 2020).

The second criterion in the Matsuno model—that SSWs are driven by an exceptional pulse of wave activity from the troposphere—is supported by the fact that SSWs are often preceded by blocking events, which amplify the tropospheric wave activity (e.g. Quiroz, 1986; Martius et al., 2009). This has led researchers to look for tropospheric precursor events that potentially give rise to additional planetary wave fluxes entering the stratosphere (e.g. Garfinkel et al., 2010; Cohen & Jones, 2011; Sun et al., 2012).

Palmer (1981) suggested that the stratospheric vortex may need to be "pre-conditioned" to accept a pulse of wave activity, based on observations of the 1979 event, a topic further explored by McIntyre (1982). Various studies have suggested that the strength and size of the vortex play a critical role in allowing wave activity to penetrate deep into the stratosphere (Limpasuvan et al., 2004; Nishii et al., 2009; Kuttippurath & Nikulin, 2012; Albers & Birner, 2014; Jucker & Reichler, 2018).

Newman et al. (2001) and Polvani and Waugh (2004) pointed out that a single precursor event will likely not cause sufficient deceleration of the stratospheric polar vortex; rather it is the accumulated wave forcing over 40-60 days that needs to be anomalously strong to cause enough deceleration to reverse the zonal mean flow around the polar cap. Sjoberg and Birner (2012) further pointed out that sustained forcing that lasts for at least 10 days, but does not need to be anomalously strong, is crucial for forcing SSWs. Processes that can lead to such a sustained increase in wave forcing from the troposphere are discussed in Section 5.

Preconditioning suggests that the state of the stratospheric vortex impacts its receptivity to accept waves from the troposphere. The "top down" perspective takes this view to the extreme, supposing that that fluctuations in tropospheric wave forcing do not play an important role at all. Rather, as long as the background wave fluxes entering the stratosphere are strong enough (such as provided by the climatological conditions in Northern Hemisphere winter) the stratosphere is capable of generating SSWs on its own.

The top down perspective has often been framed in the context of resonant growth of wave disturbances (e.g. Clark, 1974; Tung & Lindzen, 1979b). In a particularly insightful incarnation of this mechanism, the wave-mean flow interaction causes the vortex to tune itself toward its resonant excitation point (Plumb, 1981; Matthewman & Esler, 2011; Scott, 2016). Support for this perspective comes from idealized numerical model experiments that show that the stratosphere is capable of controlling the upward wave activity flux near the tropopause (Scott & Polvani, 2004, 2006; Hitchcock & Haynes, 2016) and that stratospheric perturbations can trigger SSWs even when the tropospheric wave activity is held fixed (Sjoberg & Birner, 2014; de la Cámara et al., 2017).

Preconditioning of the polar vortex, i.e., wave driving that brings it to the critical state, would clearly play a key role in this mechanism, suggesting that SSWs could potentially be predicted in advance, even in the limit where they are entirely controlled by the state of the stratospheric vortex.

The bottom up and top down SSW mechanisms are associated with a different expected lag-lead relationship in upward wave energy propagation (i.e., the Eliassen-Palm flux) between the tropospheric source and stratospheric sink. Events forced by tropospheric waves will be preceded by a build up of wave activity over time, while self-tuned resonant SSWs would be characterised by nearly instantaneous wave amplification throughout an extended deep layer, and no lag between troposphere/tropopause and stratosphere.

In this context it is important to note that fluctuations in the upward wave flux at 100 hPa are not generally representative of fluctuations in the troposphere below (Polvani & Waugh, 2004; Jucker, 2016; de la Cámara et al., 2017). The typical tropopause pressure over the extratropical atmosphere during winter is around 300 hPa, as shown in Figures 2 and 3. That is, wave flux events at 100 hPa can generally not be interpreted as tropospheric precursor signals because $\frac{2}{3}$ of stratospheric mass is below the height of the 100-hPa surface. Nevertheless, enhancements of upward wave fluxes from the troposphere at sufficiently long time scales (e.g., associated with climate variability extending over winter) tend to cause enhanced wave flux across 100 hPa into the polar vortex, which increases the likelihood for SSWs (as discussed in Section 5).

Evidence supporting both the bottom up and top down pathways has been observed, but it has become clear that the second criterion suggested by the Matsuno (1971) model—that the troposphere must drive an SSW with a pulse of enhanced wave activity—is not necessary. Birner and Albers (2017) found that only $\frac{1}{3}$ of SSWs can be traced back to a pulse of extreme tropospheric wave fluxes. Roughly $\frac{2}{3}$ of observed SSWs are more consistent with the top-down category or do not fit into either prototype (i.e., tropospheric wave fluxes are anomalously strong but not extreme). Similar ratios have been observed in modeling studies by White et al. (2019) and de la Cámara et al. (2019).

It also appears that the mechanism may vary with the type of warming. While Matsuno (1971) prescribed a wave 2 disturbance, it appears that wave 1 (displacement) events tend to be associated with the slow build up of wave activity, better matching the bottom-up paradigm, although resonant behavior has also been suggested for displacement events (Esler & Matthewman, 2011). Split, or wave 2, events are more instantaneous in nature (Albers & Birner, 2014; Watt-Meyer & Kushner, 2015), more closely matching the top-down paradigm.

5 External influences on SSWs

Because there have only been around 40 observed SSWs between 1958 and 2019, it is challenging to quantify and/or establish statistically robust changes in frequency of SSWs from external influences, especially if the observations show a subtle effect. Despite this difficulty, a range of external influences have been connected to SSWs, including the Quasi-Biennial Oscillation (QBO), ENSO, the 11-year solar cycle, the Madden-Julian Oscillation, and snow cover. Confidence in the robustness of such relationships is increased if there is a well described physical mechanism that is expected to produce the observed effect, for example through changes in the propagation and breaking of Rossby waves in the stratosphere or the generation of planetary Rossby waves in the troposphere. Similarly, confirmation of observed relationships in modelling studies also increases confidence that they are robust. Even more challenging is establishing relationships in the observations whereby two or more external influences act in concert (Salminen et al., 2020), a topic we return to in Section 10.

It has been recognized for 40 years that the stratospheric polar vortex is weaker during the easterly QBO winter than during the westerly QBO winter, known as the Holton-Tan relationship (Holton & Tan, 1980; Anstey & Shepherd, 2014). The frequency of occurrence of SSWs during each QBO phase is shown in Table 1 based on NCEP-NCAR reanalysis. SSW likelihood is higher during easterly QBO winters than during westerly QBO phase (0.9/yr vs 0.5yr), consistent with early studies (Labitzke, 1982; Naito et al., 2003). Models also simulate a weakened vortex and more SSWs during easterly QBO as compared to westerly QBO, though the magnitude of the effect tends to be somewhat weaker than that observed (e.g. Anstey and Shepherd (2014); Garfinkel et al. (2018); Rao, Garfinkel, and White (2020a)). At least four different (likely complementary) mechanisms have been proposed linking the QBO to vortex variability, and the relative importance of these mechanisms is still unclear (Holton & Tan, 1980; Garfinkel, Shaw, et al., 2012; Watson & Gray, 2014; White et al., 2015; Silverman et al., 2018).

Table 1. Revisiting the QBO-SSW relationship during 1958–2019, based on the dates computed by Charlton and Polvani (2007) for 1958–2001 and by Rao, Ren, et al. (2019) for 2002–2018 with NCEP/NCAR reanalysis data. The first column is the QBO phase. The second column is the corresponding composite size total winter (Nov–Feb mean) size. The third column is the number of SSWs events for that composite size, and the fourth column is the SSW frequency (units: events times per year). EQBO=easterly phase of QBO; WQBO=westerly phase of QBO. The unit of QBO50 is ms^{-1}. Significance for this and following tables is computed based on the following Monte Carlo test: SSWs are randomly assigned to winters while maintaining the overall SSW frequency, and then the frequency of SSWs for each phase is computed. This procedure is repeated 10,000 times, to which the observed SSW frequency is compared. If the observed frequency is less than 2.5%(5%) of the random samples, or greater than 97.5%(95%), then we can reject a null hypothesis of no relationship at the 95% or 90% confidence levels, which are indicated on the table with bold and a star. Reprinted with permission from Rao, Garfinkel, et al. (2019).

QBO-SSW relationship

QBO phase	Winter no.	SSW no.	SSW frequency
EQBO (QBO50≥5)	20	18	**0.9***
WQBO (QBO50≤-5)	36	18	0.5
Neutral (|QBO50| <5)	6	1	0.17*
Total	62	37	0.60

The relationship between the northern winter stratospheric polar vortex and ENSO, including a full discussion of possible mechanisms, has recently been reviewed in this journal (Domeisen et al., 2019). The statistical relationship between ENSO and SSWs in NCEP-NCAR reanalysis data is revisited and shown in Table 2. The likelihood of SSW events increases in both El Niño and La Niña relative to the ENSO neutral state (Butler & Polvani, 2011; Garfinkel, Butler, et al., 2012), and while the modulation of SSWs is not statistically significant, the effect of El Niño on the seasonal mean stratospheric vortex is significant and of similar strength to that of EQBO (Camp & Tung, 2007; Garfinkel & Hartmann, 2007; Domeisen et al., 2019). Increases in SSW frequency during La Niña in the observed record are not thought to be forced and, instead, are associated with internal variability or confounding climate forcings (Weinberger et al., 2019; Domeisen et al., 2019), particularly in the case of weak La Niña events (Iza et al., 2016). High-top models show a response to opposite phases of ENSO that, if anything, is generally stronger than that observed (Taguchi & Hartmann, 2006; Garfinkel, Butler, et al., 2012; Garfinkel et al., 2019) and that can be used for improving predictability over Europe (Domeisen et al., 2015).

Table 2. As in Table 1 but for the ENSO-SSW relationship during 1958–2019. The unit of Niño34 is °C. Reprinted with permission from Rao, Garfinkel, et al. (2019).

ENSO-SSW relationship

ENSO phase	Winter no.	SSW no.	SSW frequency
El Niño (Niño34≥0.5)	20	13	0.65
moderate El Niño (0.5≤Niño34≤2)	17	13	0.77
La Niña (Niño34≤-0.5)	23	15	0.65
Neutral (|Niño34| <0.5)	19	9	0.47
Total	62	37	0.60

The solar cycle may affect the stratospheric polar vortex, and earlier work reported that mid-winter SSWs tend to occur during solar minimum QBO easterly phase (i.e. classical Holton-Tan effect) *and* during solar maximum and QBO westerly phase (Labitzke, 1987; Gray et al., 2004; Labitzke et al., 2006; Gray et al., 2010). Updating these relationship for data through 2019, however, suggests that although this relationship holds, it is modest. During solar maximum/westerly QBO years, midwinter SSW frequency is 0.44/yr (Table 3). During solar minimum/easterly QBO years the frequency of midwinter SSW is increased somewhat (0.67/yr), and this increase is statistically significant at the 90% confidence level. Observations alone are not sufficient to verify that a solar-QBO-SSW relationship is robust. There is a wide spread in the ability of models to simulate an influence of solar variability on the polar stratosphere (Mitchell et al., 2015), partly related to their ability to capture the effects of solar variability on the tropical stratosphere.

October Eurasian snow cover has also been linked to subsequent variability of the stratospheric vortex, with more extensive snow leading to a weakened vortex (Cohen et al., 2007; Henderson et al., 2018) via a strengthened Ural ridge and subsequent constructive interference with climatological stationary waves (Garfinkel et al., 2010; Cohen et al., 2014). There is a slight increase in SSW frequency for winters following enhanced snow cover (Table 4), but this effect is not statistically significant. Results are similar if only early winter SSW events are considered (not shown). The relationship between October Eurasian snow and the monthly mean vortex strength is non-stationary: it peaked over the period 1991–2010 and has since collapsed (Henderson et al., 2018). Most free-running models tend to not capture the link between snow cover and a weakened vortex (Furtado et al., 2015), though there are some exceptions (Garfinkel, Schwartz, et al., 2020), and models forced with idealized snow perturbations do capture this effect to some extent (Henderson et al., 2018).

The Madden Julian Oscillation (MJO) has also been shown to influence the timing of SSW events: of the 23 events considered by Schwartz and Garfinkel (2017) and

Table 3. As in Table 1 but for the solar-SSW relationship during 1958–2019. Max=solar maximum; Min=solar minimum. The number in parentheses is SSWs during January–February (JF). Reprinted with permission from Rao, Garfinkel, et al. (2019)

solar-SSW relationship

solar phase	QBO phase	Winter no.	SSW no. (JF SSW no.)	SSW frequency
Max	EQBO	11	11 (6)	**1.0*** (0.55)
	WQBO	16	8 (7)	0.5* (0.44)
	Neutral	3	1 (0)	0.33 (0.0)
	SUM	30	20 (13)	0.67 (0.43)
Min	EQBO	9	7 (6)	0.78 (0.67*)
	WQBO	20	10 (6)	0.5 (0.3)
	Neutral	3	0.0 (0.0)	0.0 (0.0)
	SUM	32	17 (12)	0.53 (0.38)
Total		62	37(25)	0.60 (0.40)

Table 4. As in Table 1 but for the October snow cover–SSW relationship during 1968–2019. Snow cover data is sourced from `https://climate.rutgers.edu/snowcover/table_area.php?ui_set=1`, with "enhanced" and "reduced" defined as snow cover anomalies exceeding 0.5 standard deviations. Snow data is missing for October 1969.

snow-SSW relationship

Snow-coverage	Winter no.	SSW no.	SSW frequency
enhanced	14	9	0.64
reduced	17	9	0.53
Neutral	20	12	0.6
No data	1	1	–
Total	52	31	0.59

the two events since, more than half (13 of 25) were preceded by MJO phases with enhanced convection in the tropical West Pacific (6 or 7 as characterized by Wheeler and Hendon (2004)). The climatological occurrence of these phases is $\sim 18\%$ (updated from Schwartz and Garfinkel (2017)), and hence this represents an increased probability of an SSW occurring. The mechanism whereby convection in the West Pacific weakens the vortex is similar to the mechanism for the influence of ENSO and snow cover: the transient extratropical response associated with the MJO constructively interferes with the climatological planetary wave pattern (Garfinkel et al., 2014). Models simulate an effect similar to that observed (Kang & Tziperman, 2017; Schwartz & Garfinkel, 2020), and SSW probabilistic predictability is enhanced when the MJO is strong (Garfinkel & Schwartz, 2017).

6 How well can SSWs be forecast?

Prediction system models (particularly systems with high tops) are typically able to capture the onset of SSW events more than five days before the event (Tripathi et al., 2015). Fewer than 50% of ensemble members predict the SSW date at lead times of two weeks (Domeisen, Butler, et al., 2020a), though individual events can exhibit longer predictability (Rao, Garfinkel, et al., 2019). There is, however, significant event-to-event variability in predictability for the same modeling systems as demonstrated for European Centre for Medium-Range Weather Forecasts (ECMWF) forecasts by Karpechko (2018). Much of this variation in predictive skill is likely linked to the limitations in predictive skill of key tropospheric drivers of the SSW process. An interesting recent example of this is the limited skill that models had in forecasting the February 2018 SSW, which has been linked to the inability of some models to capture high pressure over the Urals (Karpechko et al., 2018) and related anticyclonic wave breaking in the North Atlantic sector (Lee et al., 2019).

There can also be substantial variation in forecasting skill for different modeling systems, both in forecasting individual SSW events (Tripathi et al., 2016; Taguchi, 2018; Rao, Garfinkel, et al., 2019; Taguchi, 2020) and in the mean aggregate skill (Domeisen, Butler, et al., 2020a). The impact of long standing stratospheric biases and how these influence the skill of different modeling systems, for example cold biases in the lowermost extratropical stratosphere, remains an area of active research interest. As noted by Noguchi et al. (2016), predictions of SSW events are also sensitive to the background stratospheric state prior to the SSW.

Nonetheless, our ability to predict SSW events into the medium-range (lead times of three to ten days) and sub-seasonal timescales and to capture changes to the seasonal likelihood of SSW events has increased substantially as forecasting systems have increased their model top, stratospheric vertical resolution, and increased the sophistication of key stratospheric physical processes like gravity wave drag (Marshall & Scaife, 2010; Domeisen, Butler, et al., 2020a).

7 Effects on weather and climate

7.1 Dynamical theories for downward influence

There are several theoretical reasons to expect that SSWs (and stratospheric variability in general) should affect surface weather. The main categories of mechanisms are:

1. The remote effects of wave driving (EP-flux divergence) in the stratosphere (Song & Robinson, 2004; Thompson et al., 2006). The downward effect through the induced meridional circulation has been termed “downward control” (Haynes et al., 1991).
2. Planetary wave absorption and reflection (Perlwitz & Harnik, 2003; Shaw et al., 2010; Kodera et al., 2016)
3. Direct effects on baroclinicity and baroclinic eddies (Smy & Scott, 2009).
4. The remote effects of stratospheric PV anomalies (Hartley et al., 1998; Black, 2002; Ambaum & Hoskins, 2002). This category includes studies such as White et al. (2020), in which deep polar temperature anomalies are prescribed, because they are equivalent to PV anomalies (Baldwin, Birner, & Ayarzagüena, 2019).

All of these mechanisms may contribute to tropospheric effects from SSWs. If we are trying to explain the surface pressure anomalies following SSWs (Figure 3), or shifts in the NAM index (e.g. Baldwin & Dunkerton, 2001), it is clear that the main observed feature is that surface effects are roughly proportional to the anomalous strength of the polar vortex in the lower stratosphere (as measured by temperature, wind, or the NAM index). In a model study, White et al. (2020) found a robust linear relationship between the strength of the lower-stratospheric warming and the tropospheric response, with the linearity also extending to sudden stratospheric cooling events. A second observation is that surface pressure anomalies are largest near the North Pole. Stratospheric wave driving (EP-flux divergence) is not, in general, proportional to the anomalous strength of the polar vortex. It therefore cannot be the primary explanation for the tropospheric response, as seen in Figure 3b. When Thompson et al. (2006) examined the connection between stratospheric wave driving and near-surface wind changes, they found that surface effects were too small, and there was no indication of a NAM-like pressure pattern, as documented in Baldwin and Dunkerton (2001).

Planetary wave absorption and reflection primarily affects tropospheric wave fields, but is not generally proportional to the anomalous strength of the stratospheric polar vortex. A small change in wind induced by an SSW can be amplified by eddy propagation of transient waves produced in the troposphere. However, this mechanism does not predict the observed NAM variations or surface amplification. Direct effects on baroclinic eddies may be important because they are expected to be proportional to the anomalous strength of the stratospheric polar vortex, and in addition momentum fluxes from transient eddies in midlatitudes drive annular modes.

The remote effects of stratospheric PV anomalies would be expected to look similar to the NAM pressure pattern, and the effects are proportional to the anomalous strength of the stratospheric polar vortex (Black, 2002). However, as pointed out by Ambaum and Hoskins (2002), the remote effects of stratospheric PV anomalies are expected theoretically to decrease through the troposphere with an e-folding depth of $\sim$5 km. PV theory explains very well the atmospheric response down to the tropopause, but it does not explain the enhanced surface pressure response in Figure 3b. Surface pressure anomalies should be only $\sim$20% of those at the tropopause. The surface pressure response is an order of magnitude larger than PV theory indicates. This "surface amplification" is well reproduced in prediction models (Domeisen, Butler, et al., 2020b).

The remote effects of stratospheric PV anomalies, combined with a mechanism to amplify the surface pressure signal, could explain the main observed SSW effects. It is clear from the observations that following an SSW, tropospheric processes act to move mass into the polar cap, raising Arctic surface pressure. The low-level build-up of mass over the polar cap cannot come from the stratosphere because the surface pressure anomalies are larger than seen at any stratospheric level. The mechanisms for this movement of mass have not been fully explained. Both synoptic-scale and planetary-scale waves are found to contribute to the tropospheric response following SSW events (Simpson et al., 2009; Domeisen et al., 2013; Garfinkel et al., 2013; Hitchcock & Simpson, 2014, 2016; K. L. Smith & Scott, 2016). Baldwin, Birner, and Ayarzagüena (2019) hypothesized that the low-level polar cap temperature anomalies (as seen in Figures 3 and 8) are responsible for the movement of mass through the mechanism of radiative cooling-induced anticyclogenesis (Wexler, 1937; Curry, 1987), also see modeling results in Hoskins et al. (1985)). If the Arctic lower troposphere cools, the air mass contracts and pulls in additional mass from lower latitudes, raising the average surface pressure over the Arctic, as is observed.

7.2 Observed and modeled downward impact for both hemispheres

Both hemispheres show significant tropospheric effects following stratospheric extreme events. In particular, SSW events tend to be followed by a negative signature of the NAM in the NH (Baldwin & Dunkerton, 1999, 2001) and the SAM in the SH. In the NH, the strongest response to SSW events is observed in the North Atlantic basin (Figure 8), where the response to SSW events often projects onto the negative phase of the North Atlantic Oscillation (NAO) (Charlton-Perez et al., 2018; Domeisen, 2019). The negative phase of the NAO is associated with cold air outbreaks over Northern Eurasia and the eastern United States (Kolstad et al., 2010; Lehtonen & Karpechko, 2016; King et al., 2019) as well as over the Barents and Norwegian Seas (Afargan-Gerstman et al., 2020), and wet anomalies over Southern Europe (Ayarzagüena et al., 2018) due to the southward shift and persistence of the North Atlantic eddy-driven jet (Maycock et al., 2020) and the storm track (Afargan-Gerstman & Domeisen, 2020). Further anomalies include positive temperature anomalies over Greenland and eastern Canada, and subtropical Africa and the Middle East. Anomalous tropospheric blocking is often observed after SSW events (Labitzke, 1965; Vial et al., 2013).

In the SH, the winter stratospheric variability is weaker compared to the NH due to less wave driving (Plumb, 1989), meaning far fewer SSWs have been observed (Sec-

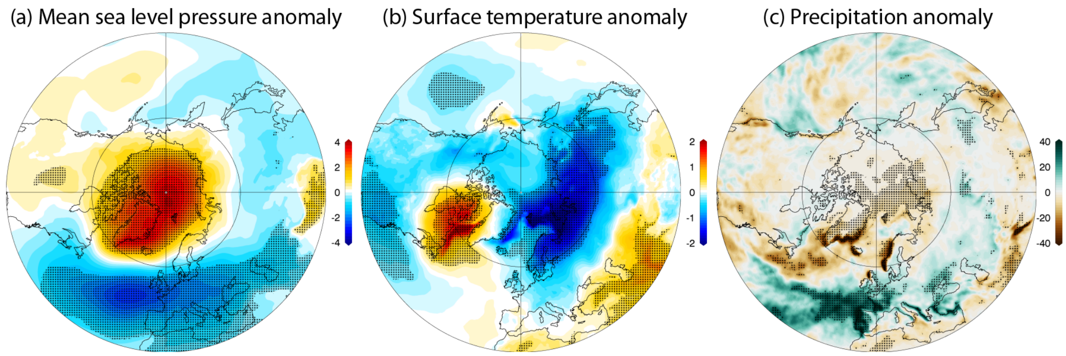

Figure 8. Composites of the 60 days following historical SSWs in the JRA-55 reanalysis for (a) mean sea level pressure anomalies (hPa), (b) surface temperature anomalies (K), and (c) precipitation anomalies (mm). Stippling indicates regions significantly different from climatology at the 95% level. [Figure from Butler et al. (2017), ©Copernicus. Used with permission.]

tion 3). Nonetheless, anomalous weakenings of the SH polar vortex, tied to shifts in the seasonal evolution of the vortex, are associated with a negative SAM pattern and significant surface impacts over Antarctica, Australia, New Zealand, and South America (Lim et al., 2018, 2019). Following the only major SSW that occurred in September 2002, the SAM stayed persistently negative from September to November (Thompson et al., 2005), with warmer and drier conditions over southeast Australia, and colder and wetter conditions over New Zealand and southern Chile (Gillett et al., 2006). Similar impacts were seen following the extreme polar vortex weakening in 2019 (Hendon et al., 2019).

Furthermore, there are significant effects of SSW events in the tropics, which contribute to a downward pathway to the troposphere through tropical convective activity. In particular, the induced meridional circulation associated with the anomalous wave driving leads to anomalous tropical upwelling and anomalous cooling in the tropical tropopause region (visible in Figure 2), modulating tropical convection (Kodera, 2006). The anomalous tropical upwelling may also lead to drying of the tropical tropopause layer (Eguchi & Kodera, 2010; Evan et al., 2015).

The downward response to SSWs tends to be well reproduced in model studies. Models ranging from idealized dynamical cores to complex coupled model systems show a tropospheric response, though its persistence is often overestimated, especially in simplified models (Gerber, Polvani, & Ancukiewicz, 2008; Gerber, Voronin, & Polvani, 2008). Additionally, idealized model experiments confirm the direction of causality, i.e., stratospheric anomalies have a downward impact even if the troposphere is perturbed and does not retain memory from potential tropospheric precursors (Gerber et al., 2009), or if a SSW is imposed without any tropospheric precursors (White et al., 2020). This stratospheric downward effect is known to contribute to surface predictability (Sigmond et al., 2013; Scaife et al., 2016; Domeisen, Butler, et al., 2020b).

While on average the "downward impact" of SSWs is robust, not all SSWs appear to couple down to the surface. Most studies agree that about two thirds (Charlton-Perez et al., 2018; Domeisen, 2019; White et al., 2019) of SSW events are characterized as having a visible downward impact (e.g., persistent negative phase of the NAM or NAO in the lower troposphere and/or the lower stratosphere, (e.g Karpechko et al., 2017; Domeisen, 2019)). One factor affecting the appearance of downward impact is the tropospheric NAM index prior to and at the time of the SSW. If the NAM is already negative, there will be a vertical connection to the negative stratospheric NAM. On the other hand, if the tropospheric NAM is strongly positive prior to the SSW, the appearance of vertical coupling is less likely, at least initially. The same is true for the NAO: if a negative NAO is present at the time of the SSW, the downward coupling is instantaneous but short-lived, while otherwise the negative NAO often appears after the SSW event (Domeisen, Grams, & Papritz, 2020). The stratosphere is one of several factors influencing the NAM, with most NAM variability being generated within the troposphere (and from surface interactions). The stratospheric influence becomes clear, only statistically, in regressions or in composites of many SSWs. Specifically, the concept of surface amplification of the polar pressure signal (Figure 3) will not be apparent during every SSW, but it becomes clear when averaging over many events. This is because the troposphere is highly variable, and the stratosphere represents a modest influence that is active during the cold season.

However, it is still not possible to predict which SSW events will have a visible downward impact. Knowing in advance or at the time of an SSW event the magnitude of its downward impact could have a significant benefit for medium-range to sub-seasonal predictions. Several studies have investigated possible stratospheric causes for the different surface impacts of SSW events:

1. The type of wave propagation during SSW events has been characterized as either absorbing or reflecting (Kodera et al., 2016) based on wave propagation during the recovery phase of the polar vortex, leading to different surface impacts. Absorbing type events are found to induce the canonical negative NAO response, while reflecting events are associated with wave reflection and blocking in the Pacific basin.
2. The type of SSW in terms of split or displacement had been suggested to produce different surface responses (Nakagawa & Yamazaki, 2006; Mitchell et al., 2013; Seviour et al., 2016). However, some other studies could not find significant difference in the annular mode response in long model simulations (Maycock & Hitchcock, 2015; White et al., 2019).
3. The duration and strength of the signal in the lower stratosphere has been suggested to contribute to the duration and strength of the surface impact (Karpechko et al., 2017; Runde et al., 2016; Rao, Garfinkel, & White, 2020b). In particular, weak vortex events that are classified as PJO events have a stronger and more persistent coupling to the troposphere than those events that lack PJO characteristics (Hitchcock et al., 2013).

Further studies have investigated tropospheric sources for different responses to stratospheric forcing, in terms of jet stream location (Garfinkel et al., 2013; Chan & Plumb, 2009), North Atlantic weather regimes (Domeisen, Grams, & Papritz, 2020), Eastern Pacific precursors (Afargan-Gerstman & Domeisen, 2020), and the characteristics of tropospheric precursors to SSW events, in particular Ural blocking (White et al., 2019). The response is also likely dependent on concurrent tropospheric climate patterns such as ENSO (Polvani et al., 2017; Oehrlein et al., 2019) and the MJO (Schwartz & Garfinkel, 2017; Green & Furtado, 2019).

8 Effects on the atmosphere above the stratosphere

The effects of SSW events are now recognized to extend well above the stratosphere, and can significantly alter the chemistry and dynamics of the mesosphere, thermosphere, and ionosphere. They are thus a significant component of the short-term variability in the upper atmosphere. This section briefly reviews the major impacts of SSWs on the upper stratosphere-mesosphere, thermosphere, and ionosphere. More detailed reviews focused solely on the upper atmosphere can be found in Chandran et al. (2014) and Chau et al. (2012).

8.1 Impacts on the Upper Stratosphere-Mesosphere

The stratopause often reforms at high altitudes (∼70–80 km) after SSW events, followed by a gradual descent to its climatological altitude of ∼50–55 km over the ensuing 2–3 weeks (Manney et al., 2008; Siskind et al., 2010). Such elevated stratopause events occur in roughly one-third of Northern Hemisphere winters (Chandran et al., 2013, 2014). Numerical simulations successfully reproduce elevated stratopause events, providing insight into the formation mechanisms. The elevated stratopause forms due to enhanced westward gravity wave forcing following SSW events, which leads to downwelling and adiabatic heating at high altitudes where the stratopause reforms (Chandran et al., 2013; Limpasuvan et al., 2016).

SSW events lead to dramatic changes in the mesosphere and lower thermosphere. This includes high latitude cooling, as well as a reversal of the zonal mean zonal winds from easterly to westerly (the opposite as in the stratosphere) (Labitzke, 1982; H. L. Liu & Roble, 2002; Hoffmann et al., 2007; Siskind et al., 2010; Limpasuvan et al., 2016). The mesosphere-lower thermosphere changes during SSWs are primarily due to changes in gravity wave drag. The weakening, and potential reversal, of the westerly stratospheric winds leads to more eastward propagating gravity waves reaching the mesosphere-lower thermosphere, where, upon breaking, they increase the eastward forcing at mesosphere-lower thermosphere altitudes. The enhanced eastward forcing leads to the reversal of the mesosphere-lower thermosphere winds, and also changes the high latitude residual circulation from downward to upward, resulting in adiabatic cooling of the mesosphere (H. L. Liu & Roble, 2002; Siskind et al., 2010; Limpasuvan et al., 2016). The altered stratosphere-mesosphere residual circulation during SSW events may also lead to a warming of the summer hemisphere mesosphere, and a decrease in the occurrence of polar mesospheric clouds (Karlsson et al., 2007, 2009; Körnich & Becker, 2010). Though Körnich and Becker (2010) originally explained the coupling between wintertime SSWs and mesospheric warmings in the summer hemisphere as due to altered wave forcing in the summer hemisphere, A. K. Smith et al. (2020) recently proposed that the inter-hemispheric coupling is due to changes in the stratosphere-mesosphere circulation, and not due to modified wave forcing in the summer hemisphere mesosphere. The mesosphere-lower thermosphere changes that occur during SSWs are only weakly correlated with the changes that occur in the stratosphere (e.g. A. K. Smith et al., 2020), and there is significant event-to-event variability (Zülicke & Becker, 2013; Zülicke et al., 2018). The lack of a direct linear correspondence between the stratosphere and mesosphere-lower thermosphere illustrates the complexity of the coupling processes.

The circulation changes in the upper stratosphere and mesosphere-lower thermosphere that are discussed above lead to notable changes in chemical transport, altering the distribution of chemical species in the stratosphere and mesosphere. Changes in chemistry are particularly notable following elevated stratopause events, when there is significantly enhanced downward transport in the lower mesosphere and upper stratosphere (e.g., Siskind et al., 2015). The enhanced downward transport leads to enhancements in NOx and CO in the stratosphere (Manney, Schwartz, et al., 2009; Randall et al., 2006, 2009). Observations of NOx during the winters of 2004-2009 are shown in Figure 9, clearly illustrating the enhanced downward transport of NOx during the winters of 2004, 2007, and 2009 during which major SSWs occurred. An increase in NOx is particularly relevant as it can lead to the loss of stratospheric ozone. Though enhanced descent of trace species is well observed, the descent in numerical models is typically too weak, leading to simulations with a deficit in NOx and CO in the stratosphere following SSW events (Funke et al., 2017). This is partly due to inadequate representation of the mesosphere-lower thermosphere dynamics (Meraner et al., 2016; Pedatella et al., 2018), though may also be due to insufficient source parameterizations (Randall et al., 2015; Pettit et al., 2019).

randall_figure_v3-eps-converted-to.pdf

Figure 9. Zonal average ACE-FTS NOx (color) in the NH from 1 January through 31 March of 2004-2009. The white contour indicates CO=2.0 ppmv. Measurement latitudes are shown in the top panel as black dots. From Randall et al. (2009).

.

The changes in stratosphere-mesosphere chemistry and zonal winds during SSWs influence solar and lunar atmospheric tides, which, in-turn, play a key role in coupling SSWs to variability in the ionosphere and thermosphere. The most notable changes are an enhancement in the migrating semidiurnal solar and lunar tides. The migrating semidiurnal solar tide is primarily generated by stratospheric ozone, and Goncharenko et al. (2012) proposed that it is enhanced during SSWs due to changes in stratospheric ozone. However, recent numerical experiments by Siddiqui et al. (2019) demonstrate that the migrating semi-diurnal solar tide in the lower thermosphere is primarily enhanced due to altered wave propagation, with ozone only being a minor (∼20-30%) contributor to the maximum enhancement. Though generally small, the migrating semidiurnal lunar tide is greatly enhanced during SSWs, and can obtain amplitudes equal to or larger than the migrating semidiurnal solar tide (e.g., Chau et al., 2015). The enhanced lunar tide is attributed to changes in the background zonal mean zonal winds, which shifts the Pekeris resonance mode of the atmosphere close to the frequency of the migrating semidiurnal lunar tide (Forbes & Zhang, 2012). The magnitude and timing of the semidiurnal lunar tide enhancements appear to be correlated with stratospheric variability (Zhang & Forbes, 2014; Chau et al., 2015), though, as discussed in Chau et al. (2015), there are events that do not follow the linear relationship.

8.2 Impacts on the ionosphere

The influence of SSWs on the ionosphere was first hypothesized several decades ago by Stening (1977) and Stening et al. (1996). However, it was not until Goncharenko and Zhang (2008) and Chau et al. (2009) that the impact of SSWs on the ionosphere was unequivocally demonstrated. Since these studies there has been considerable research into the role of SSWs on generating variability in the low-latitude and mid-latitude ionosphere.

Observations have revealed that the low-latitude ionosphere exhibits a consistent response to SSWs, with an increase in vertical plasma drifts and electron densities in the morning and a decrease in the afternoon (Figure 10). The morning enhancement and afternoon depletion gradually, over the course of several days, shifts towards later local times (e.g., Chau et al., 2009; Goncharenko, Chau, et al., 2010; Goncharenko, Coster, et al., 2010; Fejer et al., 2011). This behavior is primarily attributed to the enhancement of the solar and lunar migrating semidiurnal tides during SSWs, which influence the generation of electric fields via the E-region dynamo mechanism (Fang et al., 2012; Pedatella & Liu, 2013). The migrating semidiurnal lunar tide is thought to be especially important in producing the gradual shift of the ionospheric perturbations towards later local times. As demonstrated by Siddiqui et al. (2015), there is a linear relationship between the strength of the stratospheric disturbance and the magnitude of the semidiurnal lunar tide in the equatorial electrojet. Numerical modeling studies indicate that the influence of SSWs on the low-latitude ionosphere should be larger during solar minimum compared to solar maximum (Fang et al., 2014; Pedatella et al., 2012). Observations have, however, revealed that equally large responses can occur during solar maximum (Goncharenko et al., 2013), indicating that factors in the lower-middle atmosphere, such as the SSW strength and lifetime, may be equally as important as solar activity.

A number of studies have investigated the impact of SSWs on the low-latitude ionosphere in different longitudes. They have found that the characteristic features of the ionosphere variability during SSWs is broadly similar across longitudes (Anderson & Araujo-Pradere, 2010; Fejer et al., 2010; Siddiqui et al., 2017). There are, however, differences in the response at different longitudes. In particular, the response is strongest, and tends to occur earliest, over South America. The longitudinal differences are related to the effects of nonmigrating semidiurnal tides and the influence of Earths geomagnetic main field (Maute et al., 2015).

goncharenko_ionosphere.png

Figure 10. Observations of ionospheric behavior during the 2009 SSW event. (a) Mean total electron content (TEC) at 15 UT (morning sector, 10LT at 75°W). (b) Same as Figure 10a, except for at 21 UT (afternoon sector, 16 LT at 75°W). (c) TEC in the morning sector (15 UT) on January 27, 2009, during the SSW. (d) TEC in the afternoon sector (21 UT) on January 27, 2009. (e) Vertical drift observations by the Jicamarca incoherent scatter radar (12°S, 75°W) at 200-500 km altitude. The red line indicates observations on January 27, 2009, and the black line indicates the average behavior for winter and low solar activity. (f) Change in TEC at 75°W during the SSW as a function of local time and latitude. From Goncharenko, Chau, et al. (2010).

One of the reasons that the ionospheric variability during SSWs has attracted attention is that it potentially enables improved forecasting of ionosphere variability. Due to being primarily an externally forced system, the ionosphere and thermosphere are less sensitive to initial conditions compared to the troposphere-stratosphere (Siscoe & Solomon, 2006). This leads to skillful forecasts of the ionosphere being typically less than 24 h (Jee et al., 2007). If, however, the external drivers of ionosphere variability can be well-forecast, then the length of skillful ionosphere forecasts can be extended. The two external drivers of the ionosphere are solar activity and effects from the lower atmosphere. The relatively good predictability of SSWs means that they could enable enhanced ionosphere forecast skill by improved forecasting of the lower atmospheric driver of ionosphere variability. The ability to forecast the low-latitude ionosphere during the 2009 SSW was investigated by Wang et al. (2014) and Pedatella et al. (2018). Both studies found that ionospheric variability could be forecast $\sim$10 days in advance of the SSW, which is consistent with the ability to predict the occurrence of SSWs. SSWs may thus provide a pathway for improving forecasts of the ionosphere.

The effects of SSWs on the ionosphere extend to middle latitudes, and are, perhaps surprisingly, stronger in the SH. Fagundes et al. (2015) and Goncharenko et al. (2018) both observed notable daytime TEC enhancements in the SH middle latitude ionosphere. Goncharenko et al. (2018) also observed large decreases in nighttime ionosphere electron densities at middle latitudes. The mechanism generating variability in the middle latitude ionosphere is thought to be changes in the thermosphere neutral winds, and the greater response in the SH has been interpreted as being due to a larger amplitude semidiurnal lunar tide in the SH which propagates upwards into the thermosphere where it modulates the neutral winds (Pedatella & Maute, 2015).

Understanding the formation of small-scale irregularities in the ionosphere, often referred to as spread-F, equatorial plasma bubbles, or scintillation, is important owing to the disruptive impact of small-scale irregularities on communications and navigation (e.g., GPS) signals. Determining the role of SSWs on the formation of ionosphere irregularities is thus of considerable interest. Current observational evidence of the impact of SSWs on ionosphere irregularities is inconclusive, with some studies suggesting a suppression of irregularities (de Paula et al., 2015; Patra et al., 2014), and others an enhancement of irregularities (Stoneback et al., 2011). This is therefore an area that requires considerably more research.

8.3 Impacts on the thermosphere

The impact of SSWs on the thermosphere has received considerably less attention compared to the ionosphere. This is primarily due to the limited number of direct observations as well as generally smaller impacts of SSWs on the thermosphere. Nonetheless, investigations have revealed that there are clear impacts on the thermosphere temperature, density, and composition.

Numerical simulations by H. L. Liu and Roble (2002) first revealed that the effects of SSWs can extend into the lower thermosphere. They found that the lower thermosphere ($\sim$110-170 km) in the NH warms by $\sim$20-30 K during a SSW. Warming of the Northern Hemisphere lower thermosphere was confirmed observationally by Funke et al. (2010). Subsequent simulations by H. Liu et al. (2013) using the GAIA whole atmosphere model revealed that the zonal mean temperature changes globally, and throughout the thermosphere. In particular the GAIA simulations revealed upper thermosphere cooling in the tropics and Southern Hemisphere, and a global average cooling of $\sim$10K during the 2009 SSW. The global cooling of the thermosphere is largely attributed to the dissipation of enhanced semidiurnal solar and lunar tides during the SSW, which significantly alters the circulation of the lower thermosphere (H. Liu et al., 2014). The cooling of the thermosphere leads to a contraction of the thermosphere, and a reduction in the neutral density at a fixed altitude. Based on satellite orbital drag derived thermosphere densities, Yamazaki et al. (2015) investigated the thermosphere density response to SSW events. They found a 3-7% decrease in global mean thermosphere density at altitudes of 250-575 km.

The composition of the thermosphere is also impacted by SSWs, with model simulations and observations finding a $\sim$10% reduction in the ratio of atomic oxygen to molecular nitrogen ($[O]/[N_2]$) during SSW events (Pedatella et al., 2016; Oberheide et al., 2020). This reduction arises due to the enhancement of migrating semidiurnal solar and lunar tides during the SSW, and their influence on the mean meridional circulation. In particular, the dissipation of the tides induces a westward momentum forcing in the lower thermosphere, which drives a mean meridional circulation that is upward in the equatorial region, poleward at middle latitudes, and downward at high latitudes. This altered mean meridional circulation leads to an increase of $[O]$ and a decrease of $[N_2]$ in the lower thermosphere that is then communicated to the upper thermosphere via molecular diffusion (e.g., Yamazaki & Richmond, 2013). As thermospheric $[O]/[N_2]$ influences the production and loss of O^+, the $[O]/[N_2]$ reduction during SSWs leads to a decrease in the diurnal and zonal mean ionosphere electron densities, which are approximately equal to O^+ in the F-region ionosphere.

9 Effects on stratospheric transport and composition

The dramatic dynamical perturbations during SSWs are associated with anomalies in the transport circulation, and thus lead to anomalies in the distributions of constituents such as ozone and other trace gases throughout the lower and middle stratosphere, with the impacts on the upper stratosphere and lower mesosphere discussed in the previous section.

It has been known since the mid-twentieth century that the winter is dynamically the most active season in the stratosphere (see Baldwin, Birner, Brasseur, et al. (2019)), and it was correctly anticipated that the largest ozone changes would also occur during this season. However, measurements of both total column and profile ozone remained sparse before the 1970s and exhibited large differences among measurement stations, leading to large uncertainties in deriving knowledge on natural variability in ozone and its drivers. Nevertheless, the influence of SSWs was recognised and could be shown from observations as early as in the late 1950s, with Dütsch (1963) revealing a close spatial

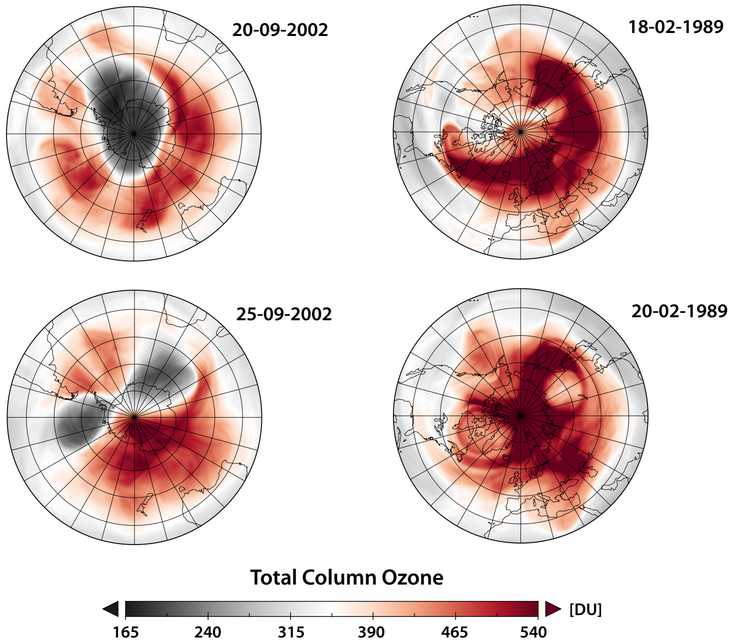

Figure 11. Total column ozone distributions in [DU] as obtained from ECMWF ERA5 before (upper panels) and after (lower panels) SSW events, for the Antarctic polar region in 2002 (left column) and the Arctic polar region in 1989 (right column), respectively.

correlation between total column ozone and temperatures in the 50–10 hPa layer during the 1957–1958 SSW over Europe. Based on averaged total column ozone observations over all available stations north of 40°N, Züllig (1973) further developed the findings by Dütsch to show that the seasonal evolution of ozone was exhibiting a much more abrupt initial increase during years with SSW events (1962–1963 and 1967–1968) than during a year without an SSW event (1966–1967).

In the early 1970s, the Backscatter Ultraviolet (BUV) instrument on Nimbus IV provided the first global ozone data from space, which served to verify the findings by Dütsch (1963) and Züllig (1973) from single measurement stations of total column ozone during SSWs (Heath, 1974). These global satellite measurements have continued to date, with a series of SBUV, TOMS, GOME, and OMI instruments flown on different satellites, providing immediate information on the impact of SSWs on total column ozone distributions in a visual manner. Figure 11 (left column) shows the total column ozone distribution over the Antarctic region in 2002 as derived from the ECWMF ERA5 reanalysis (Hersbach et al., 2020), before and after the occurrence of an SSW. This event was the first to be observed in the SH and as mentioned above led to an impressive split of the 2002 Antarctic ozone hole (Varotsos, 2002; von Savigny et al., 2005), at least partially cutting short ozone depletion during that year (Weber et al., 2003). A similar event is shown on the right for the winter 1989 over the Arctic region. While the overall ozone levels are much higher than in the SH, the split vortex can still be clearly identified.

SSWs not only leave a clear signature in total column ozone, but also affect the vertical structure of ozone (e.g., Kiesewetter et al., 2010; de la Cámara et al., 2018). With the advent of stratospheric limb sounders in the late 1970s, a wealth of observations had become available to study these features, including in trace gases other than ozone such as nitrous oxide, carbon monoxide, and nitrogen oxides (e.g., Manney, Schwartz, et al., 2009; Manney, Harwood, et al., 2009; Tao et al., 2015). As shown by Kiesewetter et al. (2010) and de la Cámara et al. (2018), after onset of an SSW, ozone anomalies become positive above 500K and negative below. The positive anomalies then slowly descend to lower altitudes, with the middle stratosphere relaxing back to normal trace gas concentrations the fastest. The enhanced poleward and downward transport during an SSW will lead to an increase in transport of other species such as carbon monoxide as well, with the breakdown of the polar vortex leading to enhanced mixing between mid and high latitudes and a flattening of the tracer gradients (Manney, Schwartz, et al., 2009). This will lead to cutting short ozone depletion by halogens in the Arctic polar stratosphere during spring, the opposite as found during the very cold and undisturbed 2013 Arctic winter that featured unprecedented Arctic ozone loss (Manney et al., 2015).

Due to the highly variable character of SSWs, observations fall short of providing the statistical information needed to fully explain trace gas transport during these events, hence models are used to more closely investigate the drivers behind the transport. Local tracer mixing ratios are the results of a balance between chemical sources or sinks and transport. In the TEM framework, the equation for a tracer mixing ratio X can be written as in equation 4:

$$\frac{\partial \overline{X}}{\partial t} = -\left[\overline{v}^* \frac{\partial}{\partial y} + \overline{w}^* \frac{\partial}{\partial z}\right] \overline{X} + \nabla \cdot M + S \tag{4}$$

The chemical sources and sinks are represented by S, while the first two terms on the right hand side represent transport. Of these, the first term describes slow residual advection, with upward transport in the tropics and downward transport in the extratropics (see also Section 4). The second term is the divergence of eddy tracer fluxes (of the form $\left(\overline{v'X'}, \overline{w'X'}\right)$), and thus describes the effect of mixing processes (M). The latter arises due to stirring of tracer contours and subsequent small-scale diffusion, leading to no net mass transport, but, in the presence of tracer gradients to tracer transport.

As described in Section 4, the strongly enhanced wave forcing prior and during a SSW event drives a strongly enhanced residual circulation. High latitude downwelling is enhanced by up to one standard deviation between about 10 days prior the SSW up to the central date (de la Cámara et al., 2018). After the central date, wave propagation is mostly prohibited and subsequently the lack of wave forcing leads to weakened polar downwelling. The weakening of the residual circulation can persist up to two months after the SSW, in particular for PJO events (de la Cámara et al., 2018; Hitchcock et al., 2013). The extended persistence in the lower stratosphere is partly a result of longer radiative timescales in this region (Hitchcock et al., 2013), but it has been shown that also enhanced diffusive PV mixing leads to the prolonged recovery phase of the polar vortex (de la Cámara et al., 2018; Lubis et al., 2018).

Next to the anomalous vertical residual advection in the polar vortex region, tracers are affected by anomalous mixing during SSW events. Mixing, as measured by effective diffusivity or equivalent length [a measure of the disturbances of a tracer contour line relative to a zonally symmetric contour line (see Nakamura (1996)], is enhanced in the aftermath of SSW events: strongest anomalies are found around 10 days after the central date at the vortex edge in the mid-stratosphere, with anomalies propagating poleward and downward in the following weeks to months (de la Cámara et al., 2018; Lubis et al., 2018). Enhanced mixing in the lower stratosphere is found to persist for more than two months for PJO events (de la Cámara et al., 2018), largely equivalent to "absorptive" events as classified by Lubis et al. (2018). Those prolonged diffusive mixing anomalies of PV delay the vortex recovery (see above); however they are not necessarily associated with enhanced eddy PV fluxes (or negative Eliassen-Palm flux divergence), but rather are compensated by wave activity transience, as revealed by an analysis of finite-amplitude wave activity (Lubis et al., 2018). The exact mechanism of the lower stratospheric mixing enhancement remains to be understood.

In summary, prior to and during an SSW tracers are affected mostly by enhanced downwelling, while after the SSW, downwelling is reduced and at the same time, enhanced quasi-horizontal mixing sets in. Together with the eroded polar vortex, and thus weakened transport barrier (see e.g., Tao et al., 2015), enhanced mixing between mid-latitude and high latitude air will affect tracer concentrations after SSW events.

10 Outlook

Despite decades of research, many key aspects of SSWs are still unclear. Even topics that have been addressed since the discovery of these phenomena, such as the mechanisms driving SSWs, present important open questions. For instance, the relative importance of tropospheric forcing versus internal stratospheric dynamics for triggering these events is still under debate.

Another “old” unclear key aspect of SSW research, investigated since the late 1970s, concerns the impact of factors such as the QBO and ENSO on the likelihood of SSWs. The underlying observational limitation is that the relatively short observational record (which has large internal variability) must be interpreted with caution (Polvani et al., 2017). For example, SSW occurrence was significantly reduced in the 1990s relative to the 2000s (Domeisen, 2019) and it is not clear if this decadal variability occurred by chance or was perhaps due in part to, say, ocean variability or sea-ice loss (Garfinkel et al., 2017; Hu & Guan, 2018; Sun et al., 2015). Separating the effects of internal variability on the occurrence of SSWs from other influences (e.g., ocean variability, solar cycles, the QBO) is essentially not feasible on a statistical basis alone, due to the short data record and multiple potential factors influencing SSWs. Fortunately, the improvement of climate models in representing stratospheric processes as well as the increasing use of model hierarchies (Maher et al., 2019) might help in quantifying these effects in the future, together with a better knowledge of theory. Further, as confidence in theory and modelling improves it is possible that somewhat different answers are obtained than from the limited observational record.

Another important category of SSW research revolves around forecasting. The first step is to develop the best possible forecasts of the stratosphere itself—currently models can predict SSWs with a lead time of approximately two weeks. What are the limitations of the predictability of SSWs within the stratosphere, and of stratospheric variability in general? To what degree are accurate stratospheric forecasts dependent on accurate forecasts of the troposphere vs. internal stratospheric dynamics?

Looking downward, we need a better dynamical understanding of how SSWs (and stratospheric variability in general) affect the troposphere and surface weather. The effects of SSWs on surface weather and climate are well quantified statistically, but not completely understood in detail. In particular, we do not have a good understanding of how the troposphere amplifies the stratospheric signal. At the same time the relative importance of characteristics of this stratospheric signal such as the morphology of vortex splits for the tropospheric fingerprint is still debated. Even interactive stratospheric chemistry has recently been suggested to modulate the tropospheric response to stratospheric variability associated with SSWs (Calvo et al., 2015; Haase & Matthes, 2019; Oehrlein et al., 2020). Consequently, we still do not have a confident answer to why some SSWs appear to have a strong surface impact, whereas the troposphere appears to be unaffected by some others.

Accurately simulating the effects of the stratosphere on surface weather will depend on identifying those aspects of the models which require improvement. This is relevant on all timescales from weather forecasts to climate projections. Ultimately, to what degree can stratospheric predictions be exploited for surface weather forecasts? One potentially important aspect is that SSWs have an influence on Arctic surface temperatures for several weeks. Can long-range forecasts of Arctic weather and sea ice movement be improved through improved stratospheric forecasts and a more accurate representation of stratosphere-troposphere coupling?

Looking upward, the effects of SSWs above the stratosphere are not well quantified and it is yet to be established if these effects are largely limited to SSWs or if the effects are proportional to stratospheric disturbances of either sign. The physical mechanisms by which SSWs impact the upper atmosphere are also not fully understood, with a number of open questions concerning how SSWs generate variability in the ionosphere and thermosphere. In a society extremely dependent on technology affected by space weather, the need for answering these questions will extend scientific curiosity.

Finally, one of the most outstanding questions is whether SSWs will change in the future by climate change. Will the frequency of SSWs be affected due to increasing greenhouse gas concentrations? Despite many efforts in the last 30 years (e.g., Rind et al., 1990; Butchart et al., 2000; McLandress & Shepherd, 2009a; Mitchell et al., 2012), the answer remains unclear. An analysis of SSWs during the climate of the Last Glacial Maximum (20,000–25,000 YBP) showed no significant difference in SSW frequency compared to today (Fu et al., 2020). Analyses of SSWs in the two most recent multi-model intercomparison projects (Chemistry Climate Models Initiative (CCMI,(Morgenstern et al., 2017)) and Coupled Model Intercomparison Project Phase 6 (CMIP6, (Eyring et al., 2016))) do not provide a robust answer. Ayarzagüena et al. (2018) showed, *on average* in CCMI models, insignificant future changes in SSWs. However, most individual CMIP6 models project significant changes, but with no consensus on the sign of the change (Ayarzagüena et al., 2020). Different reasons might explain this uncertainty. First, as already indicated, there are many unclear aspects about basic dynamics of SSWs and this translates into differences among models in how they represent it. Secondly, biases in the model representation of the mean atmospheric state and how it reacts to climate change might be another reason. In this sense, the disparity in the distribution of tropospheric warming (i.e., different relative importance of tropical and polar amplifications) among models might be a candidate to project different stratospheric forcings. In the stratosphere, the opposing signals with climate change (i.e., radiative CO_2-cooling vs. increased adiabatic warming from a faster Brewer-Dobson circulation) results in a weak amplitude of the total signal (Mitchell et al., 2012). A different relative strength of these signals among models likely contributes to a disparity in the sign of the change in frequency of SSWs.

After enumerating uncertainties in key research aspects, it becomes clear that reducing most of these uncertainties might benefit humanity through improved weather forecasts, improved climate projections, and minimising ionospheric effects on communications. Stratospheric research has the potential to benefit from evolving fields such as machine learning, big data, artificial intelligence, and data mining that are becoming more feasible as the ability to handle very large data sets becomes more routine. All these new techniques might boost future SSW research.

Acknowledgments

We thank Jian Rao for producing Table 4. BA acknowledges support from the Spanish Ministry of Science and Innovation through the JeDiS (RTI-2018-096402-B-I00) project. MPB was supported by the Natural Environment Research Council (grant number NE/M006123/1). TB and HG acknowledge support by the Transregional Collaborative Research Center SFB/TRR 165 Waves to Weather (`www.wavestoweather.de`) funded by the German Research Foundation (DFG). Funding by the Swiss National Science Foundation to D.D. through project PP00P2_170523 is gratefully acknowledged. EPG acknowledges support from the US NSF through grant AGS-1852727. CIG acknowledges the support of a European Research Council starting grant under the European Union Horizon 2020 research and innovation programme (grant agreement number 677756). NB was supported by the Met Office Hadley Centre Programme funded by BEIS and Defra. Part of the material is based upon work supported by the National Center for Atmospheric Research, which is a major facility sponsored by the U.S. National Science Foundation under Cooperative Agreement 1852977. NP acknowledges support from NASA grant 80NSSC18K1046. Snow cover data is sourced from `https://climate.rutgers.edu/snowcover/table_area.php?ui_set=1`. JRA-55 data are freely available at `https://jra.kishou.go.jp/JRA-55/index\_en.html`. ECWMF ERA5 data are accessible via the climate data store `https://cds.climate.copernicus.eu` and ERA-Interim data are avalaible online `https://apps.ecmwf.int/datasets/data/interim-full-daily/levtype=sfc/`.

References

Afargan-Gerstman, H., & Domeisen, D. I. V. (2020). Pacific modulation of the North Atlantic storm track response to sudden stratospheric warming events. *Geophysical Research Letters*, *47*, e2019GL085007. doi: 10.1029/2019GL085007

Afargan-Gerstman, H., Polkova, I., Papritz, L., Ruggieri, P., King, M. P., Athanasiadis, P. J., ... Domeisen, D. I. V. (2020). Stratospheric influence on North Atlantic marine cold air outbreaks following sudden stratospheric warming events. *Weather and Climate Dynamics*, *1*(2), 541–553.

Albers, J. R., & Birner, T. (2014). Vortex preconditioning due to planetary and gravity waves prior to sudden stratospheric warmings. *Journal of the Atmospheric Sciences*, *71*(11), 4028-4054. doi: 10.1175/JAS-D-14-0026.1

Ambaum, M., & Hoskins, B. (2002). The NAO troposphere–stratosphere connection. *Journal of Climate*, *15*(14), 1969–1978.

Anderson, D., & Araujo-Pradere, E. A. (2010). Sudden stratospheric warming event signatures in daytime ExB drift velocities in the Peruvian and Philippine longitude sectors for January 2003 and 2004. *J. Geophys. Res. Sp. Phys.*, *115*(A8). doi: 10.1029/2010JA015337

Andrews, D. G., & McIntyre, M. E. (1976). Planetary waves in horizontal and vertical shere: The generalized Eliassen-Palm relation and the mean zonal acceleration. *Journal of the Atmospheric Sciences*, *33*, 2031–2048.

Anstey, J. A., & Shepherd, T. G. (2014). High-latitude influence of the quasi-biennial oscillation. *Quarterly Journal of the Royal Meteorological Society*, *140*(678), 1–21.

Ayarzagüena, B., Barriopedro, D., Perez, J. M. G., Abalos, M., de la Cámara, A., Herrera, R. G., ... Ordóñez, C. (2018). Stratospheric Connection to the Abrupt End of the 2016/2017 Iberian Drought. *Geophysical Research Letters*, *45*(22), 12,639–12,646.

Ayarzagüena, B., Charlton-Perez, A. J., Butler, A. H., Hitchcock, P., Simpson, I. R., Polvani, L. M., ... Watanabe, S. (2020). Uncertainty in the response of sudden stratospheric warmings and stratosphere-troposphere coupling to quadrupled co2 concentrations in cmip6 models. *Journal of Geophysical Research: Atmospheres*, *125*(6), e2019JD032345. doi: 10.1029/2019JD032345

Ayarzagüena, B., Palmeiro, F. M., Barriopedro, D., Calvo, N., Langematz, U., & Shibata, K. (2019). On the representation of major stratospheric warmings in reanalyses. *Atmospheric Chemistry and Physics*, *19*(14), 9469–9484.

Ayarzagüena, B., Polvani, L. M., Langematz, U., Akiyoshi, H., Bekki, S., Butchart, N., ... Zeng, G. (2018). No robust evidence of future changes in major stratospheric sudden warmings: a multi-model assessment from CCMI. *Atmospheric Chemistry and Physics*, *18*(15), 11277–11287. doi: 10.5194/acp-18-11277-2018

Ayarzagüena, B., & Serrano, E. (2009). Monthly characterization of the tropospheric circulation over the euro-atlantic area in relation with the timing of stratospheric final warmings. *Journal of Climate*, *22*, 6313-6324. doi: 10.1175/2009JCLI2913.1

Baldwin, M. P., Birner, T., & Ayarzagüena, B. (2019). Tropospheric amplification of stratospheric variability. *EGU General Assembly Conference, Vienna, Austria.*

Baldwin, M. P., Birner, T., Brasseur, G., Burrows, J., Butchart, N., Garcia, R., ... Scaife, A. (2019, 10). 100 Years of Progress in Understanding the Stratosphere and Mesosphere. *Meteorological Monographs*, *59*, 27.127.62. doi: 10.1175/AMSMONOGRAPHS-D-19-0003.1

Baldwin, M. P., & Dunkerton, T. J. (1999). Propagation of the Arctic Oscillation from the stratosphere to the troposphere. *Journal of Geophysical Research*, *104*(D24), 30937.

Baldwin, M. P., & Dunkerton, T. J. (2001). Stratospheric harbingers of anomalous weather regimes. *Science*, *294*(5542), 581–584.

Baldwin, M. P., & Holton, J. R. (1988). Climatology of the stratospheric polar vortex and planetary wave breaking. *Journal of the Atmospheric Sciences*, *45*(7), 1123-1142. doi: 10.1175/1520-0469(1988)045⟨1123:COTSPV⟩2.0.CO;2

Baldwin, M. P., & Thompson, D. W. (2009). A critical comparison of stratosphere-troposphere coupling indices. *Quarterly Journal of the Royal Meteorological Society*, *135*(644), 1661–1672. doi: 10.1002/qj.479

Bancalá, S., Krüger, K., & Giorgetta, M. (2012). The preconditioning of major sudden stratospheric warmings. *Journal of Geophysical Research: Atmospheres*, *117*(D4), D04101. doi: 10.1029/2011JD016769

Barriopedro, D., & Calvo, N. (2014). On the Relationship between ENSO, Stratospheric Sudden Warmings, and Blocking. *Journal of Climate*, *27*(12), 4704–4720. doi: 10.1175/JCLI-D-13-00770.1

Birner, T., & Albers, J. R. (2017). Sudden stratospheric warmings and anomalous upward wave activity flux. *SOLA*, *13A*(Special Edition), 8-12. doi: 10.2151/sola.13A-002

Black, R. X. (2002). Stratospheric forcing of surface climate in the arctic oscillation. *Journal of Climate*, *15*(3), 268-277. doi: 10.1175/1520-0442(2002)015⟨0268:SFOSCI⟩2.0.CO;2

Butchart, N., Austin, J., Knight, J. R., Scaife, A. A., & Gallani, M. L. (2000). The response of the stratospheric climate to projected changes in the concentrations of well-mixed greenhouse gases from 1992 to 2051. *Journal of Climate*, *13*(13), 2142-2159. doi: 10.1175/1520-0442(2000)013⟨2142:TROTSC⟩2.0.CO;2

Butchart, N., & Remsberg, E. E. (1986). The area of the stratospheric polar vortex as a diagnostic for tracer transport on an isentropic surface. *Journal of the Atmospheric Sciences*, *43*(13), 1319-1339. doi: 10.1175/1520-0469(1986)043⟨1319:TAOTSP⟩2.0.CO;2

Butler, A. H., Charlton-Perez, A., Domeisen, D. I., Simpson, I. R., & Sjoberg, J. (2019). Predictability of northern hemisphere final stratospheric warmings and their surface impacts. *Geophysical Research Letters*, *46*(17-18), 10578-10588. doi: 10.1029/2019GL083346

Butler, A. H., & Gerber, E. P. (2018). Optimizing the Definition of a Sudden Stratospheric Warming. *Journal of Climate*, *31*(6), 2337–2344. doi: 10.1175/JCLI-D-17-0648.1

Butler, A. H., & Polvani, L. M. (2011). El Niño, La Niña, and stratospheric sudden warmings: A reevaluation in light of the observational record. *Geophysical Research Letters*, *38*(13).

Butler, A. H., Seidel, D. J., Hardiman, S. C., Butchart, N., Birner, T., & Match, A. (2015). Defining Sudden Stratospheric Warmings. *Bulletin of the American Meteorological Society*, *96*(11), 1913–1928. doi: 10.1175/BAMS-D-13-00173.1

Butler, A. H., Sjoberg, J. P., Seidel, D. J., & Rosenlof, K. H. (2017). A sudden stratospheric warming compendium. *Earth System Science Data*, *9*(1), 63–76.

Byrne, N. J., & Shepherd, T. G. (2018). Seasonal Persistence of Circulation Anomalies in the Southern Hemisphere Stratosphere and Its Implications for the Troposphere. *Journal of Climate*, *31*(9), 3467-3483. doi: 10.1175/JCLI-D-17-0557.1

Calvo, N., Polvani, L. M., & Solomon, S. (2015). On the surface impact of arctic stratospheric ozone extremes. *Environmental Research Letters*, *10*(9), 094003. Retrieved from `https://doi.org/10.1088%2F1748-9326%2F10%2F9%2F094003` doi: 10.1088/1748-9326/10/9/094003

Camp, C., & Tung, K.-K. (2007). Stratospheric polar warming by enso in winter: A statistical study. *Geophysical Research Letters*, *34*(4).

Castanheira, J. M., & Barriopedro, D. (2010). Dynamical connection between tropospheric blockings and stratospheric polar vortex. *Geophysical Research Letters*, *37*(13). doi: 10.1029/2010GL043819

Chan, C. J., & Plumb, R. (2009). The response to stratospheric forcing and its dependence on the state of the troposphere. *Journal of the Atmospheric Sciences*.

Chandran, A., Collins, R. L., Garcia, R. R., Marsh, D. R., Harvey, V. L., Yue, J., & de la Torre, L. (2013). A climatology of elevated stratopause events in the whole atmosphere community climate model. *J. Geophys. Res. Atmos.*, *118*(3), 1234–1246. doi: 10.1002/jgrd.50123

Chandran, A., Collins, R. L., & Harvey, V. L. (2014). Stratosphere-mesosphere coupling during stratospheric sudden warming events. *Adv. Sp. Res.*, *53*(9), 1265–1289. doi: https://doi.org/10.1016/j.asr.2014.02.005

Charlton, A. J., O'Neill, A., Berrisford, P., & Lahoz, W. A. (2005). Can the dynamical impact of the stratosphere on the troposphere be described by large-scale adjustment to the stratospheric pv distribution? *Quarterly Journal of the Royal Meteorological Society*, *131*(606), 525-543. doi: 10.1256/qj.03.222

Charlton, A. J., & Polvani, L. M. (2007). A new look at stratospheric sudden warmings. Part I: Climatology and modeling benchmarks. *Journal of Climate*, *20*(3), 449469.

Charlton-Perez, A. J., Baldwin, M. P., Birner, T., Black, R. X., Butler, A. H., Calvo, N., … Watanabe, S. (2013). On the lack of stratospheric dynamical variability in low-top versions of the CMIP5 models. *Journal of Geophysical Research: Atmospheres*, *118*(6), 2494–2505.

Charlton-Perez, A. J., Ferranti, L., & Lee, R. W. (2018). The influence of the stratospheric state on North Atlantic weather regimes. *Quarterly Journal of the Royal Meteorological Society*, *144*(713), 1140–1151.

Charney, J. G., & Drazin, P. G. (1961). Propagation of planetary-scale disturbances from the lower into the upper atmosphere. *Journal of Geophysical Research*, *66*(1), 83109. doi: 10.1029/JZ066i001p00083

Chau, J. L., Fejer, B. G., & Goncharenko, L. P. (2009). Quiet variability of equatorial E × B drifts during a sudden stratospheric warming event. *Geophys. Res. Lett.*, *36*(5). doi: 10.1029/2008GL036785

Chau, J. L., Goncharenko, L. P., Fejer, B. G., & Liu, H. L. (2012). Equatorial and Low Latitude Ionospheric Effects During Sudden Stratospheric Warming Events. *Space Sci. Rev.*, *168*(1), 385–417. doi: 10.1007/s11214-011-9797-5

Chau, J. L., Hoffmann, P., Pedatella, N. M., Matthias, V., & Stober, G. (2015). Upper mesospheric lunar tides over middle and high latitudes during sudden stratospheric warming events. *J. Geophys. Res. Sp. Phys.*, *120*(4), 3084–3096. doi: 10.1002/2015JA020998

Clark, J. H. E. (1974). Atmospheric response to the quasi-resonant growth of forced planetary waves. *Journal of the Meteorological Society of Japan. Ser. II*, *52*(2), 143-163. doi: 10.2151/jmsj1965.52.2_143

Cohen, J., Barlow, M., Kushner, P. J., & Saito, K. (2007). Stratosphere–troposphere

coupling and links with eurasian land surface variability. *Journal of Climate*, *20*(21), 5335–5343.
Cohen, J., Furtado, J. C., Jones, J., Barlow, M., Whittleston, D., & Entekhabi, D. (2014). Linking siberian snow cover to precursors of stratospheric variability. *Journal of Climate*, *27*(14), 5422–5432.
Cohen, J., & Jones, J. (2011). Tropospheric precursors and stratospheric warmings. *Journal of Climate*, *24*(24), 65626572.
Coughlin, K., & Gray, L. J. (2009). A Continuum of Sudden Stratospheric Warmings. *Journal of the Atmospheric Sciences*, *66*(2), 531–540. doi: 10.1175/2008JAS2792.1
Curry, J. (1987). The contribution of radiative cooling to the formation of cold-core anticyclones. *Journal of the Atmospheric Sciences*, *44*(18), 2575-2592. doi: 10.1175/1520-0469(1987)044⟨2575:TCORCT⟩2.0.CO;2
Darling, E. M. J. (1953). Winds at 100 mb and 50 mb over the united states in 1952. *Bull. Amer. Meteor. Soc.*, *34*(10), 458-461.
Dee, D. P., Uppala, S. M., Simmons, A. J., Berrisford, P., Poli, P., Kobayashi, S., ... Vitart, F. (2011). The era-interim reanalysis: configuration and performance of the data assimilation system. *Quarterly Journal of the Royal Meteorological Society*, *137*(656), 553–597. doi: 10.1002/qj.828
de la Cámara, A., Abalos, M., & Hitchcock, P. (2018). Changes in Stratospheric Transport and Mixing During Sudden Stratospheric Warmings. *Journal of Geophysical Research: Atmospheres*, *123*(7), 3356–3373. doi: 10.1002/2017JD028007
de la Cámara, A., Albers, J. R., Birner, T., Garcia, R. R., Hitchcock, P., Kinnison, D. E., & Smith, A. K. (2017). Sensitivity of sudden stratospheric warmings to previous stratospheric conditions. *Journal of the Atmospheric Sciences*, *74*(9), 2857-2877. doi: 10.1175/JAS-D-17-0136.1
de la Cámara, A., Birner, T., & Albers, J. R. (2019). Are sudden stratospheric warmings preceded by anomalous tropospheric wave activity? *Journal of Climate*, *32*(21), 7173-7189. doi: 10.1175/JCLI-D-19-0269.1
de Paula, E. R., Jonah, O. F., Moraes, A. O., Kherani, E. A., Fejer, B. G., Abdu, M. A., ... Paes, R. R. (2015). Low-latitude scintillation weakening during sudden stratospheric warming events. *J. Geophys. Res. Sp. Phys.*, *120*(3), 2212–2221. doi: 10.1002/2014JA020731
Domeisen, D. I. (2019). Estimating the Frequency of Sudden Stratospheric Warming Events From Surface Observations of the North Atlantic Oscillation. *Journal of Geophysical Research-Atmospheres*, *124*(6), 3180–3194. doi: 10.1029/2018JD030077
Domeisen, D. I., Butler, A. H., Charlton-Perez, A. J., Ayarzagüena, B., Baldwin, M. P., Dunn-Sigouin, E., ... Taguchi, M. (2020a). The Role of the Stratosphere in Subseasonal to Seasonal Prediction: 1. Predictability of the Stratosphere. *Journal of Geophysical Research: Atmospheres*, *125*(2), e2019JD030920. doi: 10.1029/2019JD030920
Domeisen, D. I., Butler, A. H., Charlton-Perez, A. J., Ayarzagüena, B., Baldwin, M. P., Dunn-Sigouin, E., ... Taguchi, M. (2020b). The Role of the Stratosphere in Subseasonal to Seasonal Prediction: 2. Predictability Arising From Stratosphere-Troposphere Coupling. *Journal of Geophysical Research: Atmospheres*, *125*(2), e2019JD030923. doi: 10.1029/2019JD030923
Domeisen, D. I., Butler, A. H., Fröhlich, K., Bittner, M., Müller, W. A., & Baehr, J. (2015). Seasonal Predictability over Europe Arising from El Niño and Stratospheric Variability in the MPI-ESM Seasonal Prediction System. *Journal of Climate*, *28*(1), 256–271. doi: 10.1175/JCLI-D-14-00207.1
Domeisen, D. I., Garfinkel, C. I., & Butler, A. H. (2019). The teleconnection of El Niño Southern Oscillation to the stratosphere. *Reviews of Geophysics*, *57*(1), 5–47. doi: 10.1029/2018RG000596

Domeisen, D. I., Grams, C. M., & Papritz, L. (2020). The role of North Atlantic-European weather regimes in the surface impact of sudden stratospheric warming events. *Weather Clim. Dynam.*, *1*, 373-388. doi: 10.5194/wcd-1-373-2020

Domeisen, D. I., & Plumb, R. A. (2012). Traveling planetary-scale Rossby waves in the winter stratosphere: The role of tropospheric baroclinic instability. *Geophysical Research Letters*, *39*(20), L20817. doi: 10.1029/2012GL053684

Domeisen, D. I., Sun, L., & Chen, G. (2013). The role of synoptic eddies in the tropospheric response to stratospheric variability. *Geophysical Research Letters*, *40*, 4933–4937. doi: 10.1002/grl.50943

Dütsch, H. U. (1963). Ozone and temperature in the stratosphere. symposium on stratospheric and mesospheric circulation. *Meteorologische Abhandlungen der Freien Universitt Berlin*, *XXXVI*, 271-291.

Edmon, H. J., Hoskins, B. J., & McIntyre, M. E. (1980). Eliassen-Palm cross sections for the troposphere. *Journal of the Atmospheric Sciences*, *37*, 2600-2616.

Eguchi, N., & Kodera, K. (2010). Impacts of Stratospheric Sudden Warming Event on Tropical Clouds and Moisture Fields in the TTL: A Case Study. *Sola*, *6*, 137–140. doi: 10.2151/sola.2010-035

Eliassen, A., & Palm, E. (1961). On the transfer of energy in stationary mountain waves. *Geofysiske Publikasjoner*, *22*, 1–23.

Esler, J., & Matthewman, N. (2011). Stratospheric Sudden Warmings as Self-Tuning Resonances. Part II: Vortex Displacement Events. *Journal of the Atmospheric Sciences*, *68*, 2505–2523.

Evan, S., Rosenlof, K. H., Thornberry, T., Rollins, A., & Khaykin, S. (2015). TTL cooling and drying during the January 2013 stratospheric sudden warming. *Quarterly Journal of the Royal Meteorological Society*, *141*, 3030–3039. doi: 10.1002/qj.2587

Eyring, V., Bony, S., Meehl, G. A., Senior, C. A., Stevens, B., Stouffer, R. J., & Taylor, K. E. (2016). Overview of the coupled model intercomparison project phase 6 (cmip6) experimental design and organization. *Geoscientific Model Development*, *9*(5), 1937–1958. doi: 10.5194/gmd-9-1937-2016

Fagundes, P. R., Goncharenko, L. P., de Abreu, A. J., Venkatesh, K., Pezzopane, M., de Jesus, R., ... Pillat, V. G. (2015). Ionospheric response to the 2009 sudden stratospheric warming over the equatorial, low, and middle latitudes in the South American sector. *J. Geophys. Res. Sp. Phys.*, *120*(9), 7889–7902. doi: 10.1002/2014JA020649

Fang, T.-W., Fuller-Rowell, T., Akmaev, R., Wu, F., Wang, H., & Anderson, D. (2012). Longitudinal variation of ionospheric vertical drifts during the 2009 sudden stratospheric warming. *J. Geophys. Res. Sp. Phys.*, *117*(A3). doi: 10.1029/2011JA017348

Fang, T.-W., Fuller-Rowell, T., Wang, H., Akmaev, R., & Wu, F. (2014). Ionospheric response to sudden stratospheric warming events at low and high solar activity. *J. Geophys. Res. Sp. Phys.*, *119*(9), 7858–7869. doi: 10.1002/2014JA020142

Fejer, B. G., Olson, M. E., Chau, J. L., Stolle, C., Lühr, H., Goncharenko, L. P., ... Nagatsuma, T. (2010). Lunar-dependent equatorial ionospheric electrodynamic effects during sudden stratospheric warmings. *J. Geophys. Res. Sp. Phys.*, *115*(A8). doi: 10.1029/2010JA015273

Fejer, B. G., Tracy, B. D., Olson, M. E., & Chau, J. L. (2011). Enhanced lunar semidiurnal equatorial vertical plasma drifts during sudden stratospheric warmings. *Geophys. Res. Lett.*, *38*(21). doi: 10.1029/2011GL049788

Forbes, J. M., & Zhang, X. (2012). Lunar tide amplification during the January 2009 stratosphere warming event: Observations and theory. *J. Geophys. Res. Sp. Phys.*, *117*(A12). doi: 10.1029/2012JA017963

Fu, Q., Wang, M., White, R. H., Pahlavan, H. A., Alexander, B., & Wallace,

J. M. (2020). Quasi-biennial oscillation and sudden stratospheric warmings during the last glacial maximum. *Atmosphere*, *11*(9), 943-954. doi: 10.3390/atmos11090943

Funke, B., Ball, W., Bender, S., Gardini, A., Harvey, V. L., Lambert, A., ... Yushkov, V. (2017). HEPPA-II model-measurement intercomparison project: EPP indirect effects during the dynamically perturbed NH winter 2008-2009. *Atmos. Chem. Phys.*, *17*(5), 3573–3604. doi: 10.5194/acp-17-3573-2017

Funke, B., López-Puertas, M., Bermejo-Pantaleón, D., García-Comas, M., Stiller, G. P., von Clarmann, T., ... Linden, A. (2010). Evidence for dynamical coupling from the lower atmosphere to the thermosphere during a major stratospheric warming. *Geophys. Res. Lett.*, *37*(13). doi: 10.1029/2010GL043619

Furtado, J. C., Cohen, J. L., Butler, A. H., Riddle, E. E., & Kumar, A. (2015). Eurasian snow cover variability and links to winter climate in the CMIP5 models. *Climate Dynamics*. doi: 10.1007/s00382-015-2494-4

Garfinkel, C. I., Benedict, J. J., & Maloney, E. D. (2014). Impact of the mjo on the boreal winter extratropical circulation. *Geophysical Research Letters*, *41*(16), 6055–6062.

Garfinkel, C. I., Butler, A., Waugh, D., Hurwitz, M., & Polvani, L. M. (2012). Why might stratospheric sudden warmings occur with similar frequency in el niño and la niña winters? *Journal of Geophysical Research: Atmospheres*, *117*(D19).

Garfinkel, C. I., & Hartmann, D. L. (2007). Effects of the el niño–southern oscillation and the quasi-biennial oscillation on polar temperatures in the stratosphere. *Journal of Geophysical Research: Atmospheres*, *112*(D19).

Garfinkel, C. I., Hartmann, D. L., & Sassi, F. (2010). Tropospheric precursors of anomalous Northern Hemisphere stratospheric polar vortices. *Journal of Climate*, *23*(12), 32823299.

Garfinkel, C. I., & Schwartz, C. (2017). Mjo-related tropical convection anomalies lead to more accurate stratospheric vortex variability in subseasonal forecast models. *Geophysical research letters*, *44*(19), 10–054. doi: 10.1002/2017GL074470

Garfinkel, C. I., Schwartz, C., Butler, A. H., Domeisen, D. I., Son, S.-W., & White, I. (2019). Weakening of the teleconnection from El Niño–Southern Oscillation to the Arctic stratosphere over the past few decades: What can be learned from subseasonal forecast models? *Journal of Geophysical Research: Atmospheres*, *124*(14), 7683–7696.

Garfinkel, C. I., Schwartz, C., Domeisen, D. I., Son, S.-W., Butler, A. H., & White, I. (2018). Extratropical atmospheric predictability from the quasi-biennial oscillation in subseasonal forecast models. *Journal of Geophysical Research: Atmospheres*, *123*(15), 7855–7866.

Garfinkel, C. I., Schwartz, C., White, I., & Rao, J. (2020). Predictability of the early winter arctic oscillation from autumn eurasian snowcover in subseasonal forecast models. *Climate Dynamics*, *55*. doi: 10.1007/s00382-020-05305-3

Garfinkel, C. I., Shaw, T. A., Hartmann, D. L., & Waugh, D. W. (2012). Does the holton–tan mechanism explain how the quasi-biennial oscillation modulates the arctic polar vortex? *Journal of the Atmospheric Sciences*, *69*(5), 1713–1733.

Garfinkel, C. I., Son, S.-W., Song, K., Aquila, V., & Oman, L. D. (2017). Stratospheric variability contributed to and sustained the recent hiatus in eurasian winter warming. *Geophysical research letters*, *44*(1), 374–382.

Garfinkel, C. I., Waugh, D. W., & Gerber, E. P. (2013). The Effect of Tropospheric Jet Latitude on Coupling between the Stratospheric Polar Vortex and the Troposphere. *Journal of Climate*, *26*(6), 2077–2095.

Garfinkel, C. I., White, I., Gerber, E. P., Jucker, M., & Erez, M. (2020). The building blocks of northern hemisphere wintertime stationary waves. *Journal of Climate*, *33*(13), 5611–5633.

Geisler, J. E. (1974). A numerical model of the sudden stratospheric warming mechanism. *Journal of Geophysical Research*, *79*(33), 4989-4999. doi: 10.1029/JC079i033p04989

Gerber, E. P., Baldwin, M. P., Akiyoshi, H., Austin, J., Bekki, S., Braesicke, P., ... Smale, D. (2010). Stratosphere-troposphere coupling and annular mode variability in chemistry-climate models. *Journal of Geophysical Research*, *115*, D00M06. doi: 10.1029/2009JD013770

Gerber, E. P., & Manzini, E. (2016). The Dynamics and Variability Model Intercomparison Project (DynVarMIP) for CMIP6: assessing the stratosphere–troposphere system. *Geoscientific Model Development*, *9*(9), 3413–3425. doi: 10.5194/gmd-9-3413-2016

Gerber, E. P., Martineau, P., Ayarzagüena, B., Barriopedro, D., Bracegirdle, T. J., Butler, A. H., ... Taguchi, M. (2020). Extratropical stratospheretroposphere coupling. In M. Fujiwara, G. L. Manney, L. Gray, & J. S. Wright (Eds.), *Stratosphere-troposphere processes and their role in climate (sparc) reanalysis intercomparison project (s-rip)* (p. Chapter 6).

Gerber, E. P., Orbe, C., & Polvani, L. M. (2009). Stratospheric influence on the tropospheric circulation revealed by idealized ensemble forecasts. *Geophysical Research Letters*, *36*, L24801.

Gerber, E. P., & Polvani, L. M. (2009). Stratosphere-troposphere coupling in a relatively simple AGCM: The importance of stratospheric variability. *Journal of Climate*, *22*, 1920–1933. doi: 10.1175/2008JCLI2548.1

Gerber, E. P., Polvani, L. M., & Ancukiewicz, D. (2008). Annular mode time scales in the Intergovernmental Panel on Climate Change Fourth Assessment Report models. *Geophysical Research Letters*.

Gerber, E. P, Voronin, S., & Polvani, L. M. (2008). Testing the annular mode autocorrelation time scale in simple atmospheric general circulation models. *Monthly Weather Review*, *136*(4), 1523–1536.

Gillett, N., Kell, T., & Jones, P. (2006). Regional climate impacts of the Southern Annular Mode. *Geophysical Research Letters*, *33*, L23704. doi: 10.1029/2006GL027721

Goncharenko, L. P., Chau, J. L., Condor, P., Coster, A., & Benkevitch, L. (2013). Ionospheric effects of sudden stratospheric warming during moderate-to-high solar activity: Case study of January 2013. *Geophys. Res. Lett.*, *40*(19), 4982–4986. doi: 10.1002/grl.50980

Goncharenko, L. P., Chau, J. L., Liu, H. L., & Coster, A. J. (2010). Unexpected connections between the stratosphere and ionosphere. *Geophys. Res. Lett.*, *37*(10). doi: 10.1029/2010GL043125

Goncharenko, L. P., Coster, A., Plumb, R., & Domeisen, D. I. (2012). The potential role of stratospheric ozone in the stratosphere-ionosphere coupling during stratospheric warmings. *Geophysical Research Letters*.

Goncharenko, L. P., Coster, A. J., Chau, J. L., & Valladares, C. E. (2010). Impact of sudden stratospheric warmings on equatorial ionization anomaly. *J. Geophys. Res. Sp. Phys.*, *115*(A10). doi: 10.1029/2010JA015400

Goncharenko, L. P., Coster, A. J., Zhang, S.-R., Erickson, P. J., Benkevitch, L., Aponte, N., ... Hernández-Espiet, A. (2018). Deep Ionospheric Hole Created by Sudden Stratospheric Warming in the Nighttime Ionosphere. *J. Geophys. Res. Sp. Phys.*, *123*(9), 7621–7633. doi: 10.1029/2018JA025541

Goncharenko, L. P., & Zhang, S.-R. (2008). Ionospheric signatures of sudden stratospheric warming: Ion temperature at middle latitude. *Geophysical Research Letters*, *35*(21), L21103.

Gray, L. J., Beer, J., Geller, M., Haigh, J. D., Lockwood, M., Matthes, K., ... others (2010). Solar influences on climate. *Reviews of Geophysics*, *48*(4).

Gray, L. J., Crooks, S., Pascoe, C., Sparrow, S., & Palmer, M. (2004). Solar and qbo influences on the timing of stratospheric sudden warmings. *Journal of the at-*

mospheric sciences, *61*(23), 2777–2796.

Green, M. R., & Furtado, J. C. (2019). Evaluating the Joint Influence of the Madden-Julian Oscillation and the Stratospheric Polar Vortex on Weather Patterns in the Northern Hemisphere. *Journal of Geophysical Research: Atmospheres*, *124*, 11693 11709. doi: 10.1029/2019JD030771

Haase, S., & Matthes, K. (2019). The importance of interactive chemistry for stratosphere–troposphere coupling. *Atmospheric Chemistry and Physics*, *19*(5), 3417–3432. Retrieved from https://acp.copernicus.org/articles/19/3417/2019/ doi: 10.5194/acp-19-3417-2019

Hardiman, S. C., Butchart, N., Charlton-Perez, A. J., Shaw, T. A., Akiyoshi, H., Baumgaertner, A., ... Shibata, K. (2011). Improved predictability of the troposphere using stratospheric final warmings. *Journal of Geophysical Research: Atmospheres*, *116*(D18). doi: 10.1029/2011JD015914

Hartley, D. E., Villarin, J. T., Black, R. X., & Davis, C. A. (1998). A new perspective on the dynamical link between the stratosphere and troposphere. *Nature*, *391*, 471474.

Hartmann, D. (1979). Baroclinic Instability of Realistic Zonal-Mean States to Planetary Waves. *Journal of Atmospheric Sciences*, *36*, 2336–2349.

Haynes, P. H., Marks, C. J., McIntyre, M. E., Shepherd, T. G., & Shine, K. P. (1991). On the downward control of extratropical diabatic circulations by eddy-induced mean zonal forces. *Journal of the Atmospheric Sciences*, *48*(4), 651–678.

Heath, D. F. (1974). Recent advances in satellite observations of solar variability and global atmospheric ozone. *International conference on structure, composition, and general circulation of the upper and lower atmospheres, and possible anthropogenic perturbations, Melbourne, Australia*, 1267-1291.

Henderson, G. R., Peings, Y., Furtado, J. C., & Kushner, P. J. (2018). Snow–atmosphere coupling in the northern hemisphere. *Nature Climate Change*, *8*(11), 954–963.

Hendon, H. H., Thompson, D. W. J., Lim, E. P., Butler, A. H., Newman, P. A., Coy, L., ... Nakamura, H. (2019). Rare forecasted climate event under way in the Southern Hemisphere. *Nature Correspondence*, *573*, 495.

Hersbach, H., Bell, B., Berrisford, P., Hirahara, S., Hornyi, A., Muoz-Sabater, J., ... Thpaut, J.-N. (2020). The era5 global reanalysis. *Quarterly Journal of the Royal Meteorological Society*, *146*(730), 1999–2049. doi: 10.1002/qj.3803

Hitchcock, P., & Haynes, P. H. (2016). Stratospheric control of planetary waves. *Geophysical Research Letters*, *43*(22), 11,884-11,892. doi: 10.1002/2016GL071372

Hitchcock, P., & Shepherd, T. G. (2012). Zonal mean dynamics of Extended Recoveries from Stratospheric Sudden Warmings. *Journal of the Atmospheric Sciences*, 120914093211006. doi: 10.1175/JAS-D-12-0111.1

Hitchcock, P., Shepherd, T. G., & Manney, G. L. (2013). Statistical Characterization of Arctic Polar-Night Jet Oscillation Events. *Journal of Climate*, *26*(6), 2096–2116. doi: 10.1175/JCLI-D-12-00202.1

Hitchcock, P., & Simpson, I. R. (2014). The Downward Influence of Stratospheric Sudden Warmings. *J. Atmos. Sci.*, *71*(10), 3856-3876.

Hitchcock, P., & Simpson, I. R. (2016). Quantifying Eddy Feedbacks and Forcings in the Tropospheric Response to Stratospheric Sudden Warmings. *Journal of the Atmospheric Sciences*, *73*(9), 3641–3657.

Hoffmann, P., Singer, W., Keuer, D., Hocking, W. K., Kunze, M., & Murayama, Y. (2007). Latitudinal and longitudinal variability of mesospheric winds and temperatures during stratospheric warming events. *J. Atmos. Solar-Terrestrial Phys.*, *69*(17), 2355–2366. doi: https://doi.org/10.1016/j.jastp.2007.06.010

Holton, J. R. (1980). The dynamics of sudden stratospheric warmings. *Annual Review of Earth and Planetary Sciences*, *8*(1), 169-190. doi: 10.1146/annurev.ea

.08.050180.001125

Holton, J. R., & Mass, C. (1976). Stratospheric vacillation cycles. *Journal of the Atmospheric Sciences*, *33*(11), 2218–2225.

Holton, J. R., & Tan, H.-C. (1980). The influence of the equatorial quasi-biennial oscillation on the global circulation at 50 mb. *Journal of the Atmospheric Sciences*, *37*(10), 2200–2208.

Hoskins, B. J., McIntyre, M. E., & Robertson, A. W. (1985). On the use and significance of isentropic potential vorticity maps. *Quarterly Journal of the Royal Meteorological Society*, *111*(470), 877-946. doi: 10.1002/qj.49711147002

Hu, D., & Guan, Z. (2018). Decadal relationship between the stratospheric arctic vortex and pacific decadal oscillation. *Journal of Climate*, *31*(9), 3371–3386.

Iza, M., Calvo, N., & Manzini, E. (2016). The stratospheric pathway of la nia. *Journal of Climate*, *29*(24), 8899-8914. doi: 10.1175/JCLI-D-16-0230.1

Jee, G., Burns, A. G., Wang, W., Solomon, S. C., Schunk, R. W., Scherliess, L., … Zhu, L. (2007). Duration of an ionospheric data assimilation initialization of a coupled thermosphere-ionosphere model. *Sp. Weather*, *5*(1). doi: 10.1029/2006SW000250

Johnson, K. W. (1969). A preliminary study of the stratospheric warming of December 1967January 1968. *Mon. Wea. Rev.*, *97*, 553-564. doi: 10.1175/1520-0493(1969)097⟨0553:APSOTS⟩2.3.CO;2

Jucker, M. (2016). Are Sudden Stratospheric Warmings Generic? Insights from an Idealized GCM. *Journal of the Atmospheric Sciences*, *73*(12), 5061-5080. doi: 10.1175/JAS-D-15-0353.1

Jucker, M., & Reichler, T. (2018). Dynamical precursors for statistical prediction of stratospheric sudden warming events. *Geophysical Research Letters*, *45*(23), 13,124-13,132. doi: 10.1029/2018GL080691

Julian, P. R., & Labitzke, K. G. (1965). A study of atmospheric energetics during the januaryfebruary 1963 stratospheric warming. *J. Atmos. Sci.*, *22*, 597-610. doi: 10.1175/1520-0469(1965)022⟨0597:ASOAED⟩2.0.CO;2

Kang, W., & Tziperman, E. (2017). More frequent sudden stratospheric warming events due to enhanced mjo forcing expected in a warmer climate. *Journal of Climate*, *30*(21), 8727–8743.

Karlsson, B., Körnich, H., & Gumbel, J. (2007). Evidence for interhemispheric stratosphere-mesosphere coupling derived from noctilucent cloud properties. *Geophys. Res. Lett.*, *34*(16). doi: 10.1029/2007GL030282

Karlsson, B., McLandress, C., & Shepherd, T. G. (2009). Inter-hemispheric mesospheric coupling in a comprehensive middle atmosphere model. *J. Atmos. Solar-Terrestrial Phys.*, *71*(3), 518–530. doi: https://doi.org/10.1016/j.jastp.2008.08.006

Karpechko, A. Y. (2018). Predictability of Sudden Stratospheric Warmings in the ECMWF Extended-Range Forecast System. *Monthly Weather Review*, *146*(4), 1063–1075.

Karpechko, A. Y., Charlton-Perez, A., Balmaseda, M., Tyrrell, N., & Vitart, F. (2018). Predicting sudden stratospheric warming 2018 and its climate impacts with a multimodel ensemble. *Geophysical Research Letters*, *45*(24), 13–538. doi: 10.1029/2018GL081091

Karpechko, A. Y., Hitchcock, P., Peters, D. H. W., & Schneidereit, A. (2017). Predictability of downward propagation of major sudden stratospheric warmings. *Quarterly Journal of the Royal Meteorological Society*, *104*, 30937.

Kiesewetter, G., Sinnhuber, B.-M., Vountas, M., Weber, M., & Burrows, J. P. (2010, 5). A long-term stratospheric ozone data set from assimilation of satellite observations: High-latitude ozone anomalies. *Journal of Geophysical Research: Atmospheres*, *115*(D10). doi: 10.1029/2009JD013362

Kim, J., Son, S.-W., Gerber, E. P., & Park, H.-S. (2017). Defining Sudden Stratospheric Warming in Climate Models: Accounting for Biases in Model Climatologies. *Journal of Climate*, *30*, 55295546. doi: 10.1175/JCLI-D-16-0465.1

King, A., Butler, A., Jucker, M., Earl, N., & Rudeva, I. (2019). Observed relationships between sudden stratospheric warmings and European climate extremes. *Journal of Geophysical Research: Atmospheres*, *124*, 13943 13961. doi: 10.1029/2019JD030480

Kobayashi, S., Ota, Y., Harada, Y., Ebita, A., Moriya, M., Onoda, H., ... Takahashi, K. (2015). The jra-55 reanalysis: General specifications and basic characteristics. *Journal of the Meteorological Society of Japan. Ser. II*, *93*(1), 5–48. doi: 10.2151/jmsj.2015-001

Kodera, K. (2006). Influence of stratospheric sudden warming on the equatorial troposphere. *Geophysical Research Letters*, *33*(6).

Kodera, K., Eguchi, N., Lee, J., Kuroda, Y., & Yukimoto, S. (2011, 7 14). Sudden changes in the tropical stratospheric and tropospheric circulation during january 2009. *Journal of the Meteorological Society of Japan*, *89*, 283–290. doi: 10.2151/jmsj.2011-308

Kodera, K., Mukougawa, H., Maury, P., Ueda, M., & Claud, C. (2016). Absorbing and reflecting sudden stratospheric warming events and their relationship with tropospheric circulation. *Journal of Geophysical Research-Atmospheres*, *121*(1), 80–94.

Kolstad, E. W., Breiteig, T., & Scaife, A. A. (2010). The association between stratospheric weak polar vortex events and cold air outbreaks in the Northern Hemisphere. *Quarterly Journal of the Royal Meteorological Society*, *136*(649), 886–893.

Körnich, H., & Becker, E. (2010). A simple model for the interhemispheric coupling of the middle atmosphere circulation. *Adv. Sp. Res.*, *45*(5), 661–668. doi: https://doi.org/10.1016/j.asr.2009.11.001

Kruger, K., Naujokat, B., & Labitzke, K. (2005). The Unusual Midwinter Warming in the Southern Hemisphere Stratosphere 2002. *Journal of Atmospheric Sciences*, *62*(3), 603–613.

Kuroda, Y., & Kodera, K. (2004). Role of the Polar-night Jet Oscillation on the formation of the Arctic Oscillation in the Northern Hemisphere winter. *Journal of Geophysical Research: Atmospheres*, *109*(D11). doi: 10.1029/2003JD004123

Kuttippurath, J., & Nikulin, G. (2012). A comparative study of the major sudden stratospheric warmings in the arctic winters 2003/2004 – 2009/2010. *Atmospheric Chemistry and Physics*, *12*(17), 8115–8129. doi: 10.5194/acp-12-8115-2012

Krnich, H., & Becker, E. (2010). A simple model for the interhemispheric coupling of the middle atmosphere circulation. *Advances in Space Research*, *45*(5), 661 - 668. doi: https://doi.org/10.1016/j.asr.2009.11.001

Labitzke, K. (1965). On the mutual relation between stratosphere and troposphere during periods of stratospheric warmings in winter. *Journal of Applied Meteorology*.

Labitzke, K. (1977). Interannual Variability of the Winter Stratosphere in the Northern Hemisphere. *Monthly Weather Review*, *105*(6), 762–770. doi: 10.1175/1520-0493(1977)105⟨0762:IVOTWS⟩2.0.CO;2

Labitzke, K. (1981). Stratospheric-Mesospheric Midwinter Disturbances - a Summary of Observed Characteristics. *Journal of Geophysical Research-Oceans and Atmospheres*, *86*(NC10), 9665–9678. doi: 10.1029/JC086iC10p09665

Labitzke, K. (1982). On the interannual variability of the middle stratosphere during the northern winters. *Journal of the Meteorological Society of Japan. Ser. II*, *60*(1), 124-139. doi: 10.2151/jmsj1965.60.1_124

Labitzke, K. (1987). Sunspots, the qbo, and the stratospheric temperature in the north polar region. *Geophysical Research Letters*, *14*(5), 535–537.

Labitzke, K., Kunze, M., & Brönnimann, S. (2006). Sunspots, the qbo and the stratosphere in the north polar region–20 years later. *Meteorologische*

Zeitschrift, *15*(3), 355–363.

Lee, S. H., Charlton-Perez, A., Furtado, J., & Woolnough, S. (2019). Abrupt stratospheric vortex weakening associated with north atlantic anticyclonic wave breaking. *Journal of Geophysical Research: Atmospheres*, *124*(15), 8563–8575. doi: 10.1029/2019JD030940

Lehtonen, I., & Karpechko, A. Y. (2016). Observed and modeled tropospheric cold anomalies associated with sudden stratospheric warmings. *Journal of Geophysical Research: Atmospheres*, *121*(4), 1591–1610. doi: 10.1002/2015JD023860

Lim, E.-P., Hendon, H. H., Boschat, G., Hudson, D., Thompson, D. W. J., Dowdy, A. J., & Arblaster, J. M. (2019). Australian hot and dry extremes induced by weakenings of the stratospheric polar vortex. *Nature Geoscience*, *12*(11), 896–901.

Lim, E. P., Hendon, H. H., & Thompson, D. W. J. (2018). Seasonal Evolution of Stratosphere-Troposphere Coupling in the Southern Hemisphere and Implications for the Predictability of Surface Climate. *Journal of Geophysical Research-Atmospheres*, *123*(21), 12,002–12,016.

Limpasuvan, V., Orsolini, Y. J., Chandran, A., Garcia, R. R., & Smith, A. K. (2016). On the composite response of the MLT to major sudden stratospheric warming events with elevated stratopause. *J. Geophys. Res. Atmos.*, *121*(9), 4518–4537. doi: 10.1002/2015JD024401

Limpasuvan, V., Thompson, D. W. J., & Hartman, D. L. (2004). The life cycle of the Northern Hemisphere sudden stratospheric warmingss. *J. Climate*, *17*(13), 2584–2596. doi: 10.1175/1520-0442(2004)017⟨2584:TLCOTN⟩2.0.CO;2

Lindgren, E. A., Sheshadri, A., & Plumb, R. A. (2018). Sudden stratospheric warming formation in an idealized general circulation model using three types of tropospheric forcing. *Journal of Geophysical Research: Atmospheres*, *123*(18), 10,125-10,139. doi: 10.1029/2018JD028537

Liu, H., Jin, H., Miyoshi, Y., Fujiwara, H., & Shinagawa, H. (2013). Upper atmosphere response to stratosphere sudden warming: Local time and height dependence simulated by GAIA model. *Geophys. Res. Lett.*, *40*(3), 635–640. doi: 10.1002/grl.50146

Liu, H., Miyoshi, Y., Miyahara, S., Jin, H., Fujiwara, H., & Shinagawa, H. (2014). Thermal and dynamical changes of the zonal mean state of the thermosphere during the 2009 SSW: GAIA simulations. *J. Geophys. Res. Sp. Phys.*, *119*(8), 6784–6791. doi: 10.1002/2014JA020222

Liu, H. L., & Roble, R. G. (2002). A study of a self-generated stratospheric sudden warming and its mesosphericlower thermospheric impacts using the coupled TIME-GCM/CCM3. *J. Geophys. Res. Atmos.*, *107*(D23), ACL 15–1–ACL 15–18. doi: 10.1029/2001JD001533

Lubis, S. W., Huang, C., Nakamura, N., Omrani, N. E., & Jucker, M. (2018). Role of finite-amplitude Rossby waves and nonconservative processes in downward migration of extratropical flow anomalies. *Journal of the Atmospheric Sciences*.

Maher, P., Gerber, E. P., Medeiros, B., Merlis, T. M., Sherwood, S., Sheshadri, A., … Zurita-Gotor, P. (2019). Model hierarchies for understanding atmospheric circulation. *Reviews of Geophysics*, *57*(2), 250-280. doi: 10.1029/2018RG000607

Manney, G. L., Harwood, R. S., MacKenzie, I. A., Minschwaner, K., Allen, D. R., Santee, M. L., … Fuller, R. A. (2009). Satellite observations and modeling of transport in the upper troposphere through the lower mesosphere during the 2006 major stratospheric sudden warming. *Atmospheric Chemistry and Physics*, *9*(14), 4775–4795. doi: 10.5194/acp-9-4775-2009

Manney, G. L., Krüger, K., Pawson, S., Minschwaner, K., Schwartz, M. J., Daffer, W. H., … Waters, J. W. (2008). The evolution of the stratopause during the 2006 major warming: Satellite data and assimilated meteorological analyses. *J.*

Geophys. Res. Atmos., *113*(D11). doi: 10.1029/2007JD009097
Manney, G. L., Lawrence, Z. D., Santee, M. L., Livesey, N. J., Lambert, A., & Pitts, M. C. (2015). Polar processing in a split vortex: Arctic ozone loss in early winter 2012/2013. *Atmospheric Chemistry and Physics*, *15*(10), 5381–5403. doi: 10.5194/acp-15-5381-2015
Manney, G. L., Schwartz, M. J., Krger, K., Santee, M. L., Pawson, S., Lee, J. N., ... Livesey, N. J. (2009). Aura microwave limb sounder observations of dynamics and transport during the record-breaking 2009 arctic stratospheric major warming. *Geophysical Research Letters*, *36*(12). doi: 10.1029/2009GL038586
Marshall, A., & Scaife, A. A. (2010). Improved predictability of stratospheric sudden warming events in an atmospheric general circulation model with enhanced stratospheric resolution. *Journal of Geophysical Research*, *115*, D16114, doi:10.1029/2009JD012643.
Martineau, P., Son, S.-W., Taguchi, M., & Butler, A. H. (2018). A comparison of the momentum budget in reanalysis datasets during sudden stratospheric warming events. *Atmospheric Chemistry and Physics*, *18*(10), 7169–7187. doi: 10.5194/acp-18-7169-2018
Martius, O., Polvani, L. M., & Davies, H. C. (2009). Blocking precursors to stratospheric sudden warming events. *Geophysical Research Letters*, *36*(14), L14806. doi: 10.1029/2009GL038776
Matsuno, T. (1971). A Dynamical Model of the Stratospheric Sudden Warming. *Journal of the Atmospheric Sciences*, *28*(8), 1479–1494. doi: 10.1175/1520-0469(1971)028⟨1479:ADMOTS⟩2.0.CO;2
Matthewman, N. J., & Esler, J. G. (2011). Stratospheric Sudden Warmings as Self-Tuning Resonances. Part I: Vortex Splitting Events. *Journal of the Atmospheric Sciences*, *68*, 2481–2504.
Maute, A., Hagan, M. E., Yudin, V., Liu, H. L., & Yizengaw, E. (2015). Causes of the longitudinal differences in the equatorial vertical E × B drift during the 2013 SSW period as simulated by the TIME-GCM. *J. Geophys. Res. Sp. Phys.*, *120*(6), 5117–5136. doi: 10.1002/2015JA021126
Maycock, A. C., & Hitchcock, P. (2015). Do split and displacement sudden stratospheric warmings have different annular mode signatures? *Geophysical Research Letters*, *42*(24), 10943–10951.
Maycock, A. C., Masukwedza, G. I. T., Hitchcock, P., & Simpson, I. R. (2020). A Regime Perspective on the North Atlantic Eddy-Driven Jet Response to Sudden Stratospheric Warmings. *Journal of Climate*, *33*(9), 3901–3917.
McInturff, R. (1978). Stratospheric warmings: Synoptic, dynamic and general-circulation aspects. *Tech.Rep. NASA-RP-1017*, *NASA Ref.*, 19.
McIntyre, M. E. (1982). How well do we understand the dynamics of stratospheric warmings. *J. Met. Soc. Japan*, *60*, 37–64.
McIntyre, M. E., & Palmer, T. N. (1983). Breaking planetary waves in the stratosphere. *Nature*, *305*, 593–600.
McIntyre, M. E., & Palmer, T. N. (1984). The "surf zone" in the stratosphere. *Journal of Atmospheric and Terrestrial Physics*, *46*, 825–849.
McLandress, C., & Shepherd, T. G. (2009a). Impact of climate change on stratospheric sudden warmings as simulated by the canadian middle atmosphere model. *Journal of Climate*, *22*(20), 5449-5463. doi: 10.1175/2009JCLI3069.1
McLandress, C., & Shepherd, T. G. (2009b). Impact of Climate Change on Stratospheric Sudden Warmings as Simulated by the Canadian Middle Atmosphere Model. *Journal of Climate*, *22*(20), 5449–5463. doi: 10.1175/2009JCLI3069.1
Meraner, K., Schmidt, H., Manzini, E., Funke, B., & Gardini, A. (2016). Sensitivity of simulated mesospheric transport of nitrogen oxides to parameterized gravity waves. *J. Geophys. Res. Atmos.*, *121*(20), 12,12–45,61. doi: 10.1002/2016JD025012
Mitchell, D. M., Charlton-Perez, A. J., & Gray, L. J. (2011). Characterizing the

Variability and Extremes of the Stratospheric Polar Vortices Using 2D Moment Analysis. *Journal of the Atmospheric Sciences*, *68*(6), 1194–1213. doi: 10.1175/2010JAS3555.1

Mitchell, D. M., Gray, L. J., Anstey, J., Baldwin, M. P., & Charlton-Perez, A. J. (2013). The Influence of Stratospheric Vortex Displacements and Splits on Surface Climate. *Journal of Climate*, *26*(8), 2668–2682. doi: 10.1175/JCLI-D-12-00030.1

Mitchell, D. M., Misios, S., Gray, L., Tourpali, K., Matthes, K., Hood, L., … Krivolutsky, A. (2015). Solar signals in CMIP-5 simulations: The stratospheric pathway. *Quarterly Journal of the Royal Meteorological Society*, *141*(691), 2390–2403.

Mitchell, D. M., Osprey, S. M., & Gray, L. J. (2012). The Effect of Climate Change on the Variability of the Northern Hemisphere Stratospheric Polar Vortex. *Journal of the Atmospheric Sciences*, *69*, 2608 – 2618.

Morgenstern, O., Hegglin, M. I., Rozanov, E., O'Connor, F. M., Abraham, N. L., Akiyoshi, H., … Zeng, G. (2017). Review of the global models used within phase 1 of the chemistry–climate model initiative (ccmi). *Geoscientific Model Development*, *10*(2), 639–671. doi: 10.5194/gmd-10-639-2017

Naito, Y., Taguchi, M., & Yoden, S. (2003). A parameter sweep experiment on the effects of the equatorial qbo on stratospheric sudden warming events. *Journal of the Atmospheric Sciences*, *60*(11), 1380-1394. doi: 10.1175/1520-0469(2003)060⟨1380:APSEOT⟩2.0.CO;2

Nakagawa, K. I., & Yamazaki, K. (2006). What kind of stratospheric sudden warming propagates to the troposphere? *Geophysical Research Letters*, *33*(4). doi: 10.1029/2005GL024784

Nakamura, N. (1996, June). Two-Dimensional Mixing, Edge Formation, and Permeability Diagnosed in an Area Coordinate. *J. Atmos. Sci.*, *53*, 1524-1537.

Newman, P. A., Nash, E. R., & Rosenfield, J. E. (2001). What controls the temperature of the Artic stratosphere during spring? *Journal of Geophysical Research: Atmospheres*, *106*, 19999–20010.

Nishii, K., Nakamura, H., & Miyasaka, T. (2009). Modulations in the planetary wave field induced by upward-propagating rossby wave packets prior to stratospheric sudden warming events: A case-study. *Quarterly Journal of the Royal Meteorological Society*, *135*(638), 39-52. doi: 10.1002/qj.359

Noguchi, S., Mukougawa, H., Kuroda, Y., Mizuta, R., Yabu, S., & Yoshimura, H. (2016). Predictability of the stratospheric polar vortex breakdown: An ensemble reforecast experiment for the splitting event in January 2009. *Journal of Geophysical Research-Atmospheres*, *121*(7), 3388–3404.

Oberheide, J., Pedatella, N. M., Gan, Q., Kumari, K., Burns, A. G., & Eastes, R. W. (2020). Thermospheric Composition O/N Response to an Altered Meridional Mean Circulation During Sudden Stratospheric Warmings Observed by GOLD. *Geophys. Res. Lett.*, *47*(1), e2019GL086313. doi: 10.1029/2019GL086313

Oehrlein, J., Chiodo, G., & Polvani, L. M. (2019). Separating and quantifying the distinct impacts of El Niño and sudden stratospheric warmings on North Atlantic and Eurasian wintertime climate. *Atmospheric Science Letters*, *20*(7), e923. doi: 10.1002/asl.923

Oehrlein, J., Chiodo, G., & Polvani, L. M. (2020). The effect of interactive ozone chemistry on weak and strong stratospheric polar vortex events. *Atmospheric Chemistry and Physics*, *20*(17), 10531–10544. doi: 10.5194/acp-20-10531-2020

O'Neill, A., Charlton-Perez, A., & Polvani, L. (2015). Middle atmosphere — stratospheric sudden warmings. In G. R. North, J. Pyle, & F. Zhang (Eds.), *Encyclopedia of atmospheric sciences (second edition)* (Second Edition ed., p. 30 - 40). Oxford: Academic Press. doi: https://doi.org/10.1016/

B978-0-12-382225-3.00230-9

Padatella, N. M., Chau, J. L., Schmidt, H., Gocharenko, L. P., Stolle, C., Hocke, K., ... Siddiqui, T. A. (2018). How sudden stratospheric warming affects the whole atmosphere. *EOS*, *99*. doi: https://doi.org/10.1029/2018EO092441

Palmeiro, F. M., Barriopedro, D., García-Herrera, R., & Calvo, N. (2015). Comparing Sudden Stratospheric Warming Definitions in Reanalysis Data. *Journal of Climate*. doi: 10.1175/JCLI-D-15-0004.1

Palmer, T. N. (1981). Aspects of stratospheric sudden warmings studied from a transformed Eulerian-mean viewpoint. *Journal of Geophysical Research: Oceans*, *86*(C10), 96799687. doi: 10.1029/JC086iC10p09679

Patra, A. K., Pavan Chaitanya, P., Sripathi, S., & Alex, S. (2014). Ionospheric variability over Indian low latitude linked with the 2009 sudden stratospheric warming. *J. Geophys. Res. Sp. Phys.*, *119*(5), 4044–4061. doi: 10.1002/2014JA019847

Pedatella, N. M., & Liu, H. L. (2013). The influence of atmospheric tide and planetary wave variability during sudden stratosphere warmings on the low latitude ionosphere. *J. Geophys. Res. Sp. Phys.*, *118*(8), 5333–5347. doi: 10.1002/jgra.50492

Pedatella, N. M., Liu, H. L., Marsh, D. R., Raeder, K., Anderson, J. L., Chau, J. L., ... Siddiqui, T. A. (2018). Analysis and Hindcast Experiments of the 2009 Sudden Stratospheric Warming in WACCMX+DART. *J. Geophys. Res. Sp. Phys.*, *123*(4), 3131–3153. doi: 10.1002/2017JA025107

Pedatella, N. M., Liu, H. L., Richmond, A. D., Maute, A., & Fang, T.-W. (2012). Simulations of solar and lunar tidal variability in the mesosphere and lower thermosphere during sudden stratosphere warmings and their influence on the low-latitude ionosphere. *J. Geophys. Res. Sp. Phys.*, *117*(A8). doi: 10.1029/2012JA017858

Pedatella, N. M., & Maute, A. (2015). Impact of the semidiurnal lunar tide on the midlatitude thermospheric wind and ionosphere during sudden stratosphere warmings. *J. Geophys. Res. Sp. Phys.*, *120*(12), 10,710–740,753. doi: 10.1002/2015JA021986

Pedatella, N. M., Richmond, A. D., Maute, A., & Liu, H. L. (2016). Impact of semidiurnal tidal variability during SSWs on the mean state of the ionosphere and thermosphere. *J. Geophys. Res. Sp. Phys.*, *121*(8), 8077–8088. doi: 10.1002/2016JA022910

Perlwitz, J., & Harnik, N. (2003). Observational evidence of a stratospheric influence on the troposphere by planetary wave reflection. *Journal of Climate*, *16*, 30113026.

Pettit, J. M., Randall, C. E., Peck, E. D., Marsh, D. R., van de Kamp, M., Fang, X., ... Funke, B. (2019). Atmospheric Effects of >30-keV Energetic Electron Precipitation in the Southern Hemisphere Winter During 2003. *J. Geophys. Res. Sp. Phys.*, *124*(10), 8138–8153. doi: 10.1029/2019JA026868

Plumb, R. A. (1981). Instability of the distorted polar night vortex: A theory of stratospheric warmings. *Journal of the Atmospheric Sciences*, *38*(11), 2514–2531.

Plumb, R. A. (1989). On the Seasonal Cycle of Stratospheric Planetary Waves. *PAGEOPH*, *130*(2/3), 233–242.

Plumb, R. A., & Semeniuk, K. (2003). Downward migration of extratropical zonal wind anomalies. *Journal of Geophysical Research: Atmospheres (1984–2012)*, *108*(D7).

Polvani, L. M., Sun, L., Butler, A., Richter, J., & Deser, C. (2017). Distinguishing Stratospheric Sudden Warmings from ENSO as Key Drivers of Wintertime Climate Variability over the North Atlantic and Eurasia. *Journal of Climate*, *30*, 19591969.

Polvani, L. M., & Waugh, D. W. (2004). Upward wave activity flux as a precursor to extreme stratospheric events and subsequent anomalous surface weather regimes. *Journal of Climate*, *17*, 3548–3554.

Quiroz, R. S. (1977). The tropospherícstratospheric polar vortex breakdown of january 1977. *Geophys. Res. Lett.*, *4*, 151-154. doi: 10.1029/GL004i004p00151

Quiroz, R. S. (1986). The association of stratospheric warmings with tropospheric blocking. *Journal of Geophysical Research: Atmospheres*, *91*(D4), 5277-5285. doi: 10.1029/JD091iD04p05277

Randall, C. E., Harvey, V. L., Holt, L. A., Marsh, D. R., Kinnison, D., Funke, B., & Bernath, P. F. (2015). Simulation of energetic particle precipitation effects during the 20032004 Arctic winter. *J. Geophys. Res. Sp. Phys.*, *120*(6), 5035–5048. doi: 10.1002/2015JA021196

Randall, C. E., Harvey, V. L., Singleton, C. S., Bernath, P. F., Boone, C. D., & Kozyra, J. U. (2006). Enhanced NOx in 2006 linked to strong upper stratospheric Arctic vortex. *Geophys. Res. Lett.*, *33*(18). doi: 10.1029/2006GL027160

Randall, C. E., Harvey, V. L., Siskind, D. E., France, J., Bernath, P. F., Boone, C. D., & Walker, K. A. (2009). NOx descent in the Arctic middle atmosphere in early 2009. *Geophys. Res. Lett.*, *36*(18). doi: 10.1029/2009GL039706

Rao, J., Garfinkel, C. I., Chen, H., & White, I. (2019). The 2019 new year stratospheric sudden warming and its real-time predictions in multiple s2s models. *Journal of Geophysical Research: Atmospheres*, *124*(21), 11155-11174. doi: 10.1029/2019JD030826

Rao, J., Garfinkel, C. I., & White, I. (2020b). Predicting the downward and surface influence of the february 2018 and january 2019 sudden stratospheric warming events in subseasonal to seasonal (s2s) models. *Journal of Geophysical Research: Atmospheres*, *125*(2), e2019JD031919.

Rao, J., Garfinkel, C. I., & White, I. P. (2020a). Impact of the quasi-biennial oscillation on the northern winter stratospheric polar vortex in cmip5/6 models. *Journal of Climate*, *33*(11), 4787–4813. doi: 10.1175/JCLI-D-19-0663.1

Rao, J., Garfinkel, C. I., White, I. P., & Schwartz, C. (2020). The southern hemisphere minor sudden stratospheric warming in september 2019 and its predictions in s2s models. *Journal of Geophysical Research: Atmospheres*, *125*(14), e2020JD032723. (e2020JD032723 2020JD032723) doi: 10.1029/2020JD032723

Rao, J., Ren, R., Chen, H., Liu, X., Yu, Y., Hu, J., & Zhou, Y. (2019). Predictability of stratospheric sudden warmings in the beijing climate center forecast system with statistical error corrections. *Journal of Geophysical Research: Atmospheres*, *124*(15), 8385–8400.

Reichler, T., Kim, J., Manzini, E., & Kröger, J. (2012). A stratospheric connection to Atlantic climate variability. *Nature Geoscience*, *5*(11), 783–787.

Rind, D., Suozzo, R., Balachandran, N. K., & Prather, M. J. (1990). Climate change and the middle atmosphere. part i: The doubled co2 climate. *Journal of the Atmospheric Sciences*, *47*(4), 475-494. doi: 10.1175/1520-0469(1990)047⟨0475:CCATMA⟩2.0.CO;2

Runde, T., Dameris, M., Garny, H., & Kinnison, D. E. (2016). Classification of stratospheric extreme events according to their downward propagation to the troposphere. *Geophysical Research Letters*, *43*(12), 6665–6672.

Salminen, A., Asikainen, T., Maliniemi, V., & Mursula, K. (2020). Dependence of sudden stratospheric warmings on internal and external drivers. *Geophysical Research Letters*, *47*, e2019GL086444. doi: 10.1029/2019GL086444

Scaife, A., Karpechko, A. Y., Baldwin, M., Brookshaw, A., Butler, A., Eade, R., … others (2016). Seasonal winter forecasts and the stratosphere. *Atmospheric Science Letters*, *17*(1), 51–56.

Scherhag, R. (1952a). Die explosionsartigen Stratosphrenerwrmungen des Sptwinters 1951/52. *Berichte des Deutschen Wetterdienstes in der US-Zone*, *6*(38), 51-63.

Scherhag, R. (1952b). Einflu von Sonneneruptionen auf Stratosphrenwetter nachgewiesen. *Wetterkarte des Deutschen Wetterdienstes in der US-Zone, 14. Mrz 1952*.

Scherhag, R. (1965). Neuere Ergebnisse der Meteorologie der Hochatmosphre. *Die Naturwissenschaften*, *11*, 279-286.

Scherhag, R., Labitzke, K., & Finger, F. G. (1970). Developments in stratospheric and mesospheric analyses which dictate the need for additional upper air data. *Meteorol. Monographs*, *11*(33), 85-90.

Schoeberl, M. R. (1978). Stratospheric warmings: Observations and theory. *Reviews of Geophysics*, *16*(4), 521-538. doi: 10.1029/RG016i004p00521

Schwartz, C., & Garfinkel, C. I. (2017). Relative roles of the mjo and stratospheric variability in north atlantic and european winter climate. *Journal of Geophysical Research: Atmospheres*, *122*(8), 4184-4201. doi: 10.1002/2016JD025829

Schwartz, C., & Garfinkel, C. I. (2020). Troposphere-stratosphere coupling in subseasonal-to-seasonal models and its importance for a realistic extratropical response to the madden-julian oscillation. *Journal of Geophysical Research: Atmospheres*, *125*(10), e2019JD032043.

Scinocca, J. F., & Haynes, P. H. (1998). Dyamical forcing of stationary planetary waves by tropospheric baroclinic eddies. *Journal of the Atmospheric Sciences*, *55*, 2361–2392.

Scott, R. K. (2016). A new class of vacillations of the stratospheric polar vortex. *Quarterly Journal of the Royal Meteorological Society*, *142*(698), 1948-1957. doi: 10.1002/qj.2788

Scott, R. K., & Polvani, L. M. (2004). Stratospheric control of upward wave flux near the tropopause. *Geophysical Research Letters*, *31*, L02115. doi: 10.1029/2003GL017965

Scott, R. K., & Polvani, L. M. (2006). Internal variability of the winter stratosphere. Part I: Time-independent forcing. *Journal of the Atmospheric Sciences*, *63*, 2758–2776.

Scrase, F. J. (1953). Relatively high stratospheric temperature of February 1951. *The Meteorological Magazine*, *82*(967), 15-18.

Seviour, W. J. M., Gray, L. J., & Mitchell, D. M. (2016). Stratospheric polar vortex splits and displacements in the high-top cmip5 climate models. *Journal of Geophysical Research: Atmospheres*, *121*(4), 1400–1413. doi: 10.1002/2015JD024178

Seviour, W. J. M., Mitchell, D. M., & Gray, L. J. (2013). A practical method to identify displaced and split stratospheric polar vortex events. *Geophysical Research Letters*, *40*, 5268–5273. doi: 10.1002/grl.50927

Shaw, T. A., Perlwitz, J., & Harnik, N. (2010). Downward wave coupling between the stratosphere and troposphere: The importance of meridional wave guiding and comparison with zonal-mean coupling. *Journal of Climate*, *23*, 63656381.

Shepherd, T., Plumb, R. A., & Wofsy, S. C. (2005). Preface. *Journal of the Atmospheric Sciences*, *62*(3), 565–566. doi: 10.1175/JAS-9999.1

Siddiqui, T. A., Maute, A., & Pedatella, N. M. (2019). On the Importance of Interactive Ozone Chemistry in Earth-System Models for Studying Mesophere-Lower Thermosphere Tidal Changes during Sudden Stratospheric Warmings. *J. Geophys. Res. Sp. Phys.*, *124*(12), 10690–10707. doi: 10.1029/2019JA027193

Siddiqui, T. A., Stolle, C., & Lühr, H. (2017). Longitude-dependent lunar tidal modulation of the equatorial electrojet during stratospheric sudden warmings. *J. Geophys. Res. Sp. Phys.*, *122*(3), 3760–3776. doi: 10.1002/2016JA023609

Siddiqui, T. A., Stolle, C., Lühr, H., & Matzka, J. (2015). On the relationship between weakening of the northern polar vortex and the lunar tidal amplification in the equatorial electrojet. *J. Geophys. Res. Sp. Phys.*, *120*(11), 10006–10019. doi: 10.1002/2015JA021683

Sigmond, M., Scinocca, J., Kharin, V., & Shepherd, T. (2013). Enhanced seasonal forecast skill following stratospheric sudden warmings. *Nature Geoscience*, *6*(2), 98.

Silverman, V., Harnik, N., Matthes, K., Lubis, S. W., & Wahl, S. (2018). Radiative effects of ozone waves on the northern hemisphere polar vortex and its modulation by the qbo. *Atmospheric Chemistry and Physics*, *18*(9), 6637–6659.

Simpson, I. R., Blackburn, M., & Haigh, J. D. (2009). The Role of Eddies in Driving the Tropospheric Response to Stratospheric Heating Perturbations. *J. Atmos. Sci.*, *66*(5), 1347–1365.

Siscoe, G., & Solomon, S. C. (2006). Aspects of data assimilation peculiar to space weather forecasting. *Sp. Weather*, *4*(4). doi: 10.1029/2005SW000205

Siskind, D. E., Eckermann, S. D., McCormack, J. P., Coy, L., Hoppel, K. W., & Baker, N. L. (2010). Case studies of the mesospheric response to recent minor, major, and extended stratospheric warmings. *J. Geophys. Res. Atmos.*, *115*(D3). doi: 10.1029/2010JD014114

Siskind, D. E., Sassi, F., Randall, C. E., Harvey, V. L., Hervig, M. E., & Bailey, S. M. (2015). Is a high-altitude meteorological analysis necessary to simulate thermosphere-stratosphere coupling? *Geophys. Res. Lett.*, *42*(19), 8225–8230. doi: 10.1002/2015GL065838

Sjoberg, J. P., & Birner, T. (2012). Transient tropospheric forcing of sudden stratospheric warmings. *Journal of the Atmospheric Sciences*, *69*(11), 3420-3432. doi: 10.1175/JAS-D-11-0195.1

Sjoberg, J. P., & Birner, T. (2014). Stratospheric wavemean flow feedbacks and sudden stratospheric warmings in a simple model forced by upward wave activity flux. *Journal of the Atmospheric Sciences*, *71*(11), 4055-4071. doi: 10.1175/JAS-D-14-0113.1

Smith, A. K., Pedatella, N. M., & Mullen, Z. K. (2020). Interhemispheric Coupling Mechanisms in the Middle Atmosphere of WACCM6. *J. Atmos. Sci.*, *77*(3), 1101–1118. doi: 10.1175/JAS-D-19-0253.1

Smith, K. L., & Scott, R. K. (2016). The role of planetary waves in the tropospheric jet response to stratospheric cooling. *Geophysical Research Letters*, *43*(6), 2904–2911.

Smy, L. A., & Scott, R. K. (2009). The influence of stratospheric potential vorticity on baroclinic instability. *Quarterly Journal of the Royal Meteorological Society*, *135*(644), 1673-1683. doi: 10.1002/qj.484

Song, Y., & Robinson, W. A. (2004). Dynamical mechanisms for stratospheric influences on the troposphere. *Journal of the Atmospheric Sciences*, *61*(14), 1711-1725. doi: 10.1175/1520-0469(2004)061⟨1711:DMFSIO⟩2.0.CO;2

Stening, R. J. (1977). Electron density profile changes associated with the equatorial electrojet. *J. Atmos. Terr. Phys.*, *39*(2), 157–164. doi: https://doi.org/10.1016/0021-9169(77)90109-X

Stening, R. J., Meek, C. E., & Manson, A. H. (1996). Upper atmosphere wind systems during reverse equatorial electrojet events. *Geophys. Res. Lett.*, *23*(22), 3243–3246. doi: 10.1029/96GL02611

Stoneback, R. A., Heelis, R. A., Burrell, A. G., Coley, W. R., Fejer, B. G., & Pacheco, E. (2011). Observations of quiet time vertical ion drift in the equatorial ionosphere during the solar minimum period of 2009. *J. Geophys. Res. Sp. Phys.*, *116*(A12). doi: 10.1029/2011JA016712

Stroud, W. G., Nordberg, W., Bandeen, W. R., Bartman, F. L., & Titus, P. (1960). Rocketgrenade measurements of temperatures and winds in the mesosphere over churchill, Canada. *J. Geophys. Res.*, *65*(8), 23072323. doi: 10.1029/JZ065i008p02307

Sun, L., Deser, C., & Tomas, R. A. (2015). Mechanisms of stratospheric and tropospheric circulation response to projected arctic sea ice loss. *Journal of Climate*, *28*(19), 7824–7845.

Sun, L., Robinson, W. A., & Chen, G. (2012). The predictability of stratospheric warming events: More from the troposphere or the stratosphere? *Journal of the Atmospheric Sciences*, *69*(2), 768-783. doi: 10.1175/JAS-D-11-0144.1
Taguchi, M. (2018). Comparison of Subseasonal-to-Seasonal Model Forecasts for Major Stratospheric Sudden Warmings. *Journal of Geophysical Research-Atmospheres*, *123*(18), 10,231–10,247.
Taguchi, M. (2020). Verification of Subseasonal-to-Seasonal Forecasts for Major Stratospheric Sudden Warmings in Northern Winter from 1998/99 to 2012/13. *Advances in Atmospheric Sciences*, *37*(3), 250–258.
Taguchi, M., & Hartmann, D. L. (2006). Increased occurrence of stratospheric sudden warmings during el niño as simulated by waccm. *Journal of climate*, *19*(3), 324–332.
Taguchi, M., & Yoden, S. (2002). Internal interannual variability of the troposphere-stratosphere coupled system in a simple general circulation model. Part I: Parameter sweep experiments. *Journal of the Atmospheric Sciences*, *59*, 3021–3036.
Tao, M., Konopka, P., Ploeger, F., Grooß, J.-U., Müller, R., Volk, C. M., … Riese, M. (2015). Impact of the 2009 major sudden stratospheric warming on the composition of the stratosphere. *Atmospheric Chemistry and Physics*, *15*(15), 8695–8715. doi: 10.5194/acp-15-8695-2015
Teweles, S. (1958). Anomalous warming of the stratosphere over North America in early 1957. *Mon. Wea. Rev*, *86*, 377396.
Teweles, S., & Finger, F. G. (1958). An abrupt change in stratospheric circulation beginning in mid-January 1958. *Mon. Wea. Rev*, *86*, 2328.
Thiblemont, R., Ayarzagüena, B., Matthes, K., Bekki, S., Abalichin, J., & Langematz, U. (2019). Drivers and surface signal of interannual variability of boreal stratospheric final warmings. *Journal of Geophysical Research: Atmospheres*, *124*(10), 5400-5417. doi: 10.1029/2018JD029852
Thompson, D., Baldwin, M., & Solomon, S. (2005). StratosphereTroposphere Coupling in the Southern Hemisphere. *Journal of the Atmospheric Sciences*, *62*, 708715.
Thompson, D., Furtado, J., & Shepherd, T. (2006). On the Tropospheric Response to Anomalous Stratospheric Wave Drag and Radiative Heating. *Journal of the Atmospheric Sciences*, *63*, 26162629.
Tripathi, O. P., Baldwin, M. P., Charlton-Perez, A., Charron, M., Cheung, J. C., Eckermann, S. D., … Stockdale, T. (2016). Examining the predictability of the Stratospheric Sudden Warming of January 2013 using multiple NWP systems. *Monthly Weather Review*, *144*, 1935–1960.
Tripathi, O. P., Baldwin, M. P., Charlton-Perez, A., Charron, M., Eckermann, S. D., Gerber, E. P., … Son, S.-W. (2015). The predictability of the extratropical stratosphere on monthly time-scales and its impact on the skill of tropospheric forecasts. *Quarterly Journal of the Royal Meteorological Society*, *141*(689), 987–1003.
Tung, K. K., & Lindzen, R. S. (1979a). A Theory of Stationary Long Waves. Part I: A Simple Theory of Blocking. *Monthly Weather Review*, *107*(6), 714–734. doi: 10.1175/1520-0493(1979)107⟨0714:ATOSLW⟩2.0.CO;2
Tung, K. K., & Lindzen, R. S. (1979b). A theory of stationary long waves. part i: A simple theory of blocking. *Monthly Weather Review*, *107*(6), 714-734. doi: 10.1175/1520-0493(1979)107⟨0714:ATOSLW⟩2.0.CO;2
Vallis, G. K. (2017). *Atmospheric and oceanic fluid dynamics.* Cambridge, U.K.: Cambridge University Press.
Varotsos, C. (2002). The southern hemisphere ozone hole split in 2002. *Environmental Science and Pollution Research*, *9*, 375-376.
Vial, J., Osborn, T. J., & Lott, F. (2013). Sudden stratospheric warmings and tropospheric blockings in a multi-century simulation of the IPSL-CM5A coupled

climate model. *Climate Dynamics*, *40*, 2401–2414.

von Savigny, C., Rozanov, A., Bovensmann, H., Eichmann, K.-U., Nol, S., Rozanov, V., ... Kaiser, J. W. (2005). The ozone hole breakup in september 2002 as seen by sciamachy on envisat. *Journal of the Atmospheric Sciences*, *62*(3), 721-734. doi: 10.1175/JAS-3328.1

Wang, H., Akmaev, R. A., Fang, T.-W., Fuller-Rowell, T. J., Wu, F., Maruyama, N., & Iredell, M. D. (2014). First forecast of a sudden stratospheric warming with a coupled whole-atmosphere/ionosphere model IDEA. *J. Geophys. Res. Sp. Phys.*, *119*(3), 2079–2089. doi: 10.1002/2013JA019481

Warnecke, G. (1962). ber die Zustandsnderungen der nordhemisphrischen stratosphre. *Meteorologische Abhandlungen, Freie Universitt Berlin*, *28*, 3.

Watson, P. A., & Gray, L. J. (2014). How does the quasi-biennial oscillation affect the stratospheric polar vortex? *Journal of the Atmospheric Sciences*, *71*(1), 391–409.

Watt-Meyer, O., & Kushner, P. J. (2015). The role of standing waves in driving persistent anomalies of upward wave activity flux. *Journal of Climate*, *28*(24), 9941-9954. doi: 10.1175/JCLI-D-15-0317.1

Weber, M., Dhomse, S., Wittrock, F., Richter, A., Sinnhuber, B.-M., & Burrows, J. P. (2003). Dynamical control of nh and sh winter/spring total ozone from gome observations in 19952002. *Geophysical Research Letters*, *30*(11). doi: 10.1029/2002GL016799

Weinberger, I., Garfinkel, C. I., White, I., & Oman, L. D. (2019). The salience of nonlinearities in the boreal winter response to enso: Arctic stratosphere and europe. *Climate Dynamics*, *53*(7-8), 4591–4610.

Wexler, H. (1937). Formation of polar anticyclones. *Monthly Weather Review*, *65*(6), 229–236. doi: 10.1175/1520-0493(1937)65⟨229:FOPA⟩2.0.CO;2

Wheeler, M. C., & Hendon, H. H. (2004). An all-season real-time multivariate mjo index: Development of an index for monitoring and prediction. *Monthly weather review*, *132*(8), 1917–1932. doi: 10.1175/1520-0493(2004)132⟨1917:AARMMI⟩2.0.CO;2

White, I., Garfinkel, C. I., Gerber, E. P., Jucker, M., Aquila, V., & Oman, L. D. (2019). The downward influence of sudden stratospheric warmings: Association with tropospheric precursors. *Journal of Climate*, *32*(1), 85–108.

White, I., Garfinkel, C. I., Gerber, E. P., Jucker, M., Hitchcock, P., & Rao, J. (2020). The generic nature of the tropospheric response to sudden stratospheric warmings. *Journal of Climate*. doi: 10.1175/JCLI-D-19-0697.1

White, I., Lu, H., Mitchell, N. J., & Phillips, T. (2015). Dynamical response to the qbo in the northern winter stratosphere: Signatures in wave forcing and eddy fluxes of potential vorticity. *Journal of the Atmospheric Sciences*, *72*(12), 4487–4507.

Wiehler, J. (1955). Die ergebnisse der berliner radiosonden-hochaufstiege der jahre 1951-1953. *Met. Abh. FU-Berlin*, *Band III*.

Willett, H. C. (1952). Atmospheric reactions to solar corpuscular emissions. *Bull. Amer. Meteor. Soc*, *33*(6), 255–258.

WMO/IQSY. (1964). *International Years of the Quiet Sun (IQSY) 1964-65. Alert messages with special references to stratwarms. WMO/IQSY Report No 6, Secretariat of the World Meteorological Organization, Geneva, Switzerland.* World Meteorological Organization.

Woollings, T., Charlton-Perez, A., Ineson, S., Marshall, A. G., & Masato, G. (2010). Associations between stratospheric variability and tropospheric blocking. *Journal of Geophysical Research: Atmospheres*, *115*(D6). doi: 10.1029/2009JD012742

Yamazaki, Y., Kosch, M. J., & Emmert, J. T. (2015). Evidence for stratospheric sudden warming effects on the upper thermosphere derived from satellite orbital decay data during 19672013. *Geophys. Res. Lett.*, *42*(15), 6180–6188. doi: 10.1002/2015GL065395

Yamazaki, Y., & Richmond, A. D. (2013). A theory of ionospheric response to upward-propagating tides: Electrodynamic effects and tidal mixing effects. *J. Geophys. Res. Sp. Phys.*, *118*(9), 5891–5905. doi: 10.1002/jgra.50487

Zhang, X., & Forbes, J. M. (2014). Lunar tide in the thermosphere and weakening of the northern polar vortex. *Geophys. Res. Lett.*, *41*(23), 8201–8207. doi: 10.1002/2014GL062103

Zülicke, C., & Becker, E. (2013). The structure of the mesosphere during sudden stratospheric warmings in a global circulation model. *Journal of Geophysical Research-Atmospheres*, *118*(5), 2255–2271.

Zülicke, C., Becker, E., Matthias, V., Peters, D. H. W., Schmidt, H., Liu, H. L., … Mitchell, D. M. (2018). Coupling of Stratospheric Warmings with Mesospheric Coolings in Observations and Simulations. *Journal of Climate*, *31*(3), 1107–1133.

Züllig, W. (1973). Relation between the intensity of the stratospheric circumpolar vortex and the accumulation of ozone in the winter hemisphere. *Pure and Appl. Geophys.*, *206*(108), 1544-1552.

Figure 1.

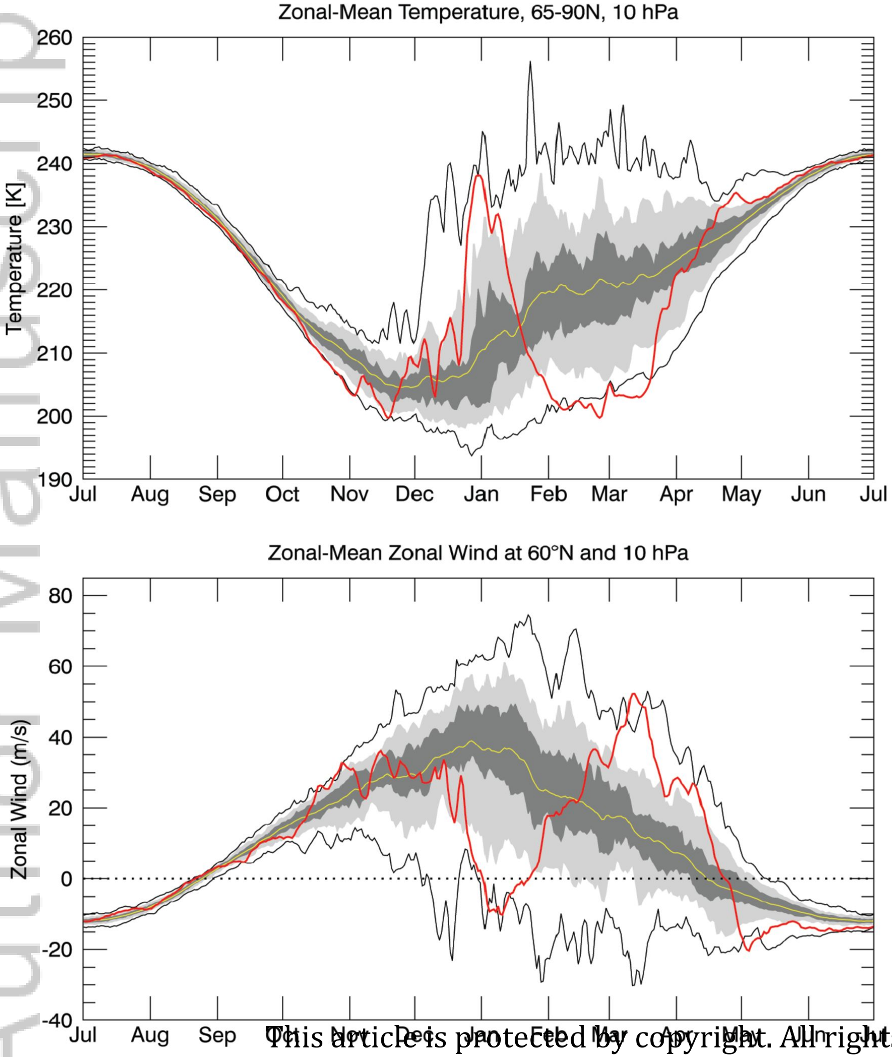
Zonal-Mean Temperature, 65-90N, 10 hPa
Temperature [K]
260
250
240
230
220
210
200
190
Jul
Aug
Sep
Oct
Nov
Dec
Jan
Feb
Mar
Apr
May
Jun
Jul
Zonal-Mean Zonal Wind at 60°N and 10 hPa
Zonal Wind (m/s)
80
60
40
20
0
-20
-40
Jul
Aug
Sep
Oct
Nov
Dec
Jan
Feb
Mar
Apr
May
Jun
Jul

Figure 2.

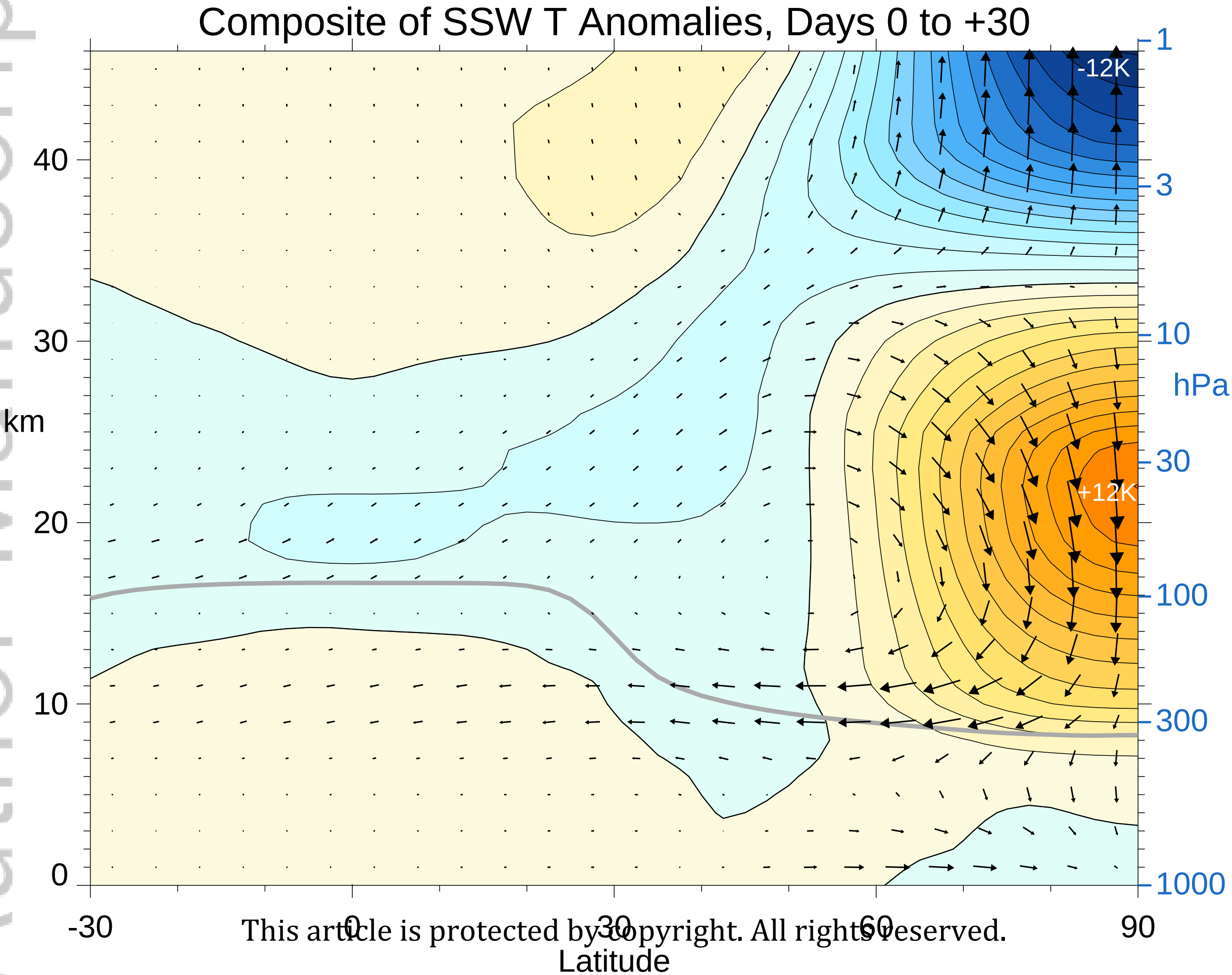
Composite of SSW T Anomalies, Days 0 to +30
-12K
+12K
km
40
30
20
10
0
1
3
10
30
100
300
1000
hPa
-30
0
30
60
90
Latitude

Figure 3.

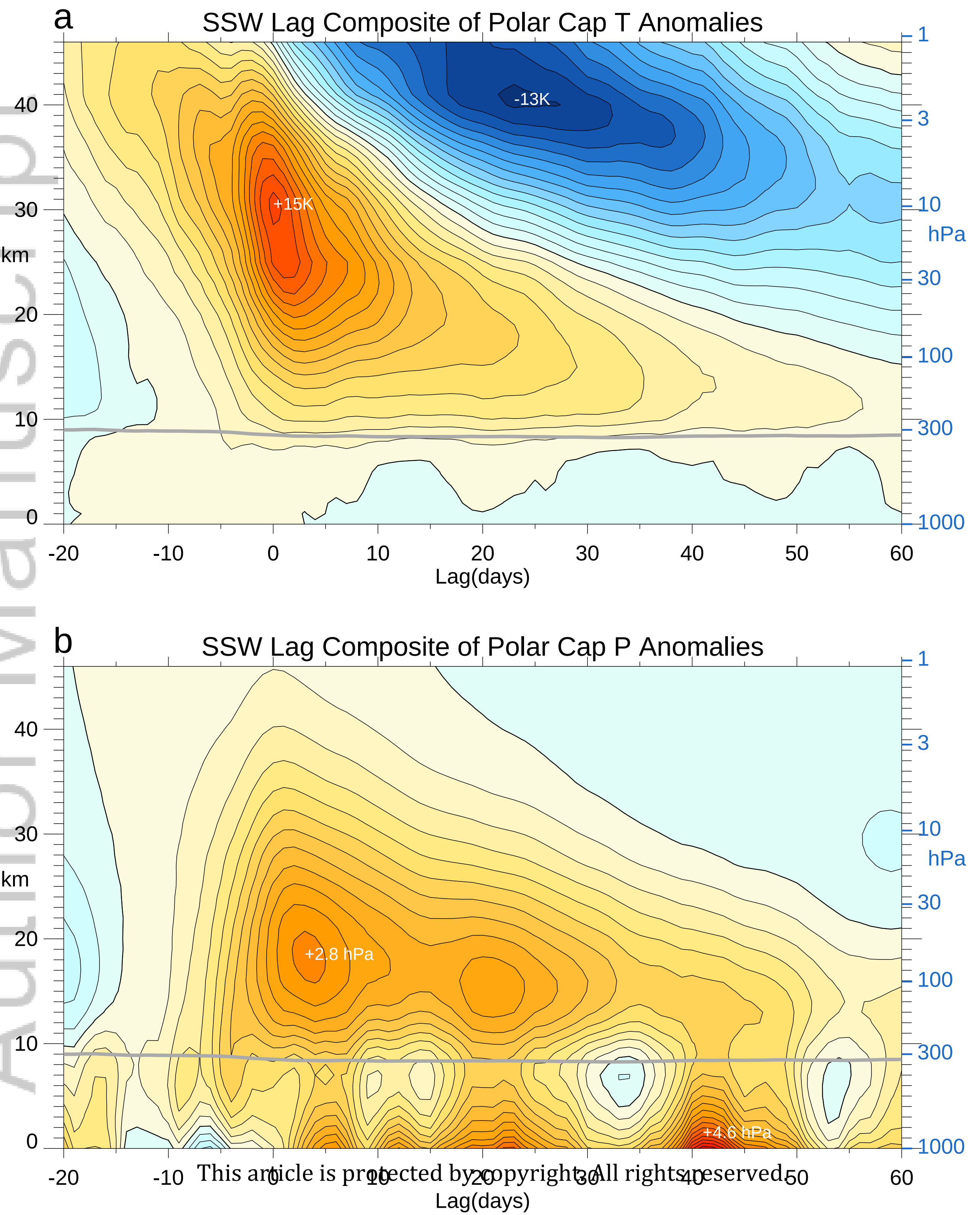

a
SSW Lag Composite of Polar Cap T Anomalies
-13K
+15K
km
hPa
Lag(days)
b
SSW Lag Composite of Polar Cap P Anomalies
+2.8 hPa
+4.6 hPa
km
hPa
Lag(days)

Figure 4.

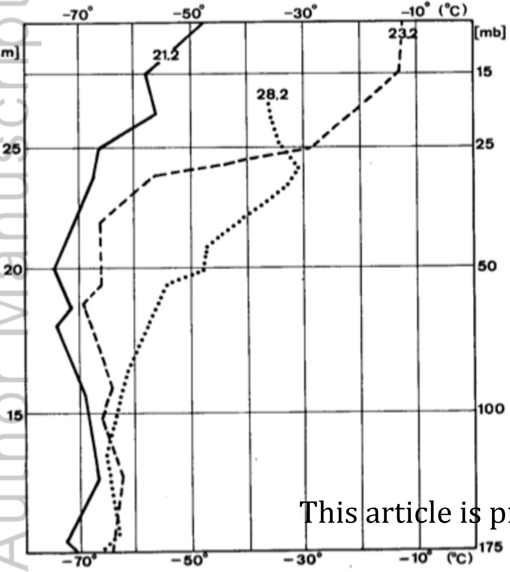

-70°
-50°
-30°
-10° (°C)
[km]
[mb]
21.2
23.2
28.2
15
25
25
20
50
15
100
175
-70°
-50°
-30°
-10° (°C)

Figure 5.

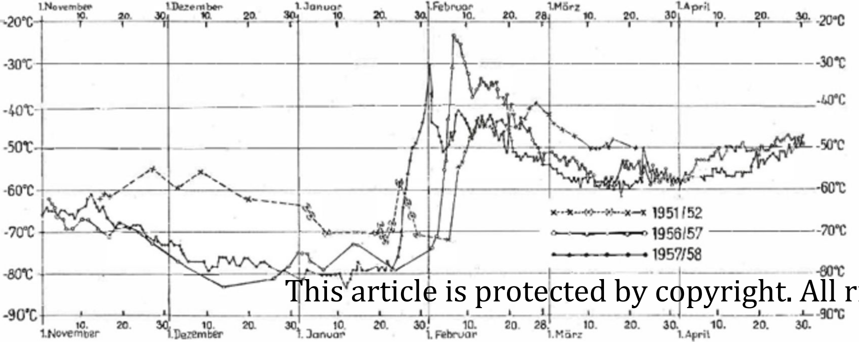

1.November
1.Dezember
1.Januar
1.Februar
1.März
1.April
10.
20.
30.
28.
-20°C
-30°C
-40°C
-50°C
-60°C
-70°C
-80°C
-90°C
1951/52
1956/57
1957/58

Figure 6.

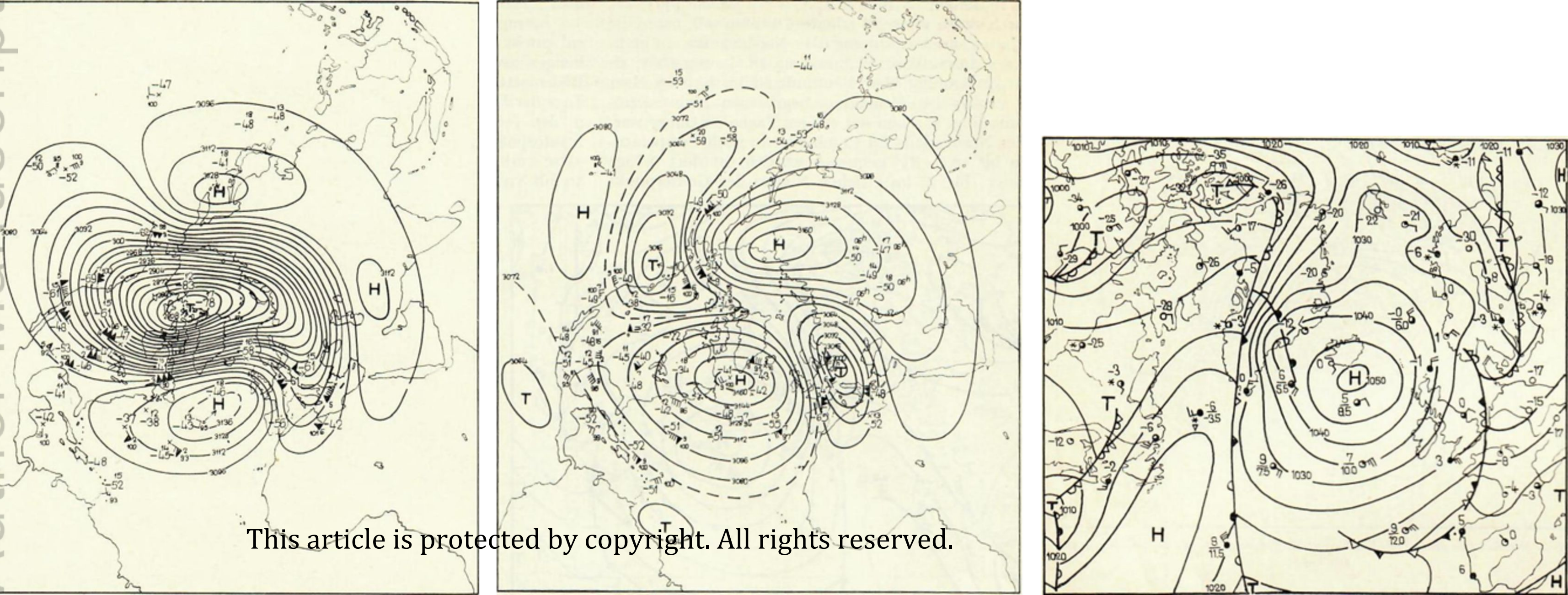

Figure 7.

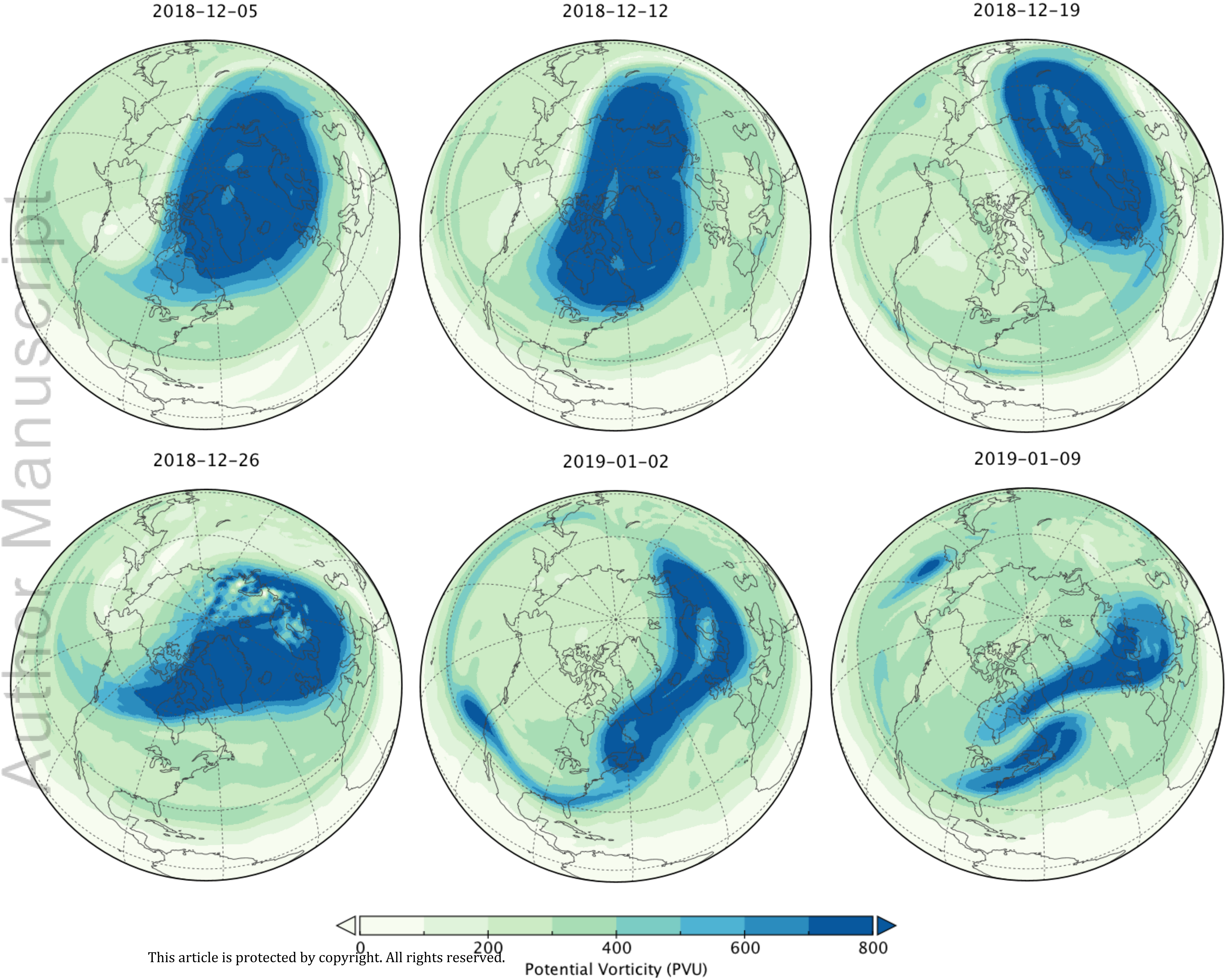
2018–12–05
2018–12–12
2018–12–19
2018–12–26
2019–01–02
2019–01–09
0
200
400
600
800
Potential Vorticity (PVU)

Figure 8.

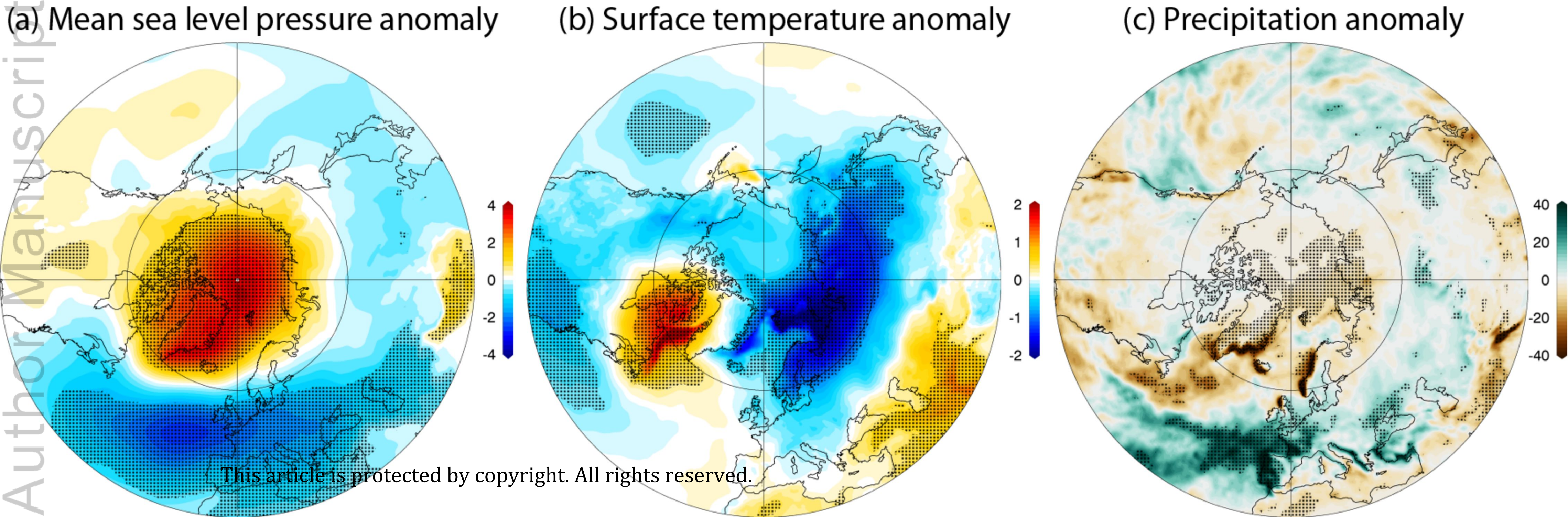
(a) Mean sea level pressure anomaly
4
2
0
-2
-4
(b) Surface temperature anomaly
2
1
0
-1
-2
(c) Precipitation anomaly
40
20
0
-20
-40

Figure 9.

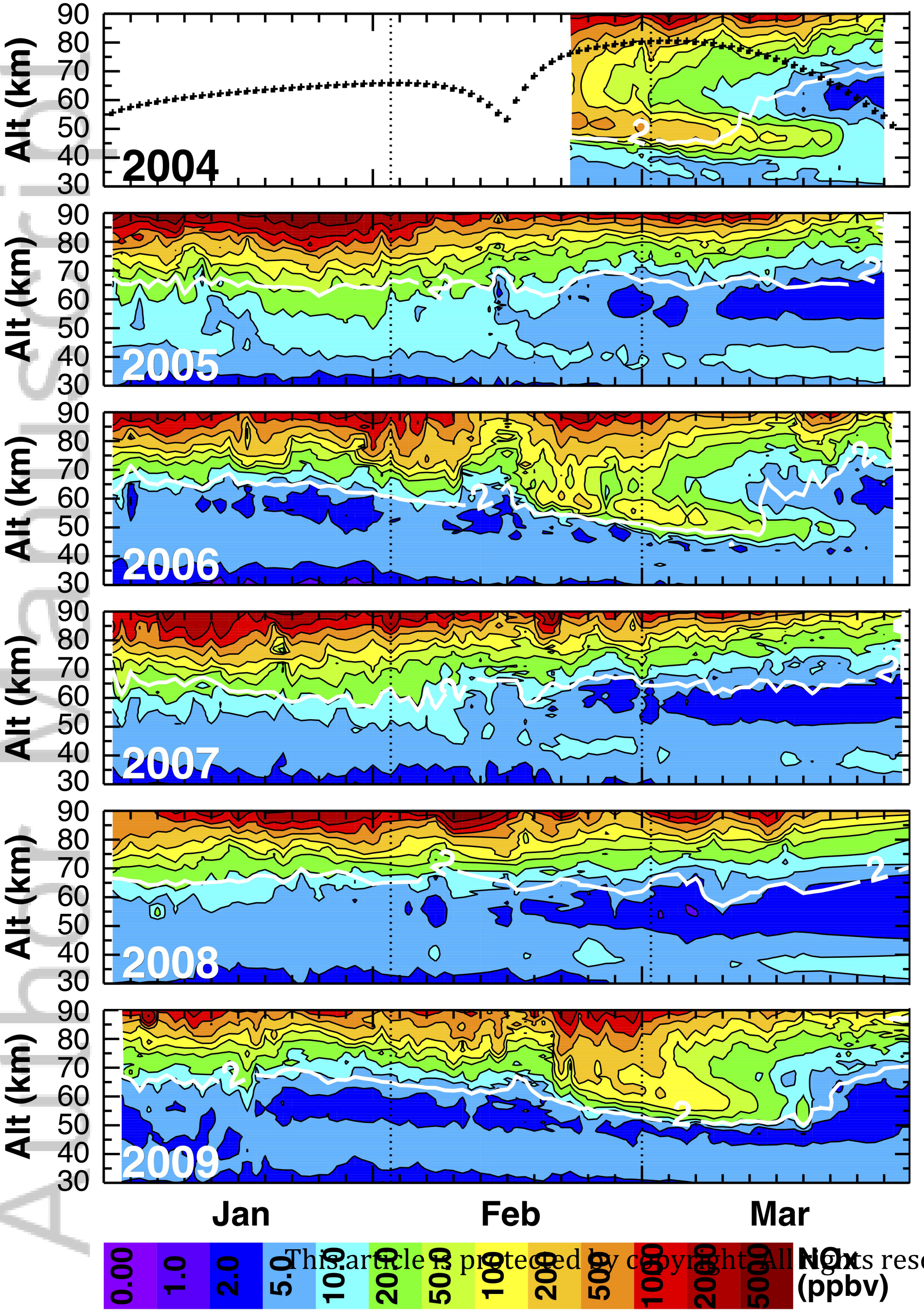

Alt (km)
90 80 70 60 50 40 30
2004
2005
2006
2007
2008
2009
2
Jan
Feb
Mar
0.00 1.0 2.0 5.0 10.0 20.0 50.0 100 200 500 1000 2000 5000
NOx (ppbv)

Figure 10.

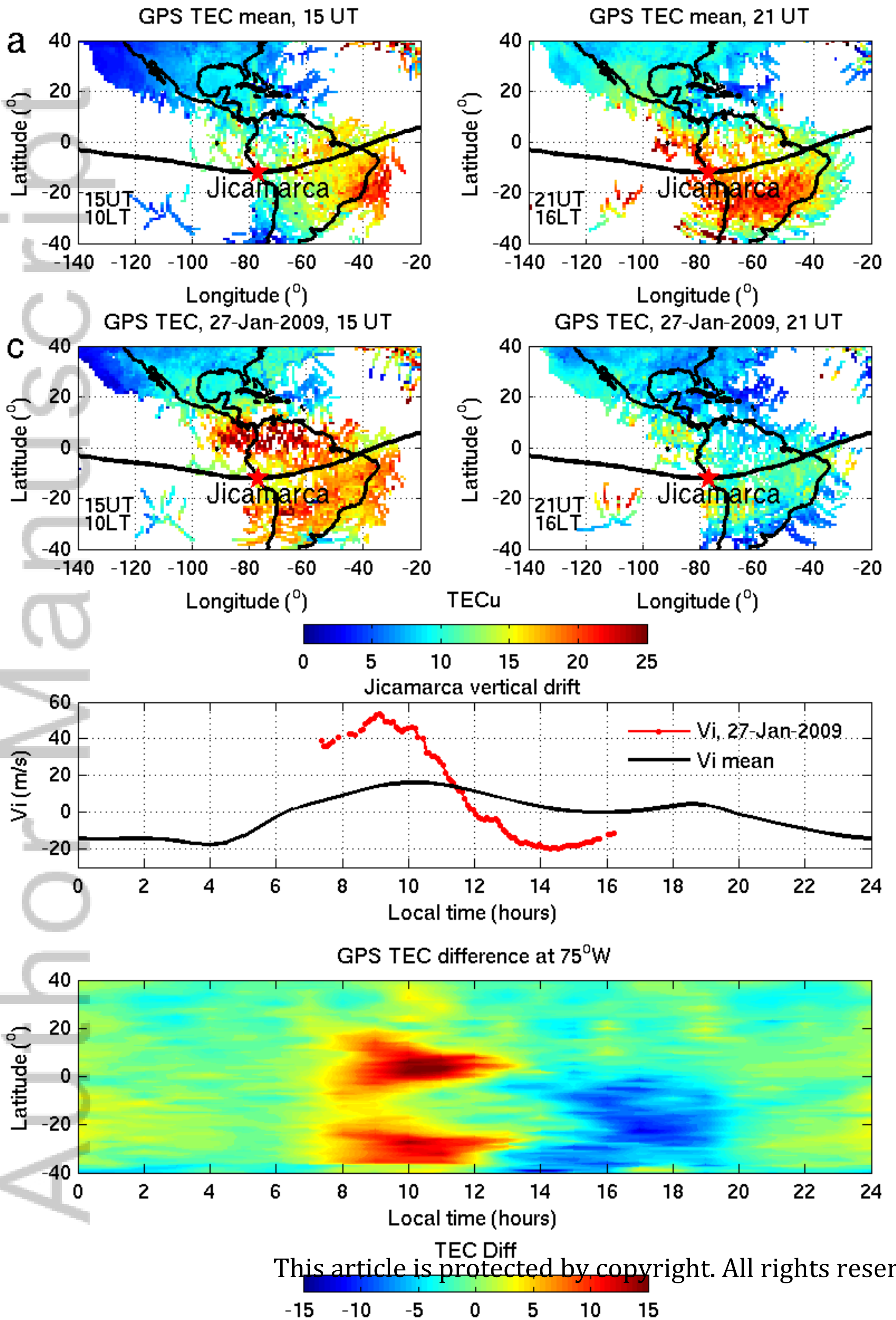

GPS TEC mean, 15 UT
GPS TEC mean, 21 UT
GPS TEC, 27-Jan-2009, 15 UT
GPS TEC, 27-Jan-2009, 21 UT
a
b
c
d
e
f
Latitude (°)
Longitude (°)
Jicamarca
15UT
10LT
21UT
16LT
TECu
Jicamarca vertical drift
Vi, 27-Jan-2009
Vi mean
Vi (m/s)
Local time (hours)
GPS TEC difference at 75°W
TEC Diff

Figure 11.

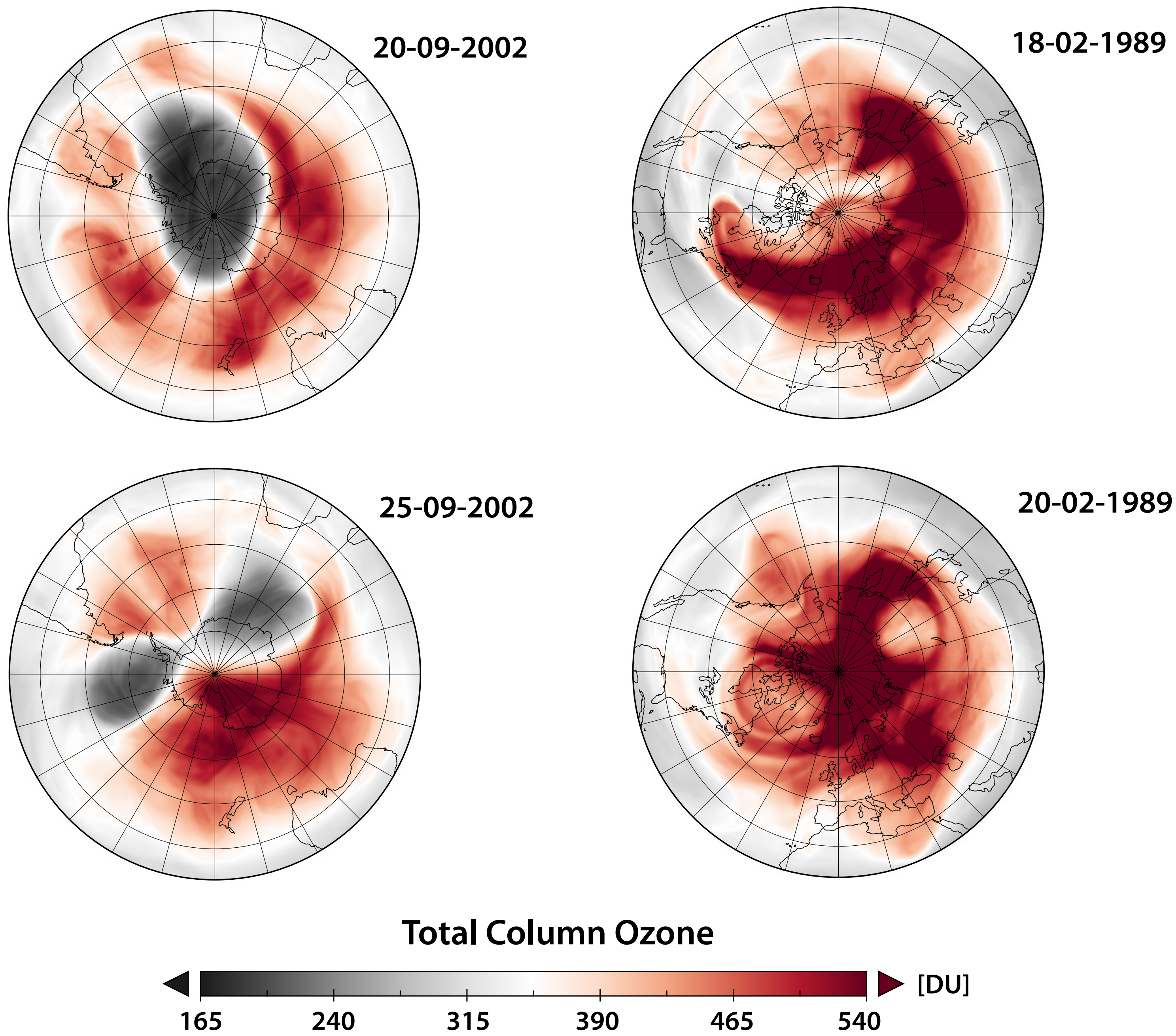
20-09-2002
18-02-1989
25-09-2002
20-02-1989
Total Column Ozone
165
240
315
390
465
540
[DU]

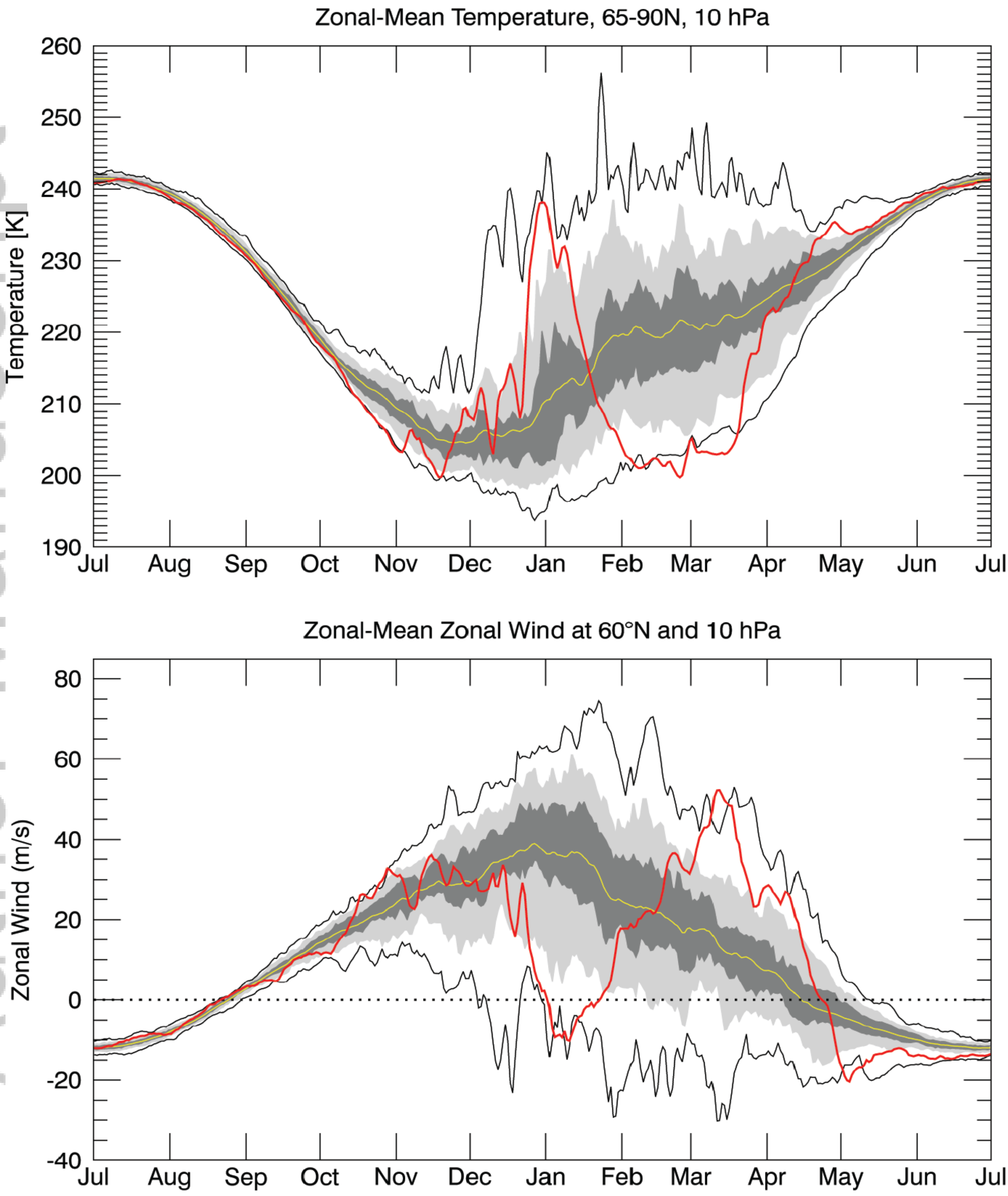

ROG_20245_2020RG000708-f01-z-.png

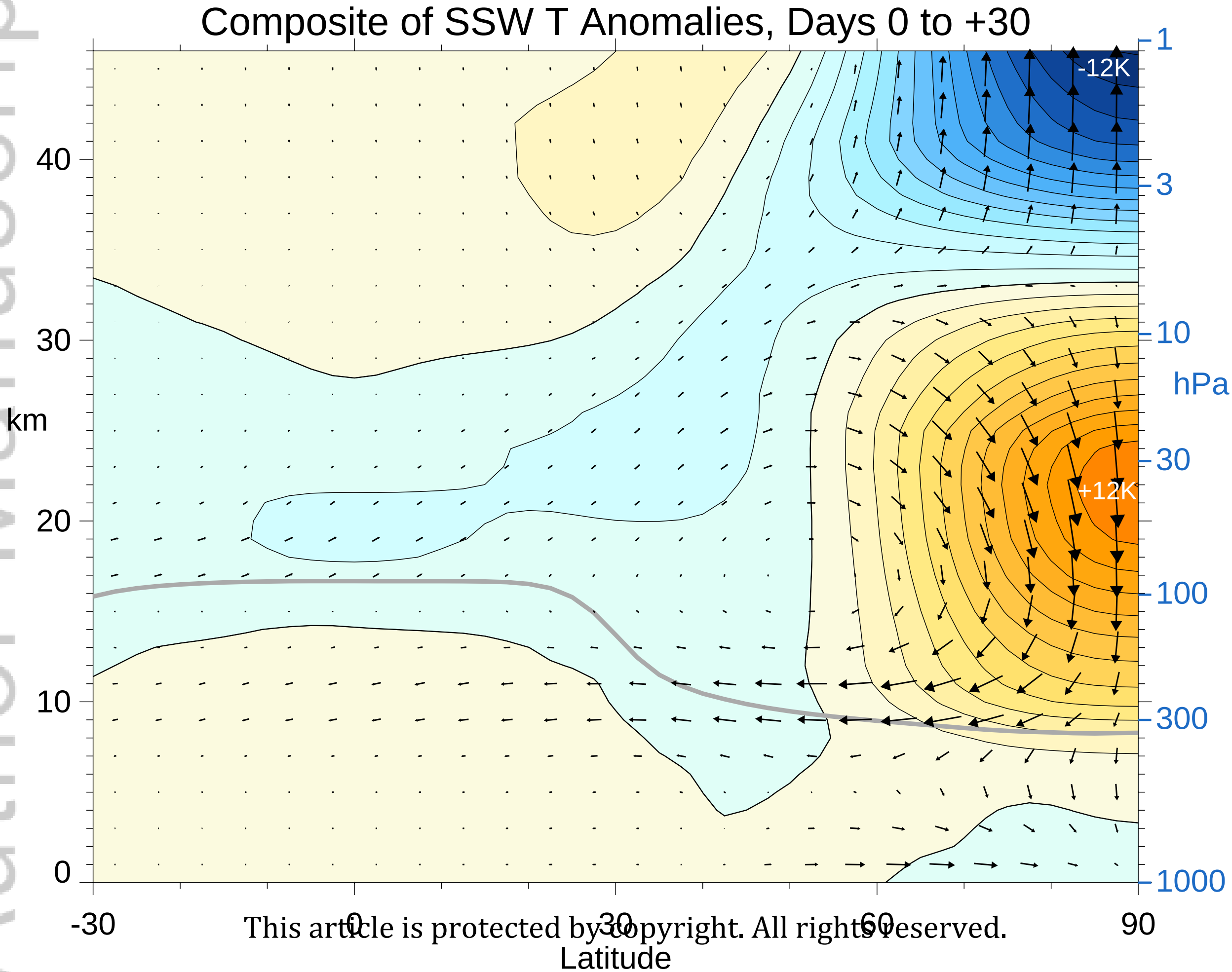

Composite of SSW T Anomalies, Days 0 to +30
-12K
+12K
km
0
10
20
30
40
hPa
1
3
10
30
100
300
1000
-30
0
30
60
90
Latitude

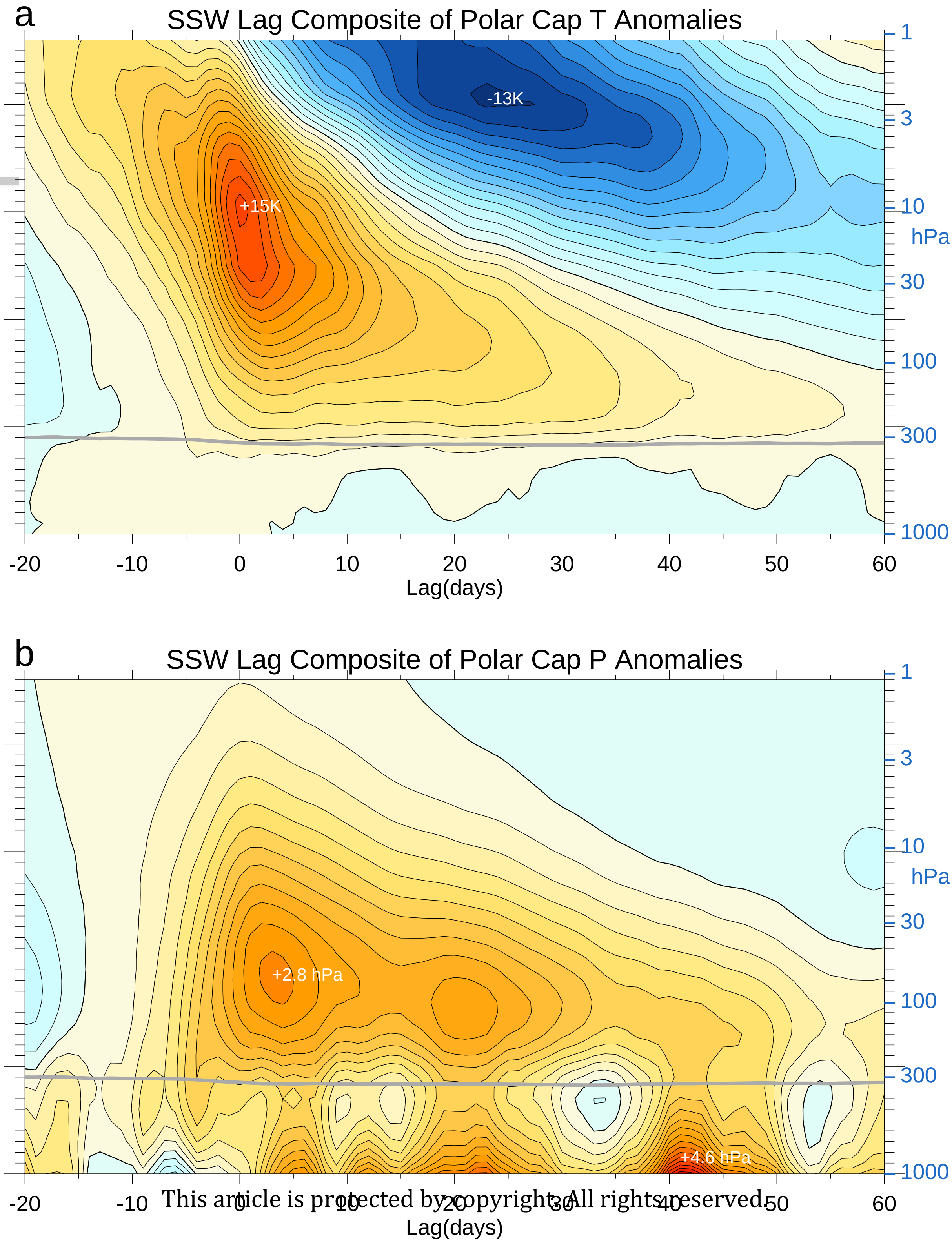
a
SSW Lag Composite of Polar Cap T Anomalies
-13K
+15K
km
hPa
Lag(days)
b
SSW Lag Composite of Polar Cap P Anomalies
+2.8 hPa
+4.6 hPa
km
hPa
Lag(days)

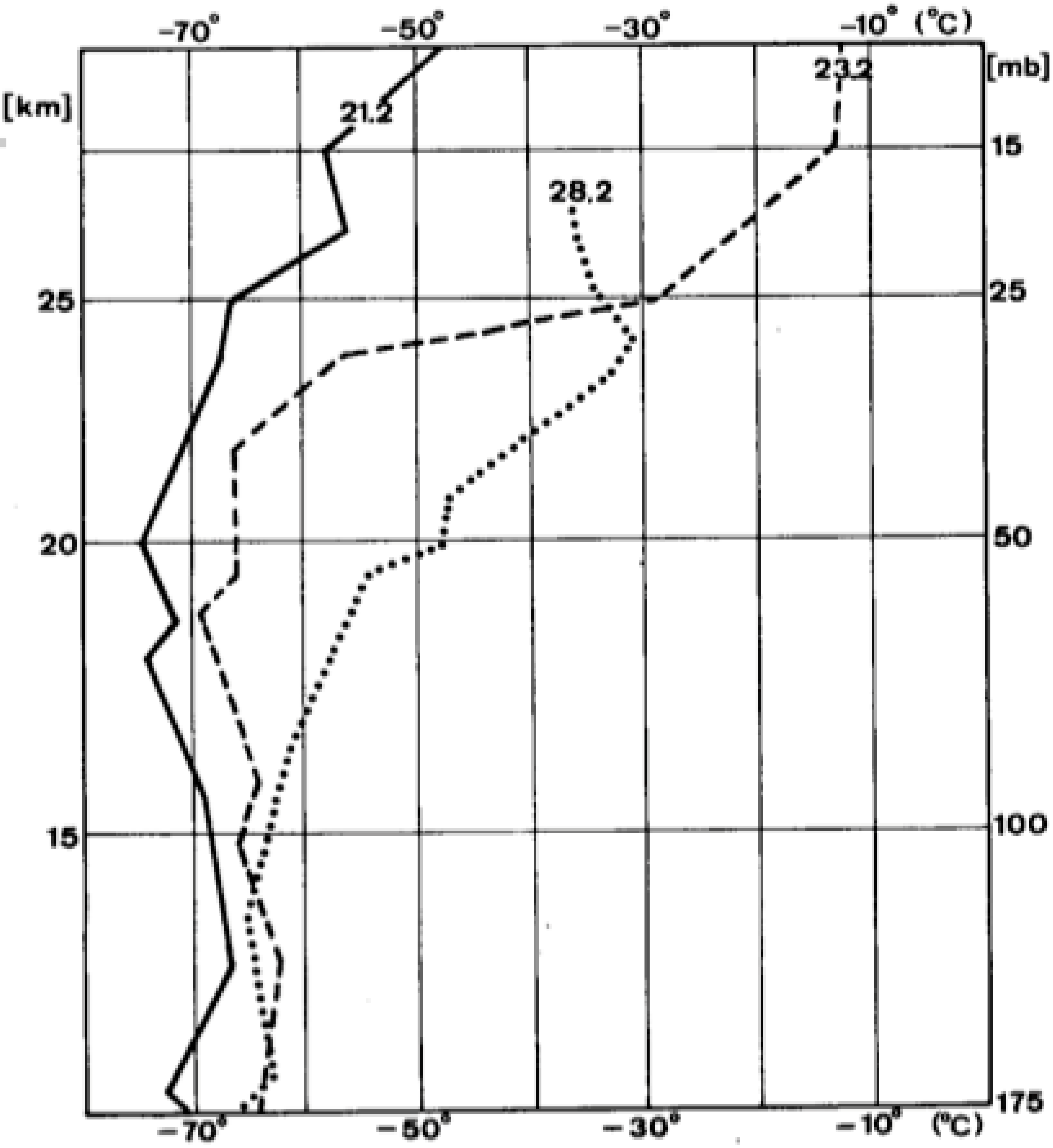

ROG_20245_2020RG000708-f04-z-.png

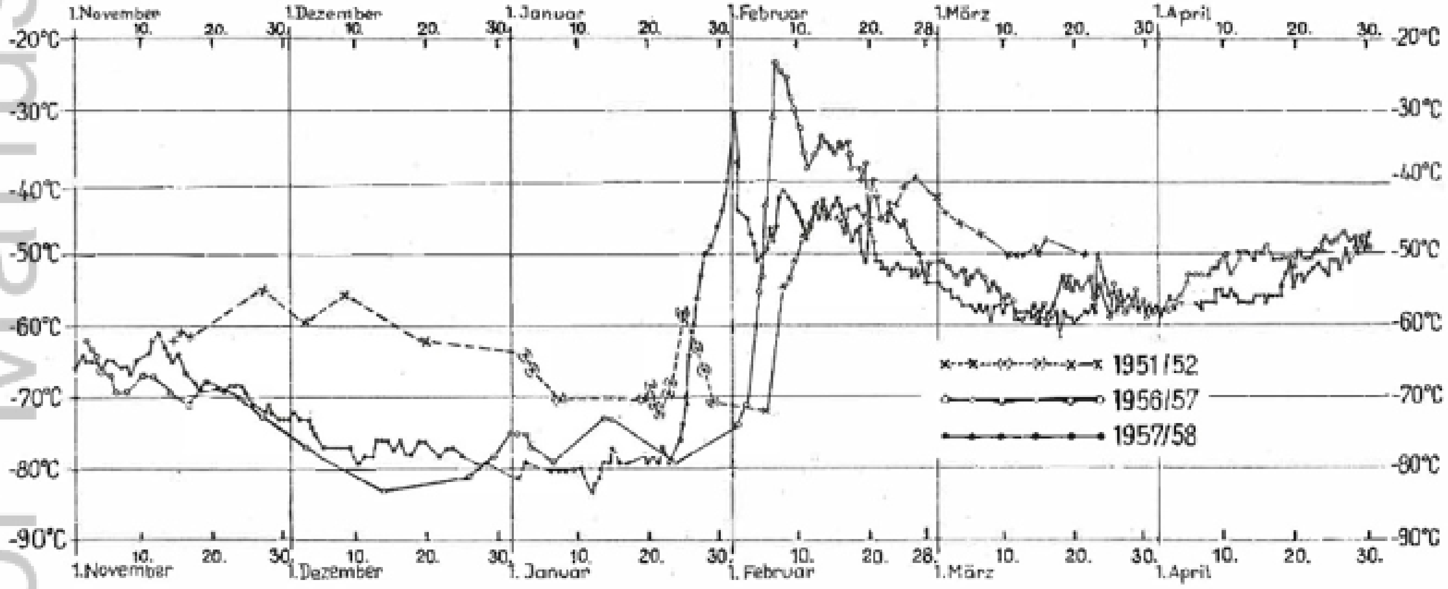

ROG_20245_2020RG000708-f05-z-.png

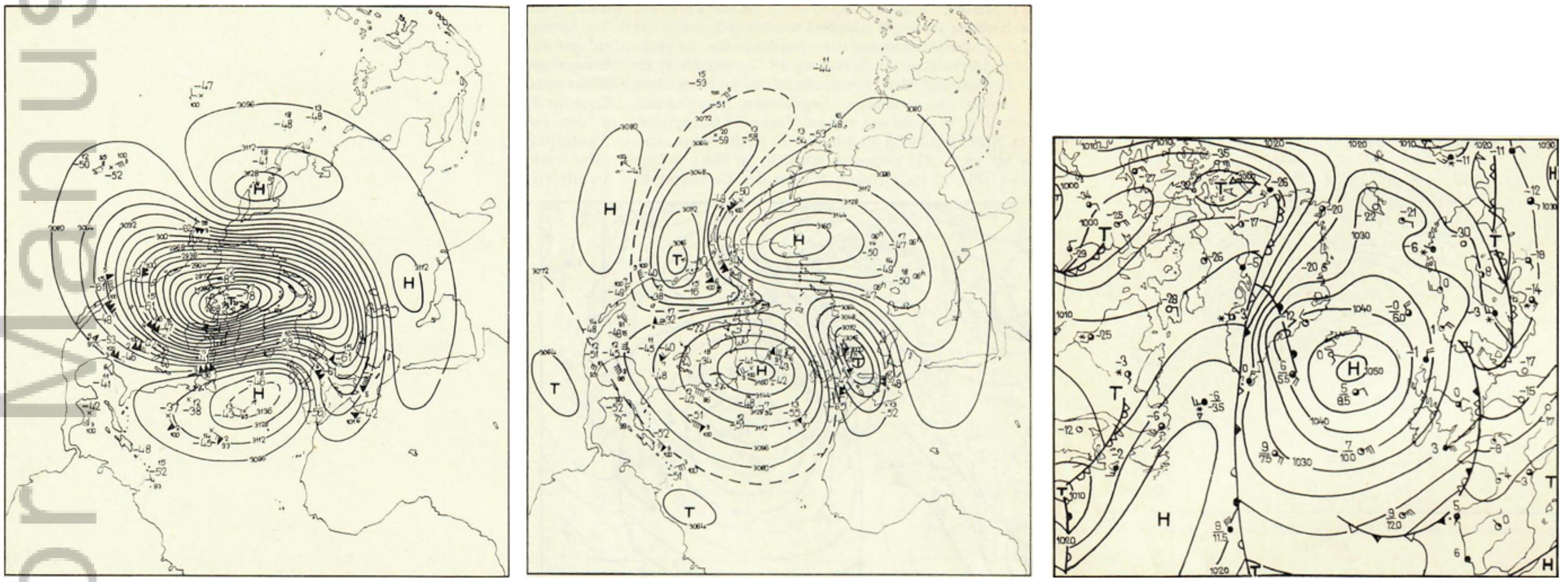

ROG_20245_2020RG000708-f06-z-.png

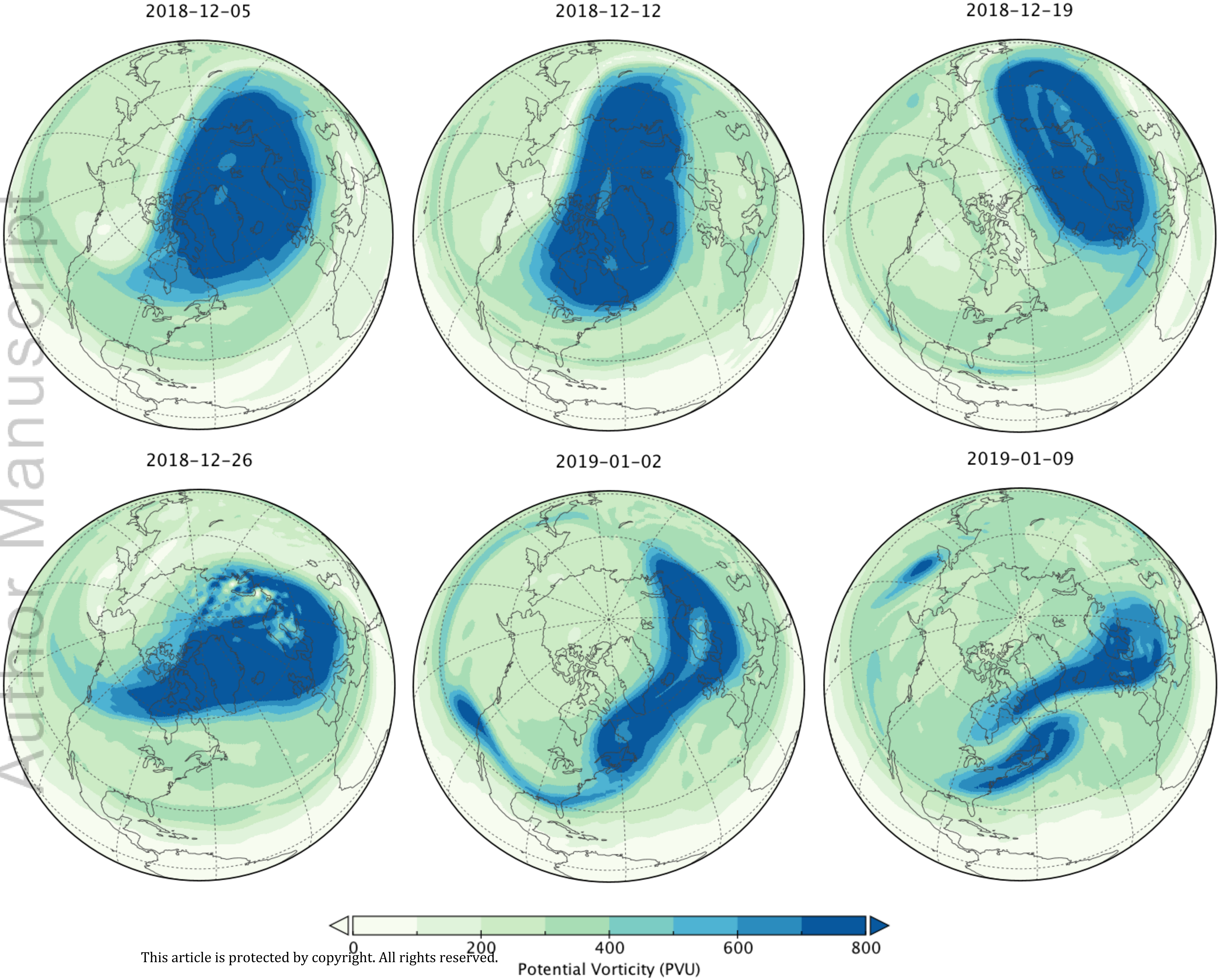
2018–12–05
2018–12–12
2018–12–19
2018–12–26
2019–01–02
2019–01–09
0
200
400
600
800
Potential Vorticity (PVU)

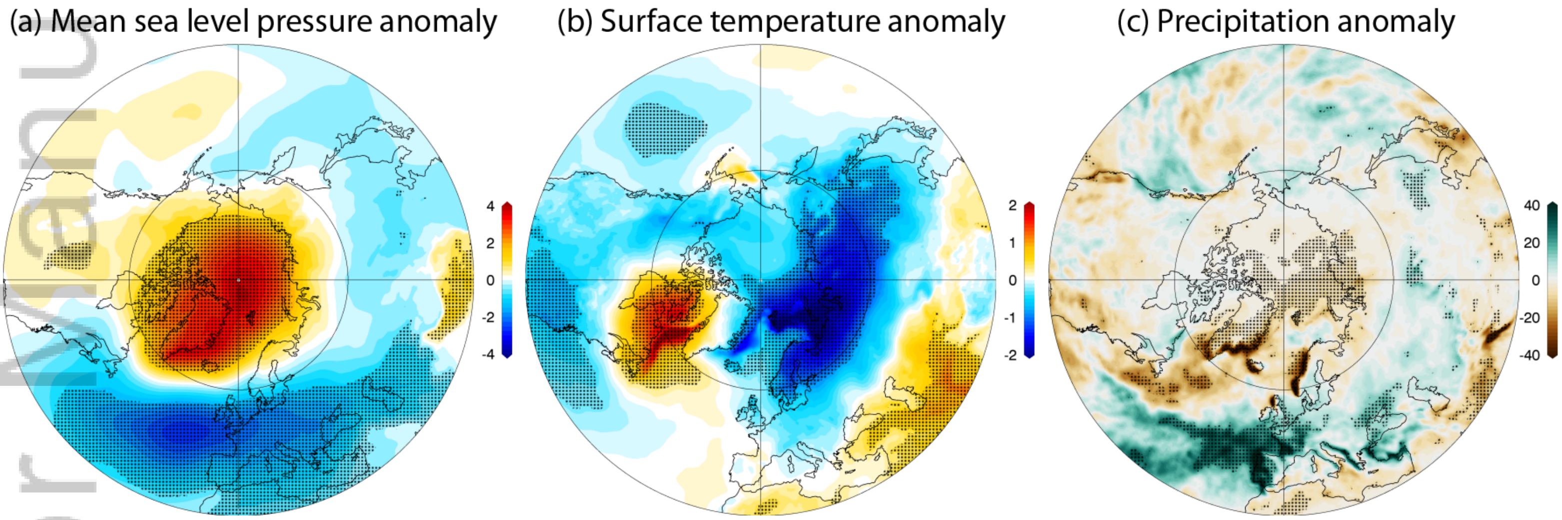

ROG_20245_2020RG000708-f08-z-.png

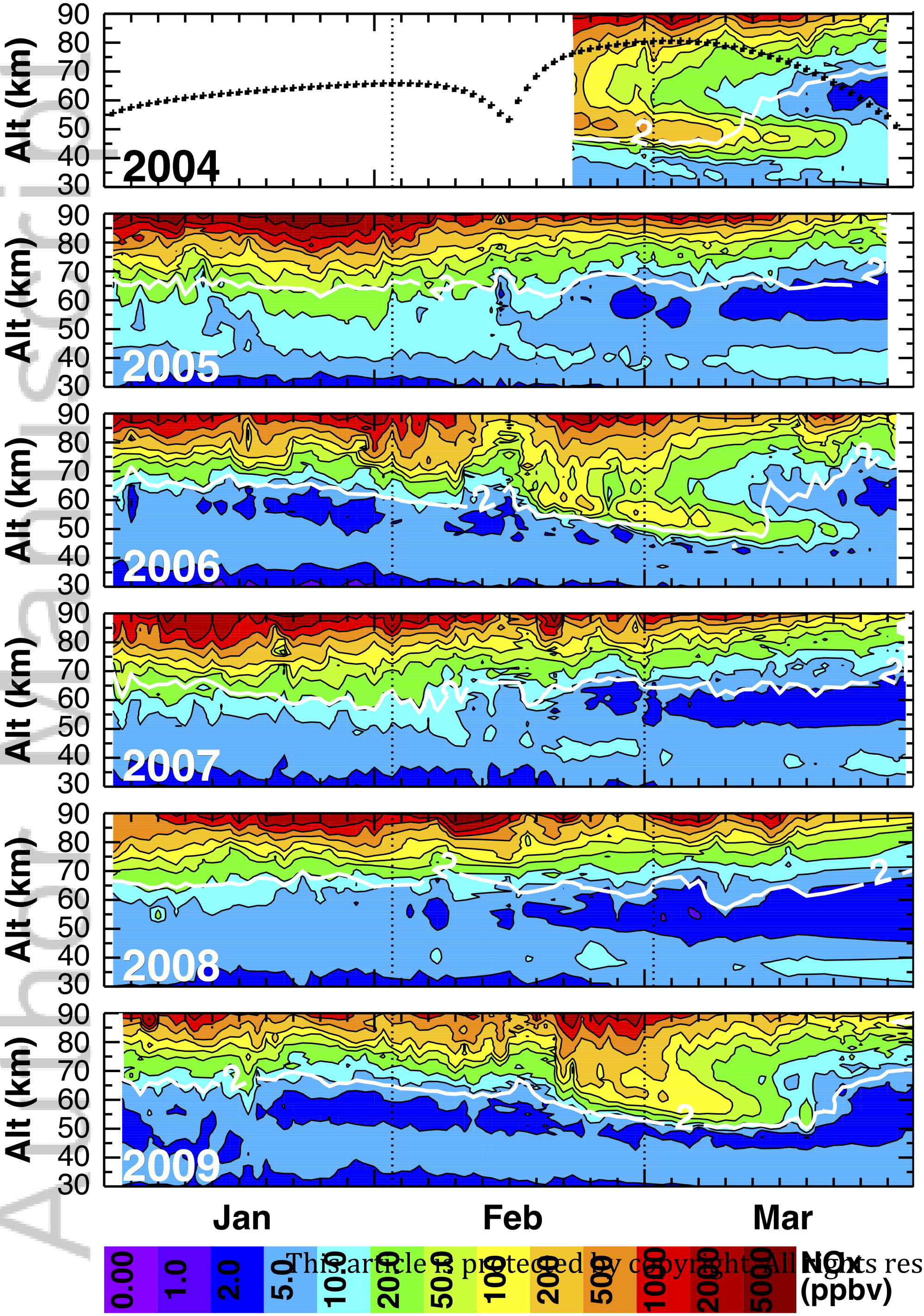

90
80
70
60
50
40
30
Alt (km)
2004
2005
2006
2007
2008
2009
2
Jan
Feb
Mar
0.00
1.0
2.0
5.0
10.0
20.0
50.0
100
200
500
1000
2000
5000
NOx
(ppbv)

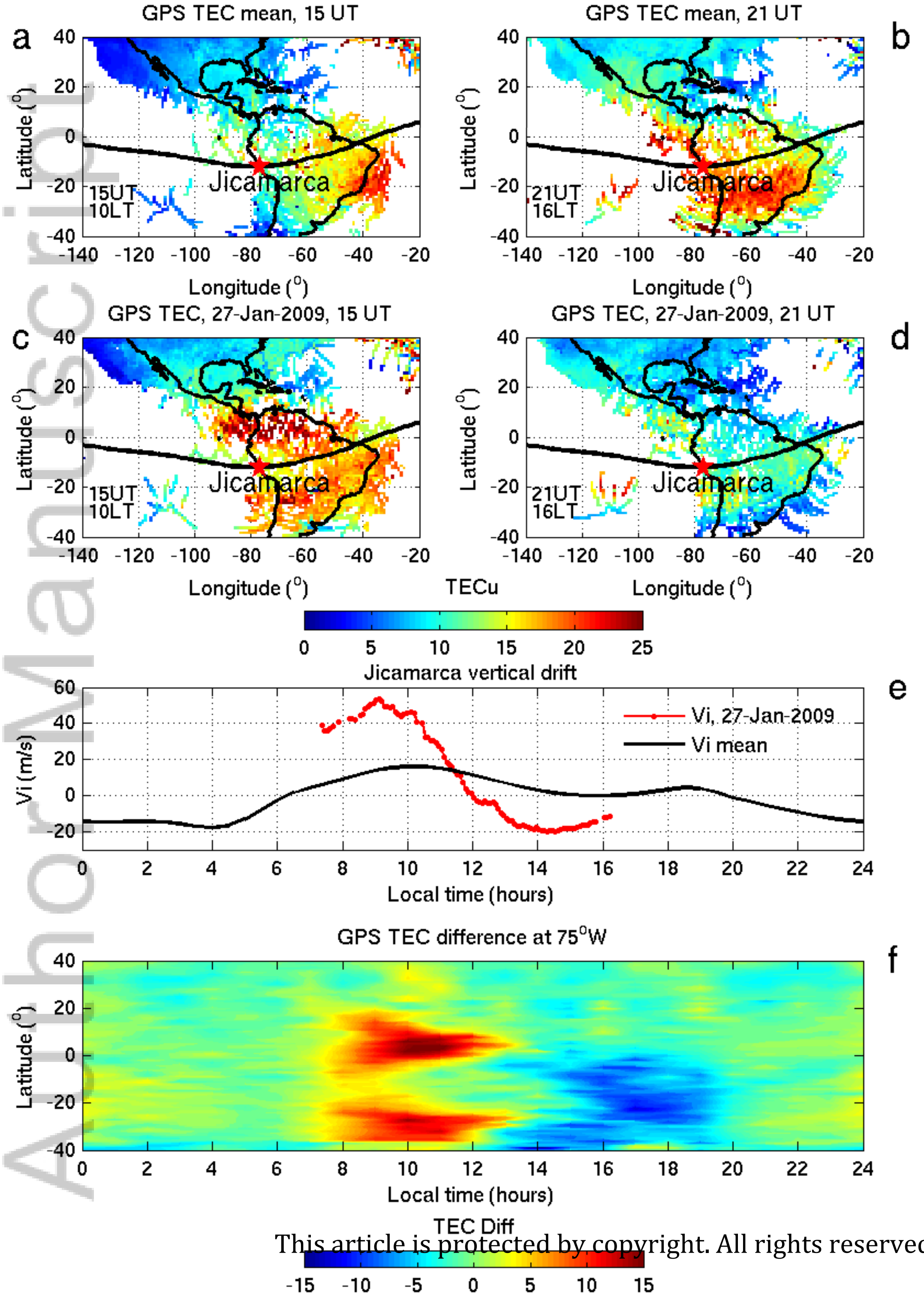
GPS TEC mean, 15 UT
GPS TEC mean, 21 UT
GPS TEC, 27-Jan-2009, 15 UT
GPS TEC, 27-Jan-2009, 21 UT
a
b
c
d
Jicamarca
15UT
10LT
21UT
16LT
Latitude (°)
Longitude (°)
TECu
Jicamarca vertical drift
e
Vi, 27-Jan-2009
Vi mean
Vi (m/s)
Local time (hours)
GPS TEC difference at 75°W
f
TEC Diff

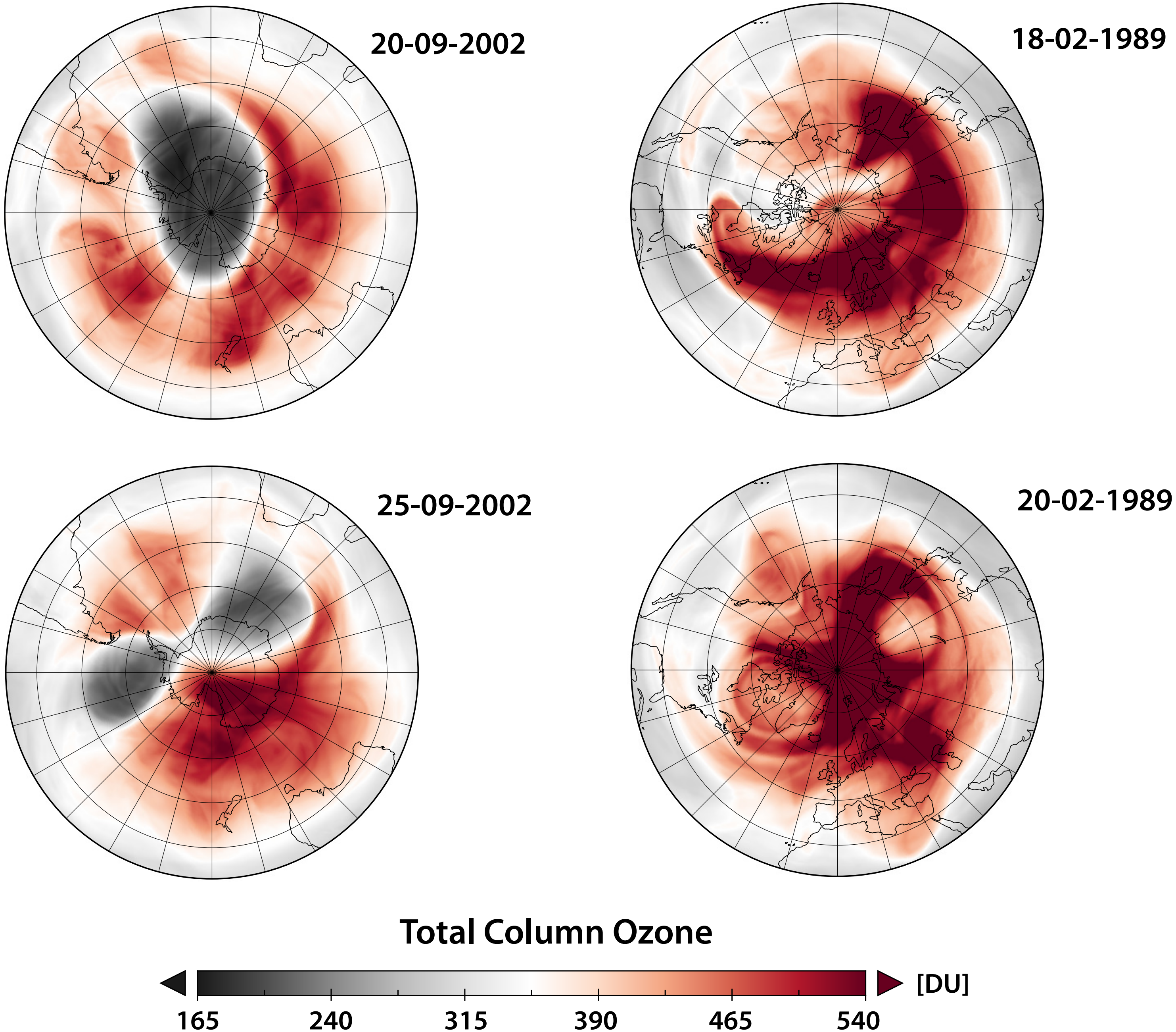
20-09-2002
18-02-1989
25-09-2002
20-02-1989
Total Column Ozone
165
240
315
390
465
540
[DU]